

CHANGES OF BREAST CANCER GROWTH AND METASTASIS IN MURINE MODELS
MODULATED BY AN AROMATASE INHIBITOR, A LOW CALCIUM DIET OR A HIGH FAT
DIET

BY

WENDAN WANG

DISSERTATION

Submitted in partial fulfillment of the requirements
for the degree of Doctor of Philosophy in Food Science and Human Nutrition
with a concentration in Human Nutrition
in the Graduate College of the
University of Illinois at Urbana-Champaign, 2015

Urbana, Illinois

Doctoral Committee:

Associate Professor Yuan-Xiang Pan, Chair
Professor William G. Helferich, Director of Research
Associate Professor Hong Chen
Professor Nicki J. Engeseth

Abstract

Breast cancer (BC) is the most commonly diagnosed cancer in women, the leading cause of cancer death in females worldwide,¹ and the second in American women (after lung cancer) according to CDCⁱ. In the most advanced stage of BC, stage IV, cancer cells metastasize from the original site to distant organs, such as bone, lung and liver. Tumor metastasis is responsible for nearly all of the morbidity and mortality associated with BC.² Treatments of BC fail in the advanced stage, when metastases have already occurred.³

To mimic late stage BC in female patients, a mouse model was utilized to create a micro-metastatic lesion by implanting a small number of metastatic murine mammary tumor cells into the marrow cavity of tibia. Subsequent lung metastasis was evaluated. Previously our group reported that estrogens and phytoestrogens stimulated BC primary tumor growth in mice.^{4,5} Estradiol stimulated ER negative BC metastasis in mice.⁶ Based on foregoing studies, the hypothesis of this study is that the aromatase inhibitor letrozole may inhibit BC metastases to lungs by suppressing estrogen synthesis. BC growth on the bone micro-metastatic site and lung metastases were monitored in live animals via Bioluminescence Imaging (BLI). Effects of ovariectomy and letrozole on body estradiol levels were examined. Tumor nodules on lungs stained with India ink were counted. Furthermore, tumor grown in lungs was analyzed via H&E staining and proliferative cell percentage in lung tumors was calculated via Ki-67 staining. Our results showed that ovariectomy lowered body estrogen level and increased bone tumor area and density as indicated by BLI, while letrozole inhibited BC lung metastases in mice inoculated with murine 4T1 cancer cells.

In a following project, the effects of a Low Calcium Diet (LCD) on BC metastases from bone to lungs, and its effects on the bone microenvironment in mice inoculated with murine 4T1 cells were studied. Bioluminescence imaging and India ink staining were used to evaluate tumor metastasis to the lungs. India ink stained lungs showed that LCD increased tumor numbers on the surface of lungs compared with control diet. LCD also induced negative impacts on the bone microenvironment where the primary tumor grows.

In the third project, the effects of a high fat diet (HFD) on BC growth and metastasis in mice inoculated with murine 4T1 or 4T1.2 BC cells were studied. HFDs have been associated with BC progression and metastasis, indicated to increase BC risk by raising estradiol level.^{7,8} In BALB/c mice, dietary fat was found to increase mammary tumor growth and metastasis, and increase mortality.⁹ In this study, effects of HFD on mammary ductal tumor growth and BC metastasis in mice were evaluated. Metastases from bone to visceral tissues were monitored by BLI. It is found in this project that HFD increased BC metastasis to lung and liver in mice

injected with 4T1.2 cells as shown by H&E staining. Mice injected with 4T1.2 cells developed more aggressive metastasis than mice with 4T1 cells, and also had higher liver weight and more liver lipid accumulation.

Acknowledgements

I would like to thank the guidance and support from my advisor, Dr. William G. Helferich, on my research projects, as well as numerous help that I received from current and previous members in the Helferich laboratory group during my graduate research and study. I would also like to thank the funding sources of the projects. These projects were supported by DOD Breast Cancer Research Program from U.S. Army Medical Research and Materiel Command [W81XWH-09-1-0689; BC085882] (WGH); National Institute on Aging; National Institute for Complementary and Alternative Medicine; Office of Dietary Supplements; and Women's Health Initiative [P01 AG024387] (WGH); and were made possible by Grant Number P50AT006268 (WGH) from the National Center for Complementary and Alternative Medicines (NCCAM), the Office of Dietary Supplements (ODS) and the National Cancer Institute (NCI). Its contents are solely the responsibility of the authors and do not necessarily represent the official views of the NCCAM, ODS, NCI, or the National Institutes of Health.

Table of Contents

CHAPTER 1: LITERATURE REVIEW.....1

CHAPTER 2: EFFECTS OF LETROZOLE ON BREAST CANCER MICRO-METASTATIC TUMOR GROWTH IN BONE AND LUNG IN MICE INOCULATED WITH MURINE 4T1 CELLS.....20

CHAPTER 3: EFFECTS OF A LOW CALCIUM DIET ON BREAST CANCER MICRO-METASTATIC BONE TUMOR GROWTH AND LUNG METASTASIS IN MICE FROM A TIME COURSE STUDY.....43

CHAPTER 4: CHANGES OF BREAST CANCER METASTASIS IN MICE INOCULATED WITH MURINE BREAST CANCER CELLS 4T1 AND 4T1.2 INDUCED BY A HIGH FAT DIET.....57

CHAPTER 5: CONCLUSION AND FUTURE RESEARCH.....79

REFERENCES.....81

APPENDIX A SUPPLEMENTAL FIGURES FOR CHAPTER 2.....91

APPENDIX B SUPPLEMENTAL FIGURES FOR CHAPTER 4.....94

Chapter 1 Literature Review

1.1 Breast Cancer (BC)

- 1.1.1 Tumor Microenvironment
 - 1.1.1.1 Bone Micrometastasis
 - 1.1.1.2 Animal Models for Bone Micrometastasis
- 1.1.2 Disseminated Tumor Cells in the Bone
- 1.1.3 Occult Micrometastasis as Circulating Tumor Cells

1.2 Letrozole

- 1.2.1 Letrozole Resistance
- 1.2.2 Effects of Letrozole on the Bone
 - 1.2.2.1 Reported No Adverse Effects from Letrozole
 - 1.2.2.2 Reported Adverse Effects from Letrozole

1.3 Low Calcium Diet (LCD) and BC

- 1.3.1 Calcium as a Growth Factor for BC Metastatic Tumor in the Bone
- 1.3.2 Clinical Trials on LCD and BC
- 1.3.3 Animal Models Used in BC and Calcium Studies
- 1.3.4 Molecular Studies on Calcium and BC

1.4 High Fat Diet (HFD) and BC

1.5 HFD and Metabolism

- 1.5.1 HFD and Hepatic Tumorigenesis
- 1.5.2 HFD and Hepatic Lipid Metabolism
- 1.5.3 Hormones Modulated by HFD
- 1.5.4 HFD and Energy Intake
- 1.5.5 HFD and Energy Expenditure
- 1.5.6 Obesity Caused by HFD

1.6 4T1 and 4T1.2 Cell Lines

- 1.6.1 4T1 Cell Line
- 1.6.2 4T1.2 Cell Line

1.1 Breast Cancer

As a global disease, breast cancer (BC) is becoming an increasingly urgent problem in low- and middle-income countries, where its incidence is on the rise as populations increasingly adopt western lifestyles. Cases increase in Africa and Asia, although prevalence is still the highest in Europe and the Americas.¹⁰ In developing countries, a large fraction of women with BC are diagnosed with advanced-stage disease and have no access to treatment or basic palliative care.¹¹ Thus a critical issue arises in regard to how we can transform existing knowledge about diet and BC into preventative or cautious practices among patients.

Metastasis is the primary cause of cancer treatment failure.¹² It usually occurs at later stages of BC, resulting in numerous comorbidities in patients. Lung is considered as a filter between the primary tumor and other secondary sites, and is therefore the organ most likely containing metastatic BC at autopsy.¹³ It was reported that isolated lung metastasis occurs in 10-20% of all women with BC and around 60-74% of patients who died of breast carcinoma developed lung metastasis.^{14,15} Another frequent site for BC metastases is bone. Around 70% of patients with BC have bone metastasis,¹⁶ and up to 75% of women with advanced BC develop bone metastasis,¹⁷ which can lead to advanced disease of bone destruction and mortality.¹⁸

During the last decade, there have been significant improvements in managing early stage BC patients. The 5-year survival rate for localized BC has increased to 98% compared to 72% in the 1940s. A decrease in mortality occurred mainly due to earlier detection and improved therapy. In contrast, metastatic BC remains essentially incurable with a 5-year survival rate of 21%. Most BC deaths result from complications of metastases rather than from the primary tumor. Tumor cells in the bone marrow of BC patients, as shown from clinical studies, correlate with a poor prognosis and predict for early recurrence.¹⁹

Studies have also found a set of genes mediating BC metastasis through their vascular remodeling functions, including EREGⁱⁱ, COX2ⁱⁱⁱ, MMP1 and MMP2^{iv}.²⁰ Specifically for lung metastasis, several extracellular modifiers were reported to cooperate, including SPARC^v, CXCL1^{vi}, VCAM1^{vii}, IL13RA2^{viii}, ROBO1^{ix}, and ID1^x.²¹ Besides, TGF β ^{xi} and NF- κ B^{xii} pathways were implicated in lung metastasis too.²² In animals implanted with BC tumors, expression of these genes can vary depending on the cell line used. Gene expressions can also be modulated by diet, and program cancer metastasis.

1.1.1 Tumor Microenvironment

As proposed in the Seed and Soil theory by Stephen Paget, the microenvironment in the secondary organs is among the three key influential factors that determines the fate of cancer metastasis. The process of metastasis involves complex interactions between tumor cells and

the environment. The capability of tumor cells to metastasize cannot be entirely explained by circulatory routes.¹⁹ The microenvironment dictates whether cancer cells of a given molecular phenotype would be supported or inhibited during metastasis.²³ The host microenvironment must provide appropriate conditions for the tumor cells to survive and proliferate. BC cells show a marked predilection for the skeletal system and can adhere to bone marrow stromal cells. The abundance of cytokines and growth factors produced by cells of the hematopoietic microenvironment are regarded to facilitate tumor cell behavior in an autocrine and/or paracrine fashion.¹⁹

There is dramatic difference between premenopausal women and postmenopausal women on the presence of growth factors in the bone pre-metastatic niche. Premenopausal women would have a lower biological activity of activin and TGF β in this niche due to presence of the inhibitors - inhibin, oestrogen and progesterone.²⁴ Whereas in post-menopausal women, high activin and TGF β activity may predispose to a tumor cell with active tumor suppressor smad2/3 signaling, macrophages polarised to an antitumor phenotype, fibroblasts with functional TGF β signaling and anti-tumor growth signaling and antiangiogenic effects of activating; eventually modify disseminated tumor cells to a less aggressive phenotype.²⁴

1.1.1.1 Bone Micrometastasis

Around 25-43% of BC patients have micrometastatic disease in the bone marrow, even after resection of their primary tumors.²⁵ Another study estimated that 12-45% of patients with primary operable BC could have tumor cells in the bone marrow as determined by immunocytochemistry.²⁶

Detection of disseminated tumor cells in the bone marrow of patients at surgery was reported to correlate with subsequent development of clinical bone metastasis.²³ Micrometastasis in bone has been shown as a biomarker for BC survival in patients. Molino A. *et al.* found evidence of longer disease-free and overall survival for patients with negative bone marrow, when the time-dependent evolution of bone marrow aspirates was taken into account. Even though the study was started in early 90s and was limited by the technical availability then, their results still hold value in interpreting the role of bone marrow micrometastasis in BC patient long term outcome, owing to the very long follow-up (13 years) and large number of bone aspirates taken.²⁷ Another study reported that immunocytochemical detection of micrometastatic cells in the bone marrow but not in lymph nodes is an independent prognostic risk factor in node negative BC that may have implications for surgery and stratification into adjuvant therapy trials.²⁸

Additionally, studies found that both the overall rate of death and rate of death from BC among patients with micrometastasis were significantly higher than the rate of death among patients without micrometastasis in the bone marrow.²⁹ There is strong evidence from clinical studies that BC patients with bone marrow micrometastasis, which is defined as the presence of single cancer cells or microscopic cancer cell-clusters in the bone marrow, have a shorter time to recurrence and decreased overall survival.²³

Besides, bone marrow may also act as a long-term reservoir of tumor cells, which can recirculate to other distant organs before growing into metastases, as reported by Vincent-Salomon A. *et al.* The high genetic heterogeneity of bone marrow micrometastatic cells might be responsible for recirculation of some cancer seeds from the bone marrow to different host organs. However, no biological or clinical study has directly reported such a process for bone marrow DTC and currently there is no direct evidence suggesting that they are responsible for the late growth of lung or liver metastases.²⁶

1.1.1.2 Animal Models for Bone Micrometastasis

The majority of animal models available for studying skeletal metastases focus on the relationship between tumor cells and bone, but clinical and experimental observations suggest that bone marrow may be the initial target tissue. Bone metastases are usually found in close association with bone marrow and frequently involve bones with a high proportion of red marrow.¹⁹

It was stated by some researchers that an ideal *in vivo* model of BC metastases to the marrow should simulate the real pathological condition. Currently, producing skeletal metastases in established models are usually achieved by manipulation of blood flow to the vertebrae, direct injection of tumor cells into the bone or left ventricular/intra-arterial injection. For example, widespread arterial dissemination of tumor cells can be generated via the intracardiac injection model by bypassing the lungs in order to seed cells to various organs. This method was employed in a study with luciferase-positive MDA-MB-231 derivative cell lines that were selected for enhanced *in vivo* metastasis to the bone in athymic nude mice.³⁰

While these systems provide valuable information, researchers argued that implanting tumor cells at the site of origin may be required for expression of the cellular properties associated with metastasis. An appropriate microenvironment may be essential for the development of metastatic phenotype. However, though orthotopic models have been described for a variety of tumor types, spontaneous bone marrow metastases from a primary breast tumor has not been described. In general, such a model is regarded necessary to evaluate the

mechanisms involved in metastasis and determine the timing and actual target (bone or bone marrow) of DTCs.¹⁹

1.1.2 Disseminated Tumor Cells in the Bone

Early BC can relapse even years after successful treatment of the primary tumor. It has therefore been hypothesized that individual tumor cells spread to secondary sites in the body where they can persist for long periods of time before initiating metastatic growth.³¹ For most patients with solid tumor, they undergo a complete resection of primary tumor, but still harbor a considerable risk of death from metastatic relapse due to minimal residual disease not eliminated by primary surgery, radio- or chemotherapy.³²

Since many advanced BC patients develop bone metastasis, it is crucial to understand the basis of bone marrow micrometastasis. Currently, little is known about the molecular mechanisms that govern dissemination of cancer cells to the bone marrow, their survival and dormancy in this niche, and progression from bone marrow micrometastasis to clinical metastasis.²³ Clinical studies have reported a link between bone marrow DTC and the onset of bone metastasis, supporting the idea of local growth of DTC into macrometastases.²⁶ Furthermore, the persistence of DTCs during adjuvant treatment of stages I-III BC predicts an increased risk of disease relapse and death.³¹ For most bone marrow DTC-positive patients, they never relapse, while others experience dramatic metastatic progression.²⁶

Now clinical manifestation of distant relapse is recognized as a consequence of early tumor cell dissemination, thus search for residual micrometastatic cells has become an issue of significant interest. With regional lymphatic spread considered as paralleled by hematogenous dissemination of tumor cells as a function of tumor load quantity,²⁸ up to 30% of node negative BC patients will recur with distant metastasis within 5 years after diagnosis, which may have arisen from occult metastatic cells present in secondary organs at diagnosis.²⁸

Besides, DTCs have been described to survive chemotherapy and hormonal therapy,³¹ and can persist in bone marrow in a dormant, non-proliferative state over many years post-surgery.³² Dormancy for DTCs is defined as the period from the dissemination of tumor cells until the appearance of clinically manifest metastases; during this time these cells appear to remain latent.²⁵ Factors that determine tumor cell dormancy are unclear, but may relate to the lack of the primary tumor microenvironment, such as the absence of stimulating growth factors and presence of growth-inhibiting cytokine.²⁶

DTC has been shown as an independent predictor of disease-free survival and overall survival in BC patients.³¹ Hartkopf A.D. *et al.* reported that DTCs were detectable in 26% of bone marrow aspirates collected from 3141 patients. As compared to DTC-negative patients,

DTC-positive patients more frequently had larger tumors, lymph node involvement, hormonal receptor positive tumors and HER2-positive tumors. DTC-positive patients were also at an increased risk of relapse and death.³¹ However, in another prospective cohort study including unselected patients before the standard procedure was established, detection of DTCs in bone marrow was not able to be confirmed as an independent prognostic marker of poor prognosis in primary BC.³³

1.1.3 Occult Micrometastasis as Circulating Tumor Cells

Besides DTCs detected in bone or other secondary organs, there are also occult haematogenous micrometastases reported in BC patients.²⁵ Depending on the detection technique used, circulating tumor cells (CTC) were found in 50-100% of patients with metastatic BC. Even in patients with no clinical signs of overt metastases, detection rates range from 10% to 60%.²⁶ It is unknown whether these cells reach secondary organs and survive there to form manifest metastases. But the number of these CTCs is reported to decrease with time after primary surgery.²⁵

The medullary space is a site of particularly intensive cell exchange between circulating blood and mesenchymal interstitium.²⁵ Two immunocytochemical studies demonstrated statistically significant correlations between DTC detection in bone marrow and CTC in blood, but bone marrow was more frequently positive than blood. Detection of DTC in bone marrow based on Real-Time rt-PCR had superior significance to CTC measurements in blood.²⁶ Another study suggested that cancer cells detected in the bone marrow are different from those in the blood, although DTCs that colonize the bone marrow pass through the blood.²³ Plus, current findings do not support an exchange of DTC in bone marrow with CTC from blood.²⁶

There is evidence showing that CTCs can be used as a biomarker for BC patient survival. In a prospective, multicenter study, 177 patients with measurable metastatic BC for levels of CTCs were tested before starting a new line of treatment and at the first follow-up visit. Specifically, the number of CTCs before treatment is an independent predictor of progression-free survival and overall survival in patients with metastatic BC.³⁴

However, other observations from studies showed that CTCs does not predict outcome in newly diagnosed BC patients. Presence of CTCs may be necessary, but is not sufficient for the development of metastases. It is argued that techniques used for the identification of micrometastatic tumor cells did not evaluate their viability or growth potential. Animal studies and clinical observations have demonstrated that metastasis is inherently an inefficient process. Studies employing tagged tumor cells have documented that micrometastases in some organs are a transient phenomenon. Evidence also suggested that very few metastatic tumor cells

actually proliferate and even fewer form macrometastases, possibly due to their clonogenicity. These cells may not have an angiogenic phenotype or the host microenvironment may be inadequate for their sustained growth, for example, lack of appropriate growth factors and/or adhesion/signaling molecules. Potentially random activation of additional genes was pointed out to be necessary to convert micrometastatic tumor cells into gross metastases.¹⁹

1.2 Letrozole

Letrozole is a third generation aromatase inhibitor which inhibits the enzyme aromatase that converts androgens to estrogens in women, mostly postmenopausal women, and is used to treat BC. After menopause, women's body estrogen is no longer supplied by ovary, but mostly generated, in much smaller amounts, from nonovarian tissues, such as the breast, the bone, the brain and the adipose tissue. Letrozole, as one of the aromatase inhibitors developed, was used to suppress estrogen production from these other sites by the enzyme aromatase, thus lower body estrogen level and suppress BC growth and development in BC patients.³⁵

Having been studied extensively in postmenopausal women with metastatic BC, as either a second-line or first-line Aromatase Inhibitor (AI) treatment or in adjuvant settings^{36,37}, the efficacy of letrozole to treat BC in premenopausal patients remains to be elucidated. Though it is mainly recommended for post-menopausal women considering their body estrogen no longer supplied from ovary but transformed by aromatase in other organs, there are studies using letrozole in premenopausal women with BC together with goserelin showing positive outcomes.³⁸⁻⁴⁰ Yet scarce data can be found regarding its use in premenopausal females as a single-agent treatment. Letrozole effectively abrogated aromatase-induced mammary hyperplasia in aromatase transgenic mice and was suggested as capable of blocking in situ estrogen production in breast tissue in premenopausal women.⁴¹ Another study in rats suggested its efficacy in suppressing mammary carcinogenesis in a premenopausal model.⁴²

Traditionally, the antiestrogen (AE) tamoxifen has been used to treat BC in patient by blocking the binding of estrogens to estrogen receptors (ER). Many organs in the body, including the mammary gland, as well as some of the mammary tumors themselves, express estrogen receptors. As a first-line or adjuvant endocrine treatment, tamoxifen has shown effectiveness in treating BC tumor growth, in mostly estrogen responsive or ER+ tumors. On the other hand, there are side effects from tamoxifen reported as well. AIs that lower estrogen level by inhibiting the enzyme aromatase and suppress mostly estrogen responsive mammary tumors have been compared with AEs and have shown fewer side effects than tamoxifen *in vitro*.³⁵ One study showed that Selective Estrogen Receptor Modulators (SERMs)/antiestrogens and AIs exhibited opposed effects on the ER expression of BC cells: tamoxifen up regulated ER α

expression, while AIs increased ER β expression. And this may contribute to the therapeutic superiority of AIs over antiestrogens.¹¹

1.2.1 Letrozole Resistance

Since letrozole directly interferes with estrogen production in the body and lowers body estradiol level, it has mostly been used to treat estrogen responsive BC or ER+ BC. Although effective as an anticancer agent, resistance to letrozole was reported in studies. It was observed in clinical trials that although AIs have been proven as an effective treatment for ER+ BC, some BC patients may eventually relapse during AI treatment while others may never regain responsiveness.⁴³ In vitro studies also showed that long-term letrozole-treated cells and tumors became insensitive to hormone therapy, probably because they adapted to the extreme conditions of estrogen deprivation.⁴⁴ Such drug resistance or non-responsiveness might develop in animal models as well. Future studies with better controlled variance are in need to explore the mechanism of this drug in animals.

The mechanism of letrozole resistance has been studied but is still vague. Sensitivity of TGF- β signaling was reported to be compromised in letrozole-resistant BC cells.⁴⁵ 4T1 cells were reported to express TGF- β receptors and blockage of TGF- β inhibits 4T1 cell migration and metastases.⁴⁶ PELP1 was also reported to be related to letrozole resistance in BC cells.⁴⁷ Down-regulation of the ER coregulator PELP1 affected the proliferative ability and migration of 4T1 cells as shown in another study.⁴⁸

To delay the development of AI resistance, blocking ER was shown effective in studies.^{44,49} Additionally, a short period without letrozole to let the tumor regain responsiveness was suggested as effective in reversing the resistance to AI and delaying the need for chemotherapy.⁵⁰

1.2.2 Effects of Letrozole on the Bone

Most of the BC patients and survivors are postmenopausal females with lower body estrogen levels, lower calcium absorption and higher bone turnover compared with premenopausal females. One of the animal models of studying late stage BC metastasis is injecting BC cells directly into the tibia to mimic micrometastatic tumor growth in the bone and subsequent metastasis, same as the model used in our research group.⁵¹ Since the bone microenvironment would dictate BC tumor growth, it would be of vital interest to know whether the treatment or diet in a study would affect the bone microenvironment or not. Moreover, any changes to the bone microenvironment from the treatment or drug, such as the action of releasing growth factors to the tumor, may influence and even exacerbate BC development in the body.

1.2.2.1 Reported No Adverse Effects from Letrozole

There were few studies showing that there is no effect of letrozole on the bone. In a study, women receiving letrozole experienced more hormonally related side effects than those receiving placebo, but the incidences of bone fractures and cardiovascular events were the same. They concluded that letrozole after tamoxifen is well-tolerated and improves both disease-free and distant disease – free survival but not overall survival, except in node-positive patients.⁵²

Though previously reported to induce bone loss, several animal studies showed that letrozole had no effect on bone turnover. In one study, letrozole inhibited BC tumor growth without inducing uterine hypertrophy or affecting Bone Mineral Density (BMD) in ovariectomized nude mice, suggesting that letrozole is an effective and safe (in terms of risk of endometrial cancer risk and osteoporosis) alternative or complement to tamoxifen treatment for BC.⁵³ In another study, OVX rats treated with letrozole had similar BMD, bone biomarkers, mechanical failure properties, and lipid levels to those of OVX controls. Thus they concluded that nonsteroidal inhibitor letrozole did not affect bone loss, bone mechanical strength, and serum cholesterol and low-density lipoprotein levels in OVX rats.⁵⁴

More studies were conducted in clinical settings, and showed that letrozole has been working when incorporated into BC therapy. For example, one study showed that primary endocrine therapy with aromatase inhibitors is an option in elderly patients unfit for or unwilling to undergo surgery. Letrozole was shown as a reasonable alternative in elderly women with early ER/PR-positive invasive BC that are unfit or unwilling to undergo standard therapy.⁵⁵

1.2.2.2 Reported Adverse Effects from Letrozole

However, women with BC, especially those receiving AIs, are indeed regarded to be at higher risk for bone loss and fracture. Postmenopausal women may already have multiple risk factors for fracture, and BC therapies compound these risks.⁵⁶ One study evaluated bone health in a prospective clinical cohort of patients recruited prior to adjuvant AI therapy, and showed that low bone mass, prevalent fractures and vitamin D insufficiency were highly prevalent among candidates to adjuvant AI for early BC.⁵⁷ In a large prospective clinical trial, about one-quarter of the patients entered discontinued the AI therapy. Musculoskeletal adverse events represent a major impediment to the use of AIs and have been the major single cause of patients discontinuing AI therapy.⁵⁸ A retrospective longitudinal analysis of a large cohort of BC patients demonstrated that AI therapies carry an increased risk of bone loss, which corroborates previous findings from smaller clinical trials.⁵⁹ In a case report, when letrozole was taken at one

dose daily (2.5mg), a patient had recurrent hypercalcemia, suggesting that letrozole may precipitate hypercalcemia in a patient with BC.⁶⁰

Letrozole, as one of the AIs, has been compared with other AIs on effectiveness to treat BC and side effects on the bone. In a prospective, open-label, randomized pharmacodynamics study designed to assess the effects of AIs on bone turnover in healthy postmenopausal women with ER+ BC, effects of letrozole on bone turnover increased with time.⁶¹ In an open, randomised Phase I study comparing three licensed AIs on bone turnover markers, lipid profiles and adrenal function, letrozole induced increases in bone resorption markers, similar as other AIs.⁶²

Studies comparing non-steroidal AI, such as letrozole, with steroidal AI on the side effects showed varied results. In a study, exemestane was compared with nonsteroidal AIs anastrozole and letrozole on serum and urine levels of biomarkers of bone turnover in healthy postmenopausal women. The steroidal aromatase inactivator exemestane did not have detrimental effects on bone in animal models, in contrast to nonsteroidal AIs.⁶³ While when tested against each other in postmenopausal women with early BC, all of the AIs, both nonsteroidal (anastrozole and letrozole) and steroidal (exemestane), were reported to cause similar increases in bone turnover markers, with no difference between the two drug classes. The absolute fracture risk in early BC patients receiving AI therapy remains relatively low, although still higher than that in the general population of postmenopausal women, and this should not be a reason for excluding patients from highly effective adjuvant treatment, such as AIs.⁶⁴

Used in premenopausal women as reported in several studies, treatment including letrozole as an adjuvant therapy showed side effects. One study showed clinical efficacies in premenopausal metastatic BC patients with combined letrozole and goserelin therapy comparable to those in postmenopausal patients treated with letrozole alone. They also showed that letrozole+ goserelin resulted in a modest increase in bone resorption.⁶⁵ Another single-arm phase II study in premenopausal women showed that letrozole as an adjuvant therapy induced side effects together with other treatments, by evaluating the feasibility of administering 2 years of ovarian suppression with letrozole to patients with BC who remained premenopausal after adjuvant tamoxifen. This study closed due to poor accrual over 3.5 years, and a quarter of enrollees stopped treatment due to toxicity. Extended therapy with GnRH-a and an aromatase inhibitor (plus optional bisphosphonate) is associated with substantial side effects in premenopausal women who have already completed > 4.5 years of adjuvant tamoxifen.⁶⁶

1.3 Low Calcium Diet (LCD) and BC

1.3.1 Calcium as a Growth Factor for BC Metastatic Tumor in the Bone

The bone microenvironment serves as the soil, once cancer colonized in this niche, the soil produces growth factors to create an environment conducive for tumor to grow. On the other hand, this is rather a two-way communication than a single-way monologue. BC cells produce regulating factors in this fertile environment, facilitating their growth in this secondary site.⁶⁷ Micrometastasis thus forms, when BC cells begin to proliferate in this new site.⁶⁸

Growth factors secreted from the bone microenvironment include TGF, IGF-1, FGF, PDGF, BMPs, cytokines, chemokines, and cell adhesion molecules. Calcium ions are also among these important factors secreted from the bone to promote tumor growth. The high extracellular calcium concentration provides a physical environment favorable for tumor growth.⁶⁷ Besides, these growth factors from the mineralized bone matrix can also feedback to promote further production of osteolytic and osteoblastic factors from the bone.⁶⁹ Concurrently in this process, cancer cells secrete factors to increase bone resorption. These growth factors from cancer cells include PTHrP, which mimics the action of PTH, interleukin-8, and MIP1 alpha in multiple myeloma.⁶⁸

Tumor metastasis in the bone involves changes on the network of gene and protein expressions, such as matrix metalloproteinases, interleukin-6, Jagged 1–Notch, GLI2, RUNX2, hypoxia-induced growth factor 1 α , calcium and the calcium-sensing receptor.⁶⁹

1.3.2 Clinical Trials on LCD and BC

Su X. *et al.* studied the association between calcium intake during adolescence and benign breast tissue, which is a marker of increased breast cancer risk, and did not find an association.⁷⁰ Although it was previously reported that calcium may have anticarcinogenic properties including regulations on cell differentiation, proliferation and apoptosis, yet Anderson L.N. *et al.* did not find a significant association of calcium supplement intake and reduced breast cancer risk in pre- or post-menopausal women, but observed a significant inverse trend.⁷¹ In a case control study in Japan, Kawase T. *et al.* found that calcium intake is protective against breast cancer risk in postmenopausal women only, and the association is modified by tumor receptor status (significant only in ER+ and/or PR+/HER2 + postmenopausal BC and ER+ and/or PR+ /HER2- postmenopausal BC); while no association was found in premenopausal women.⁷²

In a large European prospective cohort study, Abbas S. *et al.* did not find any association between dietary vitamin D or calcium intake and BC risk; in postmenopausal women, there was a borderline significant inverse association ($P_{trend} = 0.05$).⁷³ They suggested that since blood calcium level in humans is tightly regulated, it may not be a good marker indicating calcium

status or dietary calcium intake. Thus it is difficult to derive an association from dietary calcium intake and BC risk. They also mentioned that most cohort studies so far have suggested an inverse association between calcium intake and BC risk in premenopausal women only, but not postmenopausal women; while there are also studies finding no association at all.⁷³

It is still inconclusive regarding the evidence from clinical trials on calcium intake and BC risks among women. Some studies suggested an inverse trend despite no association was found among women⁷¹, while others found no overall association but inverse trend in premenopausal women; among postmenopausal women, some reported protective effects⁷², or borderline significant inverse association⁷³. Intriguingly enough, Almquist M. *et al.* conducted a prospective cohort study of 7,847 women and reported in 2007 that serum calcium level was inversely associated with BC risk in premenopausal women in a dose-response manner.⁷⁴ The same group conducted a prospective nested case-control study and reported in 2010 that serum calcium level was positively associated with BC risk in premenopausal women.⁷⁵

In the first study in 2007, they found no overall association between serum calcium levels and BC; while serum calcium levels were inversely associated with BC incidence in premenopausal women dose-responsively, but the p for trend was not significant ($p=0.25$). They also found that serum calcium rises with menopause: there was higher percentage of women in peri-postmenopausal stages, and these women are also in higher calcium quartiles. This may be explained by the fact that with declining body estrogen in these women, bone becomes more sensitive to PTH, and results in higher serum calcium.⁷⁴ In their second study in 2010, they had opposite findings that serum calcium was positively associated with BC risk in premenopausal women. However, they did mention that it was based on a small number of cases ($n=39$), and the confidence interval for the positive association was wide (1.33–7.22). They hence suggested that larger-scale prospective studies are needed for a robust conclusion.⁷⁵

In the second trial by Almquist M. *et al.*, they also examined the associations between PTH, vitamin D levels and BC risk, since blood levels of these two are closely related to calcium levels. PTH was suggested by experimental studies to have carcinogenic and tumor promoting effects; while vitamin D was shown to have tumor protective effects such as inhibiting invasiveness and angiogenesis. Since calcium levels in serum is associated, or maybe stimulated by PTH and vitamin D, the effects of calcium itself on BC seem quite inconclusive, though experimental studies suggest that high calcium level have a tumor protective effect. Besides, the disease of BC itself may cause hypercalcemia (hypercalcemia of malignancy), which adds difficulty to elucidate the association of serum calcium and BC risk. It was hypothesized that in postmenopausal women, serum calcium level may reflect more of PTH

level instead of vitamin D level. On the contrary, in premenopausal women, serum calcium more represents vitamin D level.⁷⁴

1.3.3 Animal Models in BC and Calcium Studies

Hu Z. *et al.* showed in an animal study that mice injected with BC cells into the left heart ventricle and developed bone metastasis had higher serum calcium levels than control mice. Basal calcium levels in normal sera were 7.18 ± 0.13 mg/dl; while mice that received tumor cells followed by buffer had significantly higher calcium levels: 13.33 ± 1.43 mg/dl ($p=0.0006$).⁷⁶

Animal models aimed to develop bone metastasis have included efforts to inject cancer cells into the heart, so that tumor cells can travel to the bone via circulation; or directly inject cancer cells to the bone. The second model has been recognized as having the advantage of excluding potential metastasis to other visceral organs which might be brought about in the first case.⁷⁷

1.3.4 Molecular Studies on Calcium and BC

Molecular studies examined the mechanisms of how calcium could modulate or interact with BC cells *in vitro*. D'Ambrosio J. *et al.* reported that osteoblasts can protect BC cells from cell death caused by increased cytosolic Ca^{2+} . This mechanism as part of the reciprocal interaction of tumor cells and bone microenvironment, can lead to macroscopic skeletal metastasis of BC.⁷⁸

Vitamin D and calcium insufficiency may cause impairment of VDR and CaSR signaling, lead to cellular dysfunction, and thus increase the risk of certain diseases, including BC.⁷⁹ Increased extracellular Ca^{2+} will activate CaSR signaling, and can either reduce cell proliferation (as reported in human colon cancer, or ovarian surface epithelial cells), stimulate cell growth (reported in malignant Leydig cells), or protect from apoptosis (reported in prostate cancer cells).⁷⁹ Functions of CaSR, together with VDR, have been implicated in how vitamin D and calcium can regulate neoplastic mammary gland cell growth *in vivo*.⁷⁹⁻⁸¹

As an intracellular messenger, calcium has been involved in different cell processes including proliferation, apoptosis and cell signaling. High calcium level in extracellular environment has an “estrogen-like” effect mediated through the calcium sensing receptor (CaSR) and even involves estrogen receptor (ER). Yet there is quite inconclusive *in vitro* evidence so far regarding calcium and BC growth.⁷⁵

Molecular studies have suggested the involvement of calcium sensing receptor (CaSR) in the interaction or modulation of calcium on BC cells. CaSR functions to allow extracellular Ca^{2+} to enter the cells and participate in calcium signaling pathways. The Ca^{2+} /CaSR signaling is also closely linked to some functions of the vitamin D receptor (VDR) activated pathways, regulating

osteoblast and bone formation, inhibiting colorectal cancer cell proliferation, as well as inducing Ca^{2+} influx into BC cells and activating apoptosis signaling.⁸² CaSR is highly expressed in organs involved in the regulation of mineral ion metabolism in the body, such as the parathyroid, kidney, and bone. It is also expressed in the mammary gland⁷⁹, the gut, the vasculature and the lung.⁸³

CaSR has been closely related to BC bone metastasis. Mihai R. *et al.* examined the histology materials of 65 patients who died from metastatic BC, and found that CaSR is highly expressed in those patients who had bone metastasis than visceral metastasis.⁸⁴ Liu G. *et al.* found that CaSR is involved in how extracellular Ca^{2+} down regulated cell proliferation, invasion and growth of two human BC cell lines: the ER+ MCF-7 cells and the ER- MDA-MB-435 cells. Thus loss of CaSR may promote malignancy as they suggested.⁸⁵ Saidak Z. *et al.* reported that activation of CaSR via calcium is a necessary step and produces a strong chemoattractant effect on how extracellular Ca^{2+} modulates the migration of bone metastatic BC cells to a Ca^{2+} rich environment, such as those near the resorbing bone.⁸⁶

Studies also showed that calcium can even interact and activate ER following the activation of CaSR by calcium. Leclercq G. reported that high level of extracellular calcium, through interacting with CaSR could enhance ER α transcription and confer an active conformation to ER.⁸⁷ Divekar S.D. *et al.* identified several potential sites on the ER α ligand-binding domain for calcium to activate the receptor, and suggested that calcium can mediate the cross-talk between ER α activating signaling pathways.⁸⁸

Several other calcium channels were identified in how calcium can affect BC. Peters A.A. *et al.* found that plasma membrane calcium channel TRPV6 is overexpressed in some BC cell lines (ER negative), and also suggested that elevated expression of calcium channels and pumps is a characteristic of certain BC.⁸⁹ Britschgi A. *et al.* found that a calcium-activated chloride channel anoctamin 1 (ANO1) is amplified and highly expressed in BC cells and can promote BC progression.⁹⁰

1.4 HFD and BC

Several animal studies have linked HFD to increased mammary cancer development or BC tumor growth.^{91,92,93} Response to HFD in mice may be strain-dependent. BALB/c mice, referred to as obesity resistant in some studies, would have different metabolism and cancer related responses when fed HFD, compared with the C57BL/6 mice, which are more prone to weight gain on HFD.⁹⁴ Effects of HFD on BC may also depend upon sources of dietary fat. Plant source fat was indicated to reduce BC risk whereas animal source fat increased BC risk.⁹⁵

Western diet (WD) high in fat, sucrose and cholesterol has been introduced in animal models, especially in studies on metabolic syndromes. Studies have shown that western diet is linked with increased body oxidative stress,⁹⁶ or increased mammary carcinogenesis.⁹⁷ However, there is one study showing that a diet containing 5% typical anhydrous milk fat (representing ~70% of the total dietary fat component) fed to Balb/c mice delayed the appearance of subcutaneous 4T1 BC tumors and inhibited metastasis to the lung and liver, when compared to the control diet containing soybean oil as the only fat component. Instead of using HFD, they used a diet with fat content in the normal range. This study promoted using milk fat as an adjuvant to inhibit tumor metastasis during cancer chemotherapy, and to spare patients from debilitating side-effects of cytotoxic drugs.⁹⁸

1.5 HFD and Metabolism

1.5.1 HFD and Hepatic Tumorigenesis

HFD affects lipid metabolism in liver and energy homeostasis in the adipose tissue by modulating gene expressions. There seems to be an inherent link between liver lipid metabolism, body inflammatory state, and hepatic tumorigenesis. Itoh *et al.* reported that, after feeding mice with HFD for one year, there is chronic inflammation marked by increased macrophage infiltration and fibrotic changes in adipose tissue, leading to hepatocellular carcinoma.⁹⁹ Kampschulte *et al.* reported that feeding a western diet for around 9 months in ApoE^{xiii}-LDLR^{xiv} double-deficient mouse model of atherosclerosis led to hepatic steatosis, fibrosis, and tumorigenesis.¹⁰⁰ Tajima *et al.* also found liver tumorigenesis induced by HFD in C57Bl/6 mice with altered inflammatory cytokine gene expressions, such as MCP-1^{xv} and NADPH^{xvi} oxidase complex.¹⁰¹

1.5.2 HFD and Hepatic Lipid Metabolism

A number of studies in rodents reported that HFD modulates lipid metabolism in liver.^{102,103,104} However, more studies on HFD and metabolism were conducted in C57/Bl mice. Lipogenic genes, such as SREBP1c^{xvii}, PPAR γ , SCD1^{xviii}, CPT1a^{xix}, Hmgcr^{xx}, GPAT^{xxi}¹⁰⁵ and gluconeogenic genes, like PCK1^{xxii} and G6Pc^{xxiii} were usually target genes in these studies.¹⁰⁶ Genes regulating fatty acid metabolism were also measured in studies on HFD and liver lipids, including liver PPAR α and its downstream target medium-chain acyl-CoA dehydrogenase, and fatty acid oxidation genes including ACO^{xxiv}, AMPK^{xxv}, PGC-1 α/β ^{xxvi} and VLAD^{xxvii}.^{105, 107}

1.5.3 Hormones Modulated by HFD

In mammals, adipose tissue is a major site controlling fatty acid (FA) metabolism and energy homeostasis. White adipose tissue (WAT), as an endocrine organ,¹⁰⁸ secretes several cytokines, also known as adipokines, like leptin, adiponectin, resistin, IL6, and TNF- α , which

play important roles in FA metabolism and can be modulated by a HFD.¹⁰⁹ Among them, leptin functions to decrease food intake, increase energy expenditure, and inhibit lipogenesis.¹¹⁰ Another hormone carnitine transports CoA-activated fatty acid into mitochondria and out of peroxisomes. Higher plasma acetylcarnitine level reflects stimulated β -oxidation of fatty acids.¹¹¹ Besides FA oxidation, another mechanism that increases energy expenditure is brown adipose tissue (BAT^{xxviii})-mediated thermogenesis. Thermogenic genes in BAT include PGC1 α , PPAR γ , Cidea^{xxix}, protein kinase IKK ϵ ^{xxx}, and TIF2^{xxxi}.¹⁰⁹ Enhanced thermogenesis was reported to be modulated by up-regulation of UCP1 in BAT, PPAR α , PPAR γ , and PGC1 α in WAT.¹⁰⁹ PGC1 α regulates the expression of UCP1, which creates a proton leak in mitochondria that dissipates energy produced by oxidative metabolism.¹⁰⁹ Expression of UCP^{xxxii} can be tested in both BAT and WAT^{xxxiii}.¹¹² Other key regulators of adipocyte gene expression and differentiation, which could be modified by a HFD, also encompass C/EBP^{xxxiv}s, ADD1^{xxxv}, RXR^{xxxvi} isotypes, GATA^{xxxvii}, and KLF-4^{xxxviii}.

1.5.4 HFD and Energy Intake

Mice fed a HFD usually have increased energy intake (EI) and increased body weight (BW) than control. Increased thermogenesis in BAT is a mechanism by which rodents fed HFD can compensate for increased EI. In one study, female C57BL/6J mice received a low (10 kcal% fat), medium (45 kcal% fat), or high-fat diet (60 kcal% fat) for 12 weeks. Mice with greater resting metabolic rates (RMRs) also had greater food intakes (FIs), with an extent sufficient to offset the greater energy expenditure.¹¹³

However, studies also showed that mice on a HFD can have lower or comparable EI than control, while still maintaining higher body weight. With their incipient capability to regulate EI, mice could decrease FI and reduce EI when fed a HFD, to compensate for the greater energy density and higher apparent energy absorption efficiency (AEAE). Animals failing to match the adjusted intake to expenditure gained weight; while others showed resistance and maintained their body mass on a diet providing 60% calories from fat. Hambly *et al.* reported that a reduction in intake overcompensated for the increased energy and absorption efficiency of the diet so that animals actually absorbed less energy on HFD than on the relatively low-fat chow. There was no change in animal body weight over 3-week exposure to HFD, suggesting that those mice made additional modulations of their expenditure to balance their energy budgets.¹¹⁴ Ishii *et al.* reported that rats fed a HFD had a comparable calorie intake, yet higher body weight compared with control. In their study, rats on a control diet had an increased calorie intake over time, while those on a HFD had a slightly decreasing calorie intake.¹¹⁵

Several other studies on HFD and BC showed similarly lower EI in HFD animals. Lane *et al.* reported that diets high in fat, particularly fat as corn oil, promoted mammary tumors in rats treated with 7,12-dimethylbenz(a)anthracene (DMBA) or N-nitroso-N-methylurea. Tumorigenic effects of HFD seem to be the strongest during promotional phase of tumorigenesis; this effect may be enhanced by high body weight. In their study, Balb/c mice fed HFD consumed significantly less food, had a decreasing and lower EI, and lost more body weight during DMBA treatment than control.¹¹⁶

Lane *et al.* also suggested that organisms can react to reductions in EI by reducing their basal energy level, activity level and growth rate. In their study, energy consumption was highest in standard diet-fed groups followed by HFD-fed groups. They also mentioned it was previously reported that sedentary rats fed a HFD consumed less energy than sedentary rats on a standard AIN-76A diet. Besides, consumption of HFD may induce thermogenesis, which would affect tumor incidence.¹¹⁷

1.5.5 HFD and Energy Expenditure

Haramizu *et al.* pointed out that body weight increase induced by high-fat feeding in their study was related to reduced energy expenditure, higher respiratory quotient, and lower fatty acid beta-oxidation in liver. They tested genes regulating fatty acid uptake and oxidation, such as PPAR α , PPAR γ , PPAR δ and their co-activator PGC-1 γ . Among them, PPAR α is predominantly expressed in liver, and its activation up-regulates beta-oxidation enzymes, resulting in reduced body fat accumulation. By comparing two mice strains, they found that BALB/c mice had higher liver PPAR α , MCAD and UCP2 mRNA levels than C57BL/6J mice.¹¹⁸

Vaanholt *et al.* reported that mice reduced food intake and increased body fat mass and plasma leptin levels on HFD. They had elevated daily energy expenditure, increased spontaneous cage activity and higher RMR on HFD than standard chow diet. Compared to chow diet group, HFD females had lower food intake and yet higher body weight. Their food intake was initially decreasing over time and later became stable. They concluded that mice on HFD obtained more energy with greater food efficiency.¹¹⁹

Satyanarayana *et al.* found that ablation of the *Id1* gene, the protein of which is highly expressed in BAT and WAT and was suggested to have a role in adipogenesis, enhanced energy expenditure and improved insulin sensitivity. Other potential target genes affected by HFD on energy expenditure include critical regulators of adipocyte gene expression and differentiation, like CCAAT/enhancer binding proteins(C/EBPs), PPAR, adipocyte differentiation determinant-dependent factor 1(ADD1), retinoid X receptor(RXR) isotypes, GATA, and KLF-4.

Key regulators of mitochondrial energy production and/or lipid mobilization also include protein kinase A regulatory subunit 2 alpha (RII alpha), adipose triglyceride lipase (ATGL)¹²⁰, as well as genes involved in mitochondrial oxidative phosphorylation (COX1) and β -oxidation (CPT1b, PDK4, and FABP3).¹²¹ Elevated expression of PGC-1 α is a hallmark of BAT, which is specialized for consumptive metabolism of thermogenesis. Fatty acid transporter 1 (FATP1) is also reported as a critical regulator of BAT metabolism.¹²⁰ General adipogenic markers, such as aP2 and adiponectin (AdipoQ) could also be affected by a HFD.¹²¹

1.5.6 Obesity Caused by HFD

When animals were fed high-fat diet for 20 weeks, mMCP6, F4/80, and cleaved caspase-3 gene expressions were increased in C57BL/6 mice, while adiponectin, leptin, IL-6, and MCP-1 gene expression levels were lower in epididymal fat of obese than lean mice. TNF- α and IL-10 gene expression were higher in epididymal fat of obese mice. Cytokines, like tumor necrosis factor- α (TNF- α), interleukin-6 (IL-6), interleukin-10 (IL-10), and monocyte chemoattractant protein-1 (MCP-1) have profound effects on metabolism.¹²² In another study by Morita *et al.*, mRNA levels of energy metabolism-related IGFBP1 was tested in hepatocytes.¹²³

1.6 4T1 and 4T1.2 cell lines

1.6.1 4T1 cell line

The murine 4T1 BC cell line used in our experiments was originally isolated from the Karmanos Cancer Institute, and has been extensively used in animal studies on BC, especially stage IV BC, due to its strong capabilities of metastasis to lungs, liver, bone and other sites.¹²⁴

4T1 cells have been regarded as one of the best models to study late stage BC.^{124,125} Unlike some previous studies using xenograft human BC cells on immuno-compromised athymic nude mice, where their immune functions were totally disrupted; with 4T1 cells, immunocompetent Balb/c mice can be used as hosts.¹²⁶ Once injected into Balb/c mice, 4T1 multiply rapidly and develop metastases aggressively and spontaneously metastasize to lung, lymph nodes, liver, bone, and other sites in a pattern analogous to human BC.¹²⁶

The current laboratory group has been studying effects of different phytoestrogens on BC growth in mouse model for years. It is of great concern whether the cell line is estrogen responsive in studies of BC in response to either a diet containing phytoestrogens or a drug/agent that can modulate body estrogen level. In the first project, effects of letrozole (an aromatase inhibitor) on BC metastasis were studied and thus the estrogen responsiveness of 4T1 cell line needs to be considered. In vitro studies showed that 4T1 cells are E2 non-responsive.¹²⁷ Estrogens can affect tumor growth and metastasis by interacting with the secondary organs hosting metastatic BC tumors, such as bone and lung.^{128,129} Hence in our

study the involvement of the microenvironment in the context of BC growth and metastasis should be considered.

The 4T1 cell line is among the clonal lines derived originally from a spontaneously arising mammary tumor in a Balb/cfC3H mouse. Compared with other clonal lines that were either non-metastatic (67NR), or metastasized only to lung (66cl4), 4T1 cells metastasized to liver in addition to lung. Tester *et al.* established a murine model to investigate BC metastasis to bone by injecting 4T1 cells into the mammary gland of mice. Among the first to show spontaneous metastasis of BC cells from the primary site to bone, their model closely mimics the pattern of metastatic spread observed in human BC. According to this study, their model provides a more complete representation than existing models that require the cancer cells to be injected into the arterial system via the left ventricle or directly into the tibia to induce bone metastasis.¹³⁰

1.6.2 4T1.2 cell line

Lelekakis M *et al.* reported that clonogenic cells can be detected in spines of 4T1 bearing mice.¹³¹ The highly metastatic 4T1.2 cell line is derived from single cell cloning of its parental cell line, 4T1.¹³¹ The 4T1.2 cells metastasize to the bone, and reproducibly form metastases in numerous sites in addition to bone following orthotopic inoculation into the mammary fat pad.¹³⁰

4T1.2 cells are highly metastatic to lymph nodes, bone, lungs and other organs, and were originally selected based on its aggressive properties. Similar as its parental line, 4T1 cells, the advantage of the model using 4T1.2 cells is that immunocompetent mice can be used, in contrast to xenogeneic tumor models that utilize athymic nude mice or other immunocompromised animals.¹²⁶ Thus 4T1.2 cells provide a rare and valuable model that closely resembles the events that occur in metastatic BC in humans, with spontaneous metastasis from the mammary gland to distal sites, including spine and femur.¹³² In one study, Matrigel invasion in Boyden chamber was progressively higher in the more metastatic lines 4T1.2, together with higher MMP-2 activation potential, MMP-9 secretion, and migration over either type I or IV collagen than other BC cell lines.¹³⁰

Chapter 2 Effects of Letrozole on Breast Cancer Micro-metastatic Tumor Growth in Bone and Lung in Mice Inoculated with Murine 4T1 Cells

Abstract

Breast cancer (BC) is the leading cancer in women worldwide. Metastasis occurs in stage IV BC with bone and lung being common metastatic sites. Aromatase inhibitors (AI) like letrozole suppress the conversion of androgens to estrogens and inhibit estrogen-responsive mammary tumor growth. The goal of this study was to evaluate the effects of letrozole on BC micro-metastatic tumor growth in bone and lung metastasis in intact and ovariectomized (OVX) mice with murine estrogen receptor negative (ER-) BC cells inoculated in tibia. Forty-eight BALB/c mice were randomly assigned to one of four groups: OVX, OVX+Letrozole, Intact, and Intact+Letrozole, and injected with 4T1 cells intra-tibially. Letrozole was subcutaneously injected daily for 23 days at a dose of 1.75 µg/g body weight. Tumor progression was monitored by bioluminescence imaging. OVX mice had lower serum estradiol than intact mice and greater tumor area and integrated density in the inoculated limb on D14 and D17. Letrozole decreased serum estradiol levels and reduced lung surface tumor numbers in intact animals. Mice receiving letrozole had significantly fewer tumor colonies and fewer proliferative cells in the lung than OVX and intact controls based on H&E and Ki-67 staining, respectively. In conclusion, tumors were larger with greater integrated density in inoculated limbs of OVX animals and letrozole reduced BC metastases to lungs, suggesting that though 4T1 cells are considered estrogen unresponsive, by lowering systemic estrogen level and possibly through interacting with the host organ, breast cancer metastasis to the lung was still effectively reduced by the aromatase inhibitor letrozole.

Introduction

Breast cancer (BC) is the leading cancer type in women worldwide, and the second in estimated deaths.¹ Stage IV BC is the most advanced stage, in which cancer cells metastasize from the original site to distant tissues, such as bone, lung and liver. The invasiveness and metastatic spread of tumor cells are responsible for most of the morbidity and mortality associated with BC, and are considered as the primary cause of cancer treatment failure.¹² In general, BC therapies often fail in advanced stage BC, after metastasis has already occurred.³ Considered as a filter between primary tumor and other secondary sites, lung typically contains metastatic BC at autopsy.¹³ Bone is another frequent site for BC metastases.¹³³ Once BC metastasizes to bone, bone destruction occurs, inducing higher risk of fracture, hypercalcemia, paralysis due to spinal cord compression, and associated bone pain in BC patients.^{133,134}

Occult BC tumors are commonly present in BC patients. Also 7% of women that have died from unrelated causes had small, occult, undiagnosed BC in situ in breast at autopsy.¹³⁵ Micro-metastatic BC cells, also known as disseminated tumor cells, can stay dormant in bone for years.¹³⁶ These metastatic cells were found in the bone of up to 80% of patients who died from BC, and skeleton is the second largest reservoir for BC metastasis after lymph nodes.¹³⁷ Braun *et al.* reported that 30% of BC patients had bone micrometastasis at diagnosis of BC, and these patients often had larger tumors and hormone receptor-negative BC.²⁹ To understand why metastatic BC cells specifically harbor in certain organs like bone and lung, the intriguing interaction between host organ and tumor cells needs to be considered.¹³⁸

Estrogens play a critical role in the development and progression of BC. About 70% of BCs express estrogen receptors (ER). Estrogens interact with ER alpha (ER α) and beta (ER β) to mediate BC cell growth through distinct mechanisms.¹³⁹ The majority of patients with BC are postmenopausal women. Most estrogens (estrone and estradiol) in postmenopausal women are synthesized from androgens (androstenedione and testosterone) at extragonadal sites, including breasts, and exert their effects locally.^{35,41} This led to the development of a third-generation BC therapy, aromatase inhibitors (AIs), which inhibit the enzyme aromatase converting androgens to estrogens. AIs are currently the most widely prescribed hormonal therapy for postmenopausal women with early stage or advanced ER+ BC.¹⁴⁰

Among the third generation aromatase inhibitors, letrozole is one of the most effective therapies for lowering estrogen in the breast tissue and plasma. It decreased estrone, estradiol, and estrone sulfate by 98.8%, 95.2% and 98.9% respectively in postmenopausal BC patients.^{141,142} *In vitro* and *in vivo* studies indicate that letrozole inhibits tumor growth. In ER+ MCF-7 cells, it suppressed cell proliferation and inhibited type IV collagenase expression,

through a mechanism possibly involving other estrogen-dependent pathways besides inhibiting aromatase, and was suggested as of value in suppressing mammary tumor growth and invasiveness.¹² In clinical trials, letrozole reduced distant metastases risk among BC patients.^{141,143} However, there are reported side effects from this drug, including bone loss.^{58,59} In this study, the effects of letrozole on BC metastasis were evaluated by using intact and ovariectomized (OVX) mice as models for pre and post-menopause, respectively.

BC cells not expressing ER, progesterone receptor or HER2 are considered “triple negative” cells. Women bearing this kind of tumor were usually diagnosed at a later stage, with a more aggressive phenotype and poorer survival rate regardless of stage.¹⁴⁴ Based on the fact that postmenopausal women with ER- BC cannot be effectively treated with antiestrogen tamoxifen, a generally accepted view regarding ER- tumors is that they do not respond to estrogen, unlike estrogen responsive ER+ tumors.¹²⁸ It is of importance to note that in the current study, 4T1 cells are triple negative (ER-, PR-, HER2-). However, we and others have observed an enhancement of whole animal estrogen action on BC metastasis with ER- 4T1 tumor cells, which is likely due to an overall systemic estrogenic effect that alters the microenvironment of organs and allows ER- tumor to grow.^{145,6}

The murine model utilized in this study aims to mimic late stage BC in female patients by implanting a small number of metastatic murine mammary tumor cells into the marrow cavity of tibia to model a micrometastatic lesion. Subsequent lung metastasis was evaluated. Based on prior studies on letrozole and ovariectomy, the hypothesis is that ovariectomy will increase tumor growth in bone, while letrozole will reduce BC metastases to lungs. To assess this, BC growth in the bone micro-metastatic site and lung metastases in live animals was monitored via Bioluminescence Imaging (BLI), examined effects of ovariectomy and letrozole on circulating estradiol levels, and tumor nodule count on lungs. Furthermore, lung tumors were analyzed with H&E and Ki-67 staining. Our results suggest that ovariectomy increases BC tumor growth in bone, while letrozole reduces BC metastases from bone to lungs in mice inoculated with murine 4T1 cancer cells.

Materials and methods

Materials

Murine 4T1 cells tagged with firefly luciferase were provided by Dr. David Piwanica-Worms (Washington University, St. Louis, MO). Heat-Inactivated Fetal Bovine Serum (HI-FBS) was purchased from Atlanta Biologicals (Lawrenceville, GA). Modified IMEM, Penicillin/Streptomycin, Fungizone, and Trypsin-EDTA were purchased from Invitrogen (Carlsbad, CA). L-Glutamine was purchased from Sigma Chemical Co. (St Louis, MO). MatrigelTM matrix was purchased from BD Biosciences (San Jose, CA). AIN-93G pellet diet was purchased from Research Diets (New Brunswick, NJ). D-luciferin potassium salt was purchased from Regis Technologies (Morton Grove, IL). Isoflurane was purchased from Baxter Healthcare Corporation (Deerfield, IL). India ink was purchased from Sanford (Bellwood, IL).

Cell culture

4T1 murine mammary cancer cells were cultured with IMEM, supplemented with 10% HI-FBS, 100 unit/mL Penicillin, 100 µg/mL Streptomycin, 1% L-Glutamine, and 0.1% Fungizone in a humidified incubator containing 5% CO₂ at 37°C. Cells were harvested at 70% confluence, centrifuged (0°C, 700 rpm, 5 minutes), and resuspended in Matrigel^{TX} for injection.^{3,146}

BALB/c mice

Forty-eight female BALB/c mice (intact) were purchased from Charles River Laboratories (Wilmington, MA). Mice were 7 months of age when cancer cells were injected into their tibia. During the study, animals were singly caged and maintained under the standard light-dark cycle (12 h light and 12 h dark), with *ad libitum* access to food and water. All studies were carried out under animal experiment protocols approved by the Institutional Animal Care and Use Committee (IACUC) at the University of Illinois at Urbana-Champaign.

Methods

Mice were randomly assigned to 1 of 4 groups (n=12/group): OVX, OVX+Letrozole, Intact, and Intact+Letrozole. The OVX and OVX+Letrozole groups were ovariectomized and inoculated with 4T1 cells. The Intact and Intact+Letrozole groups were inoculated with 4T1 cells. Each animal in the Intact+Letrozole group and OVX+Letrozole group was injected daily with the drug subcutaneously at a dose of 1.75 µg/g body weight for the 3 week duration of treatment. Dosage of letrozole (40 µg per day) was determined based on the results of a pilot study performed in our laboratory showing that lower doses were ineffective. The dose chosen in this study is in the range (10-50 µg per day) reported in the literature.^{49,147-152} Mice were ovariectomized in our facility following procedures as previously described.¹⁵³ Letrozole treatment was initiated on postoperative day 1 and continued until the end of the study. Letrozole (0.4 mg/mL) was made in dimethyl sulfoxide

(0.08%), ethanol (0.8%) and 0.3% HPC-PBS (99%). Animals were weighed once a week and prior to sacrifice. Mice were sacrificed with CO₂ asphyxiation.

Intra-tibial injection

Mice were anesthetized with isoflurane/oxygen and placed in a supine position during operation. After an incision was made on the right knee of the animal, 1,000 4T1 cells suspended in 2.5µL Matrigel™ were inoculated. A 26-gauge needle connected to a syringe was first inserted into the bone marrow cavity to create space for the subsequent injection, and then replaced by a 27-gauge for injection. The incision was sealed with tissue adhesive (3M Vetbond) and closed with a surgical staple. Banamine (2.3 µg/g body weight) was subcutaneously administered at surgery and 12 hours post-surgery for pain relief.

Bioluminescence imaging

Mice were injected with 15 mg/mL luciferin dissolved in PBS at a dose of 10 µL luciferin per gram of body weight 3 minutes prior to BLI. Each mouse was anesthetized with continual administration of isoflurane gas from an inlet tube and imaged with BLI twice per week. The whole body scan of one mouse takes three minutes. BLI signals were detected by a camera set inside of the imaging unit. Pictures taken by the camera were transferred to a computer. Images and movies were acquired and compiled by the Piper Control software (Stanford Photonics, Palo Alto, CA). Images obtained were later analyzed by the software Image J (NIH, Bethesda, MD) and Photoshop Elements (Adobe, San Jose, CA). The background image of the mouse body was combined with the image showing only the luminescence of the tumor. Tumor area and integrated density (the product of area and the intensity of luminescence) on the bone were analyzed using ImageJ.

Serum collection

Venous blood was collected from each animal from inferior vena cava, allowed to clot at room temperature, and centrifuged to separate serum, which was frozen and stored at -20°C until analysis. Serum concentrations of E2 were measured using LC/MS/MS since typical immunochemical approaches are known to be unreliable for very low physiological levels of E2, like those present in OVX females. Method details and validation were previously published.¹⁵⁴ Briefly, 10-100 µL aliquots of individual mouse serum samples were subjected to liquid-liquid extraction, dansyl chloride derivatization, and isotope dilution LC/MS/MS analysis. The limit of detection (LOD) for E2 was 1.5 pg/mL (5 pM). When calculating group mean values, samples <LOD were replaced with a value of 0. Using a value of 1/2LOD (0.8 pg/mL) for those samples <LOD was also tried. There is no difference in statistical analysis result between these two methods. All analyses were performed without an enzymatic hydrolysis step using B-

glucuronidase/arylsulfatase, so only “free” (i.e., active, unconjugated) E2 concentrations were obtained.

India ink staining

Lungs of mice were perfused with India ink to stain the lobes and visualize the tumor following the method described by Wexler.^{155,156} Briefly, ribs were cut to expose the lung and trachea, and India ink was slowly injected into the lung via trachea until the lung fully expanded. The fully infused lung was harvested and fixed in fekete solution (90% of 70% EtOH, 9% of 37% formaldehyde, and 1% of 9% acetic acid). After being kept in fresh fekete solution for 24 hours, tumor nodules on lung lobes were counted by three individuals. Tumors were distinguished as white extrudates not being stained while normal lung tissue was stained black. The mean value of the three individuals' counts is reported.

Histopathological analysis

Lung sections were embedded in paraffin, trimmed and sliced into 5 µm slices. Each slice was mounted on a glass slide, and tissue slides were deparaffinized, rehydrated, and stained with H&E. Stained tissues were observed under the 5X objective of an AxioSkop 40 microscope (Carl Zeiss, Thornwood, NY), and photographed using Axio Cam HRc (Carl Zeiss, Thornwood, NY). Tumors on each slide were counted and tumor area was determined using the software ImageJ. Tumor area percentage on the lung from each animal was calculated by dividing the total tumor area (with individual tumor area added together) by the total area of lung lobes.

To evaluate proliferative cell percentage by Ki-67 staining, deparaffinized and rehydrated tissue slides were incubated with anti-Ki-67 antibody (Pharmingen, San Diego, CA) and biotinylated secondary antibody (Vector Laboratories, Burlingame, CA). Slides were then stained by diaminobenzidine substrate and counter stained by hematoxylin. Proliferating cells expressing Ki-67 were stained brown and were considered as positive cells. By contrast, cells stained blue by hematoxylin were considered as negative cells. The immunostained slides were photographed under an AxioSkop 40 microscope and Axio Cam HRc. Tumor images were analyzed using Adobe Photoshop Elements. To assess the percentage of proliferating cells, the proportion of Ki-67-positive nuclei was determined. According to H&E staining results, four animals with the H&E tumor count most close to the group average were selected from each group. Ki-67 stained positive and negative cells were counted on slides of these four animals, with at least 24 viable tumor areas evaluated under high-power (40X objective) fields.

Statistical Analysis

All parametric data, including BLI tumor area, integrated density, uterine wet weights, serum estradiol level and proliferating cell percentage from Ki-67 staining were analyzed using ANOVA

Two Way by SAS GLM procedure to determine the significant difference between groups. The non-parametric tumor colony numbers on lungs stained with India ink were analyzed using Wilcoxon rank sum test. Tumor numbers by H&E staining, also as non-parametric data, were analyzed using the Poisson model. All data are reported as mean \pm SEM. All hypotheses were tested in a two sided way and significance was set at $p < 0.05$. All statistical tests were done in SAS (SAS Institute, Cary, NC).

Results

Ovariectomized mice had larger tumor area and stronger integrated density in the bone

BLI is proven as effective to monitor tumor growth and progression and determine an appropriate ending point of a study.⁶ Tumor progression was evaluated by BLI on day 4, 7, 10, 14, 17, 21, and 23. Representative BLI images (Figure 2.1) show that while there was primary tumor growth in situ in tibia, no metastasis to the lung occurred until on Day 7 in most animals (Figure 2.2). Most of mice started to show metastases to lungs on Day 17. By day 23, the lung tumors had grown into a large luminescent area in most of the animals (Figure 2.1). OVX mice had greater BLI tumor area and integrated density of the micrometastatic bone tumor compared with intact animals on both Day 14 and Day 17 (Figure 2.2), whereas there was no difference on either tumor area or integrated density on other days from BLI (Figure A.1).

Ovariectomy lowered serum estradiol level; letrozole lowered estradiol level in intact mice

Serum estradiol in Intact group was significantly higher ($p < 0.05$) than Intact+Letrozole group (Figure 2.3). Ovariectomy significantly decreased serum estradiol level, consistent with uterine wet weight measured during necropsy that OVX mice had significantly lower uterine weight than intact animals (data not shown). Serum estradiol levels of mice in OVX+Letrozole group were all below the detection level (1.5 pg/mL) and thus recorded as 0.

Letrozole reduced metastatic progression of 4T1 cells to lungs in intact mice

Tumor colony numbers on lungs stained with India ink were counted to assess severity of lung metastases. Lungs stained with India ink harvested during necropsy show that several animals had severe lung metastasis, with many visible tumor nodules spread on the outer surface of the lung. This observation was consistent with our findings from BLI images. Tumor colony numbers of Intact+Letrozole group were significantly lower ($p < 0.05$) than that of Intact group; while there was no significant difference in OVX animals (Figure 2.4). There was no difference in lung surface tumor numbers between OVX and intact animals.

Letrozole reduced metastatic progression of 4T1 cells to lungs in both OVX and intact mice; Intact mice had more lung tumors than OVX mice.

Tumor numbers and tumor areas were analyzed in histological lung sections stained with H&E to assess the severity of lung metastasis. Tumor numbers in H&E stained lungs in OVX+Letrozole group were significantly lower ($p < 0.05$) than OVX group (Figure 2.5 a). A similar pattern was observed in intact mice that there were fewer ($p < 0.05$) tumors inside the lung of

Intact+Letrozole group compared with Intact (Figure 2.5 a). Noticeably, Intact group had a higher tumor number than OVX group. There was no significant difference in tumor area percentage on lungs among different groups (Figure A.2).

Letrozole reduced tumor proliferation in lungs in both OVX and intact mice

Proliferative cells on lung tumors were analyzed with Ki-67 staining to show cancer cell proliferation in the lung. Letrozole was found to reduce lung tumor proliferation in both OVX and intact mice. There is a significant major effect from letrozole in reducing tumor proliferation, which means the proportion of Ki-67 positive cells, positively stained brown compared to the negatively blue-stained cells, in the lungs of mice treated with letrozole was significantly lower than mice not treated with the drug, irrespective of OVX status (Figure 2.6 a).

Discussion

Microenvironment is important in determining whether cancer cells of a given molecular phenotype would be supported or inhibited during metastasis.²³ As pointed out by Stephen Paget in the seed and soil theory in 1889, cancer cells metastasize to distinct organs and tissues dependent on specific characteristics of the cells, the blood flow pattern and local environment of those secondary sites.¹⁵⁷ As a complex process, metastasis involves interactions between both 'seed' and 'soil', and cannot be solely explained by circulatory routes. For cancer cells to survive and proliferate, secondary organs need to provide a conducive environment with enough 'nutrients' and appropriate conditions.¹⁵⁸ Among them, bone and lungs are two primary metastatic organs for late stage breast carcinoma.¹⁵⁸ It was reported that BC cells can adhere to bone marrow stromal cells. Cytokines and growth factors from hematopoietic microenvironment via autocrine and/or paracrine secretion provide fertile 'soil' for tumors to grow in the local environment.¹⁹ The current study is the first to evaluate effects of letrozole on ER- BC micrometastatic tumor growth in bone and subsequent lung metastases in mice. In this study, OVX mice had larger tumor area and greater integrated density in bone on D14 and D17 compared with intact mice (Figure 2), due potentially to a more susceptible environment for BC to grow in the bone of OVX animals.

There are many growth factors released during osteoclast-mediated bone resorption, which constantly takes place in the bone environment of OVX mice. For example, TGF- β is one of the factors involved in aiding BC progression. Muraoka *et al.* reported that 4T1 cells express TGF- β receptors and blockage of TGF- β inhibits 4T1 cell migration and bone metastases.⁴⁶ Masri *et al.* found that sensitivity of TGF- β signaling was compromised in letrozole-resistant BC cells.⁴⁵ According to Wilson *et al.*, in post-menopausal women, there is a predilection for tumor cells to stay in bone with activated TGF- β and activin signaling.²⁴ In a post-menopausal bone environment, higher levels of TGF- β and activin are present due to significantly decreased inhibin, estrogen and progesterone, which leads to upregulated CXCL4 and bone-derived growth factors, leading to an environment susceptible for BC in the bone. In contrast, in premenopausal women, higher levels of inhibin, estrogen and progesterone would impair the signaling pathway by inhibiting bone resorption-mediated TGF- β and activin release.²⁴

Metastatic tumors in the lung were rather sporadic and variable with regard to tumor area and density measured by BLI. As previously pointed out,^{159,160} BLI is a semi-quantitative measurement and to evaluate lung metastasis, histopathology analysis was needed. It is found in this project that letrozole reduced lung metastasis, likely due to systemic decrease of estradiol by the aromatase inhibitor, as well as modulations of host cell interactions on the

secondary metastatic site - lung.^{127,128} As is known, ER+ mammary tumor growth is stimulated by estrogens. Previously our group reported that phytoestrogens, such as genistein, stimulate growth of human BC cells in mice with plasma estradiol concentrations comparable to those found in postmenopausal women, and can even negate the inhibitory effect of letrozole on human BC cell growth *in vivo*.^{4,5} Dietary daidzein was also found to significantly stimulate human mammary tumor growth in mice.¹⁶¹ Using an experimental metastasis model, our previous study showed that estradiol stimulated ER- BC metastasis in mice.⁶

Murine 4T1 BC cell line was originally isolated by Fred Miller and colleagues and have been used in BALB/c mice or tissue culture.¹⁶² Due to high frequency of metastasis to lung, liver, bone and other sites, 4T1 cells have been widely used in animal studies of BC, especially stage IV BC.¹²⁴ The syngeneic nature of this cell line enables both innate and acquired immune responses in mice, providing an advantage over human originated BC cells used in immunocompromised mice for metastatic BC studies. Additionally, 4T1 cells multiply rapidly and develop metastases aggressively once injected into BALB/c mice. For the above-mentioned reasons, 4T1 cells have been regarded as a useful model to study late stage BC.^{124,125}

Previously, we demonstrated that estrogens and phytoestrogens stimulate ER+ BC primary tumor growth in mice.^{4,5} In this study, letrozole significantly lowered serum estradiol levels, consistent with some previous studies. In a clinical trial, letrozole reduced serum estrone and estradiol to nearly undetectable levels.¹⁶³ To evaluate effects of letrozole on BC metastases to lungs, lung surface tumor nodules were counted, and there were fewer tumors on the lung in Intact+Letrozole group than Intact group. H&E staining showed that letrozole reduced metastatic progression of cancer to lungs in both OVX and intact mice. The intact group had the highest tumor numbers, probably resulting from higher estrogen level, which is consistent with higher uterine weight (data not shown). Ki-67 protein expression in cell nuclei indicates proliferating cancer cells. A previous study from our laboratory reported that dietary soy isoflavones, including genistein, daidzein, equol and a mix of isoflavones increased breast cancer lung metastasis by increasing Ki-67 expression in the lung metastatic tumors.⁵¹ In the present study, it was demonstrated that the aromatase inhibitor letrozole lowered proliferative cell percentages in lung tumors possibly by lowering estrogen levels, consistent with previous findings in our group on how estradiol and soy isoflavones increased proliferative cell percentages on lung metastatic tumors in a similar model utilizing murine 4T1 cells.^{6,51} We hence propose that letrozole can reduce lung metastasis of ER- 4T1 cells, by decreasing tumor proliferation in both intact and OVX mice.

In vitro studies showed that 4T1 cells are E2 non-responsive.¹²⁷ Using RT-PCR, Michigami *et al.* presented ER β gene expressions in 4T1 cells.¹⁶⁴ Estrogen was reported to promote the growth of ER- cancers by acting on cells distinct from tumors to stimulate angiogenesis.¹²⁸ Iyer *et al.* found that estrogen can promote the outgrowth of murine xenograft tumors established from patient-derived ER- BC cells by influencing the mobilization and recruitment of proangiogenic bone marrow-derived myeloid cells.¹²⁹ Furthermore, E2 increased tumor burden in lungs of mice injected with E2 non-responsive 4T1 cells by influencing host cells instead of cancer cells.¹²⁷ Signaling pathways other than ER mediated ones were reported as involved in ER- BC metastasis, including ER coregulator-PELP1,⁴⁸ and aryl hydrocarbon receptor (AHR) pathways.¹⁶⁵ In distant BC metastasis, receptor conversions were also reported. Receptor phenotypes in metastatic tumors differ from its original tumor phenotypes.¹⁶⁶ In the current study, letrozole may have modulated BC lung metastasis by directly acting on the metastatic site, lung.

Although 4T1 cells are considered as triple negative, pulmonary endothelial cells, however, do express ERs.^{127,167} Compared with mice uterine and MCF-7 tumors, which highly express ER α , lung was not a major organ with ER α expression (data not shown). Yet ER β is reported as predominant in the lung.¹⁶⁸ As reported in previous studies, host-cell interactions including the process of estrogens binding with ER on the lung may be involved in how letrozole reduces lung metastasis, besides its systemic effect on lowering estrogenic activities.

In summary, letrozole was effective in reducing BC metastases to lungs in mice inoculated with murine 4T1 cancer cells in the tibial marrow cavity. There were larger tumor areas and higher integrated density in bone on D14 and D17 in OVX animals. Both ovariectomy and letrozole lowered serum estradiol levels. Letrozole decreased tumor numbers on lungs by significantly reducing cell proliferation. Therefore, letrozole can be a potent agent to reduce ER- BC metastases. The model developed in this study can be further used to evaluate effects of other agents on bone micrometastatic tumor growth and lung metastases in mice.

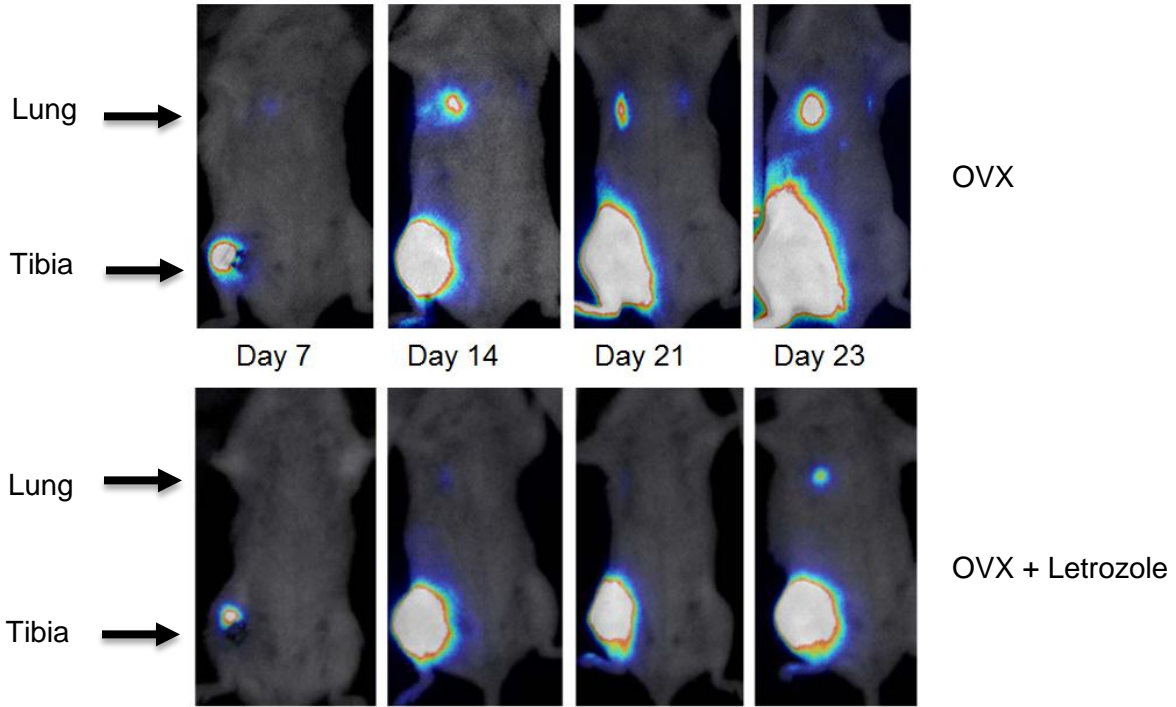
Acknowledgments

We thank the funding sources of this project as below: NCCAM BRC (P50 AT006268), DOD Breast Cancer Research Program from U.S. Army Medical Research and Materiel Command (W81XWH-09-1-0689; BC085882). The views expressed in this paper do not necessarily reflect those of the U.S. Food and Drug Administration.

Figures

Figure 2.1

(a)



(b)

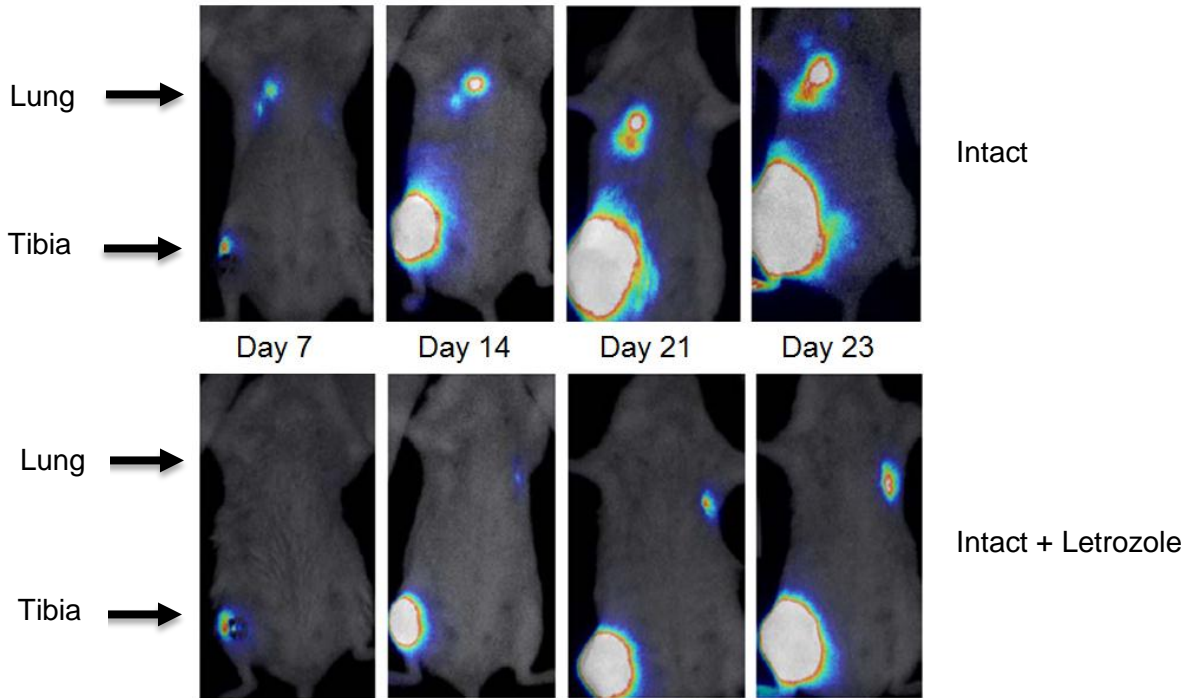
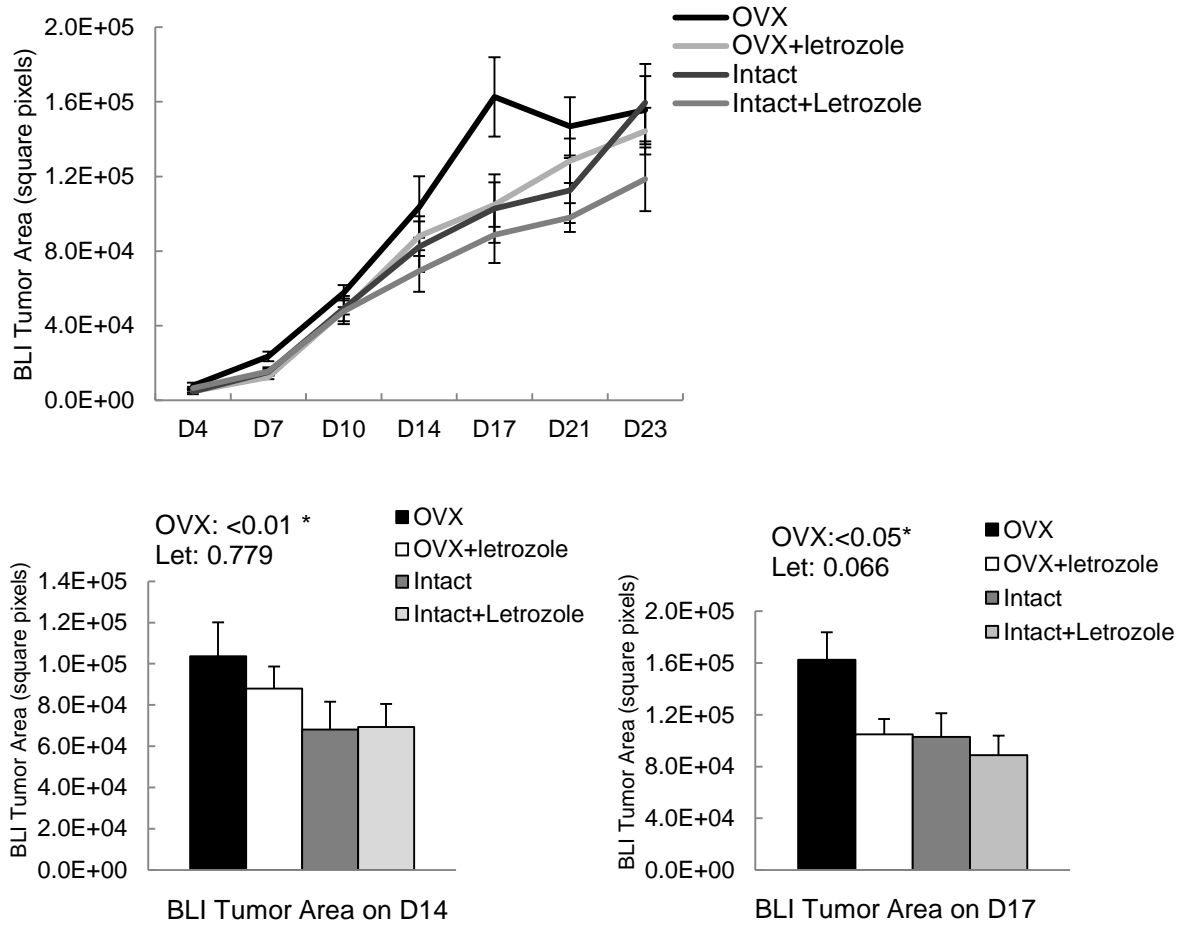


Figure 2.1 Metastatic progression of 4T1 cells monitored by bioluminescence imaging (BLI)

The date for cell injection and ovariectomy surgery was set as day 1. BLI was conducted on seven separate days of the study: day 4, day 7, day 10, day 14, day 17, day 21, and day 23. Representative images of one animal in each group on day 7, day 14, day 21, and day 23 are presented, showing progressive stages of tumor development. Tumor area and integrated density from the bone tumor on BLI images were measured and compared between OVX and intact animals, also between groups treated with letrozole and groups not being treated, as results shown in Figure 2 and Figure A. (a) Representative images of ovariectomized (OVX) animals: images from a mouse in ovariectomy (OVX) group are shown in the upper panel, showing tumor aggressively metastasized to lungs; images from a mouse in OVX+Letrozole group are shown in the lower panel, showing tumor slowly developed moderate metastases to lungs. (b) Representative images of intact animals: images from a mouse in Intact group are shown in the upper panel, showing tumor aggressively metastasized to lungs; images from a mouse in Intact+Letrozole group are shown in the lower panel, showing tumor slowly developed moderate metastases to lungs.

Figure 2.2

(a)



(b)

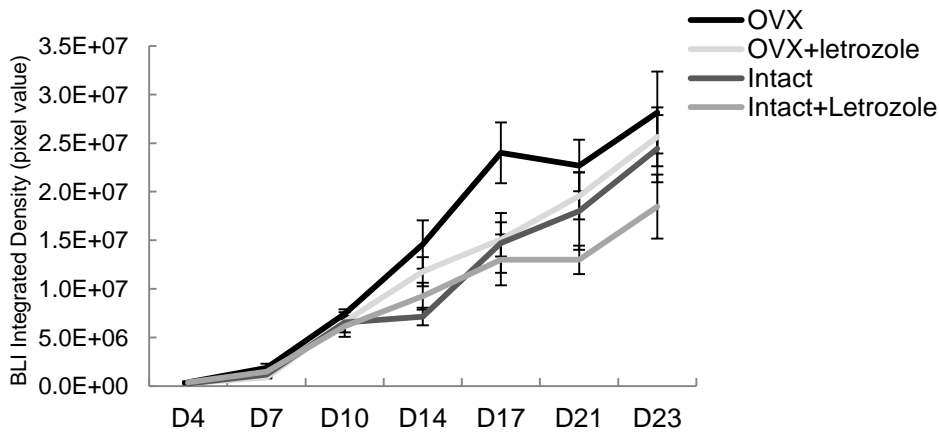


Figure 2.2 (cont.)

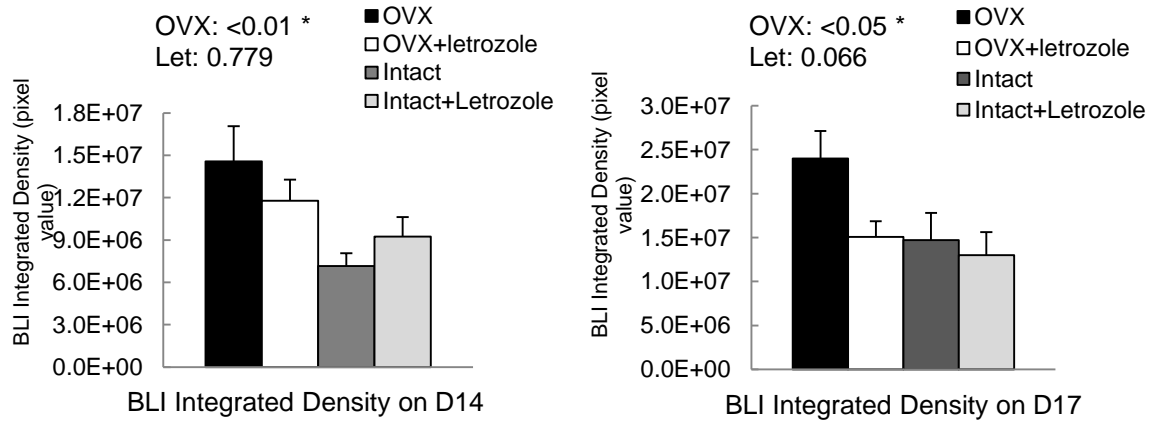


Figure 2.2 OVX animals had greater area and density on bone micrometastatic tumor on D14 and D17 shown by BLI.

(a) BLI tumor area: tumor area growth in bone over time, as well as the tumor area on D14 and D17 measured by BLI in the four groups is shown in Figure 2 a. The significance levels of the major effect from OVX or Letrozole were shown above the figure. Groups treated with letrozole were compared with groups not treated with the drug. OVX groups were compared with intact groups. (b) BLI integrated density: integrated density of tumor on the bone over time, as well as the integrated density on D14 and D17 in the four groups is shown in Figure 2 b. The significance levels of the major effect from OVX or Letrozole were shown above the figure. Data are presented as mean \pm SEM. P values show that OVX animals had significantly greater tumor area and integrated density than intact animals.

Figure 2.3

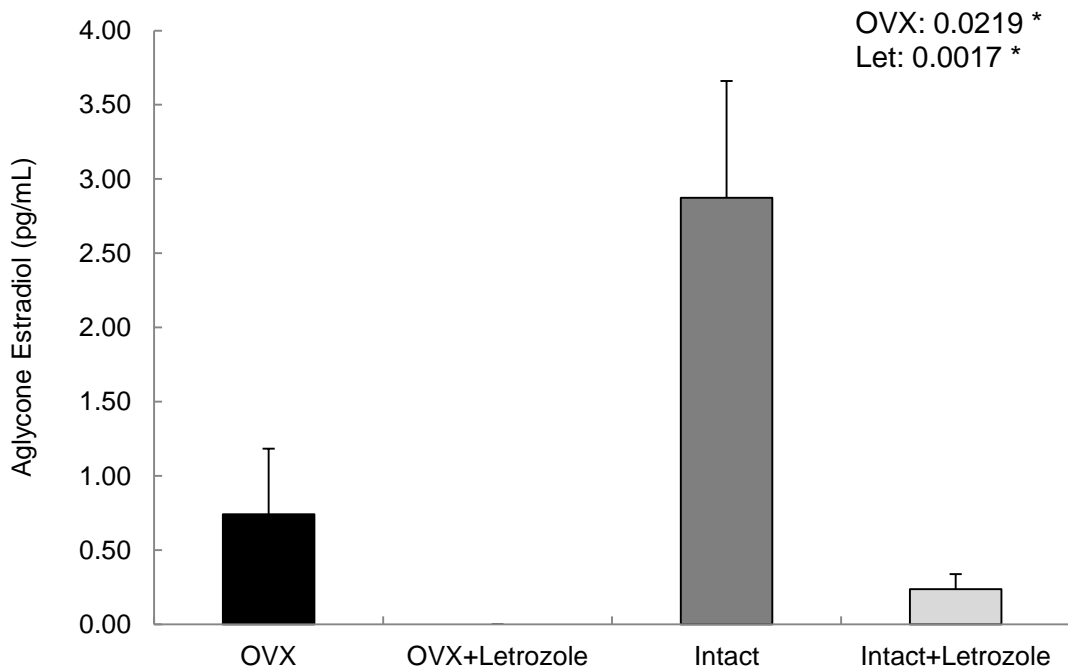


Figure 2.3 Intact mice had higher serum estradiol level than OVX mice, and letrozole reduced serum estradiol level in OVX and intact mice.

Serum was collected at necropsy and analyzed by LC-MS/MS. Serum aglycone estradiol levels are shown in this figure and presented as mean \pm SEM. Serum level below the detection level (0.5 pg/mL) was recorded as 0. The significance levels of the major effect from OVX or Letrozole were shown above the figure. Groups treated with letrozole were compared with groups not treated with the drug. OVX groups were compared with intact groups. P values show that both ovariectomy and letrozole significantly reduced estradiol levels.

Figure 2.4

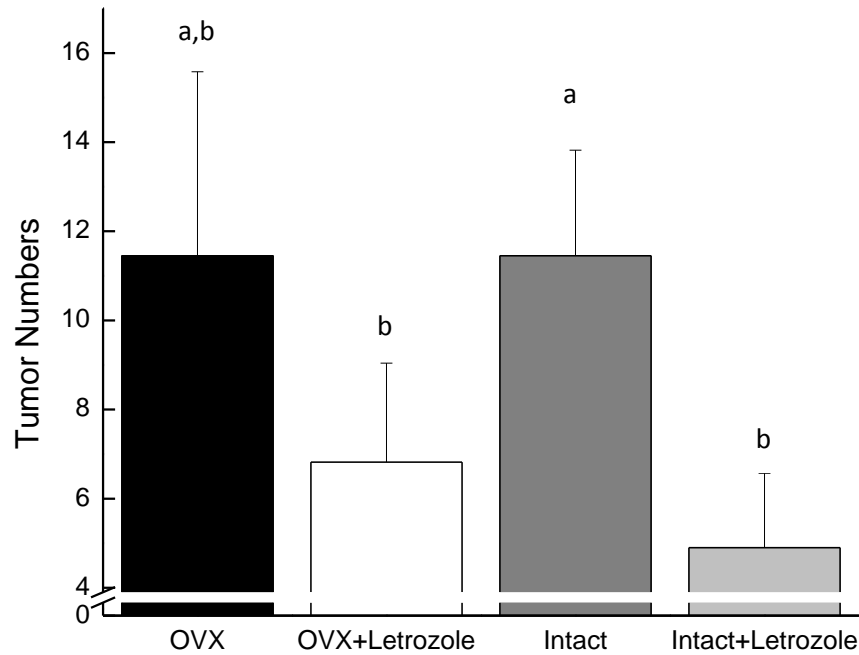
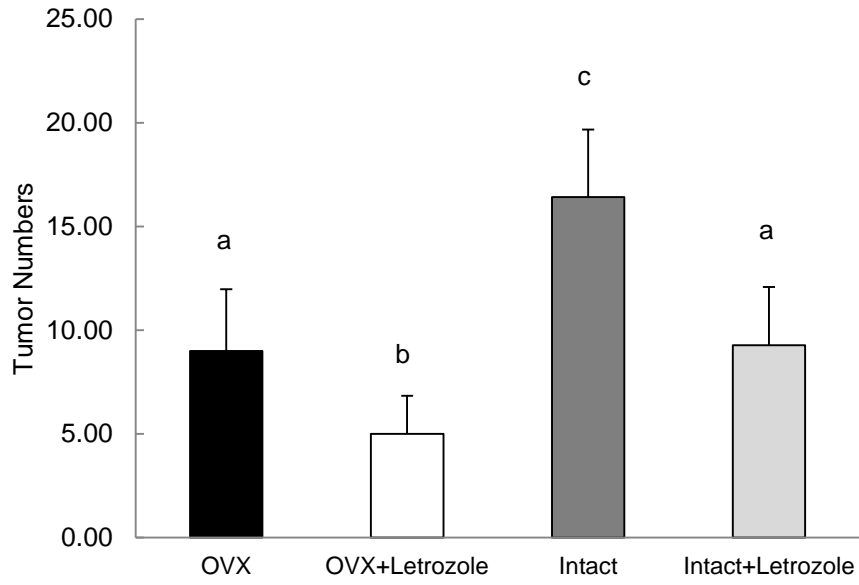


Figure 2.4 Letrozole reduced metastatic progression of 4T1 cells to lungs shown by India ink staining.

Tumor colony numbers on lungs stained with India ink are presented. Groups treated with letrozole were compared with groups not treated with the drug. OVX groups were compared with intact groups. Intact+Letrozole group has fewer tumors compared with Intact group. Data are presented as mean \pm SEM. Bars with different letters are significantly different ($p < 0.05$).

Figure 2.5

(a)



(b)

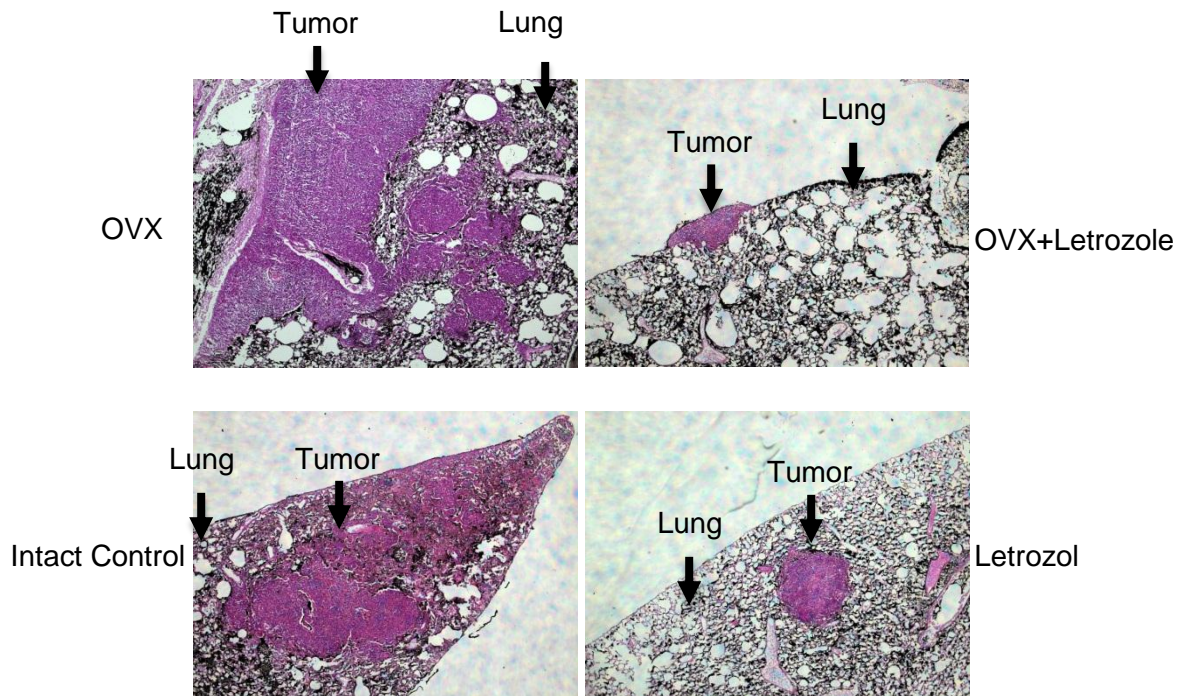
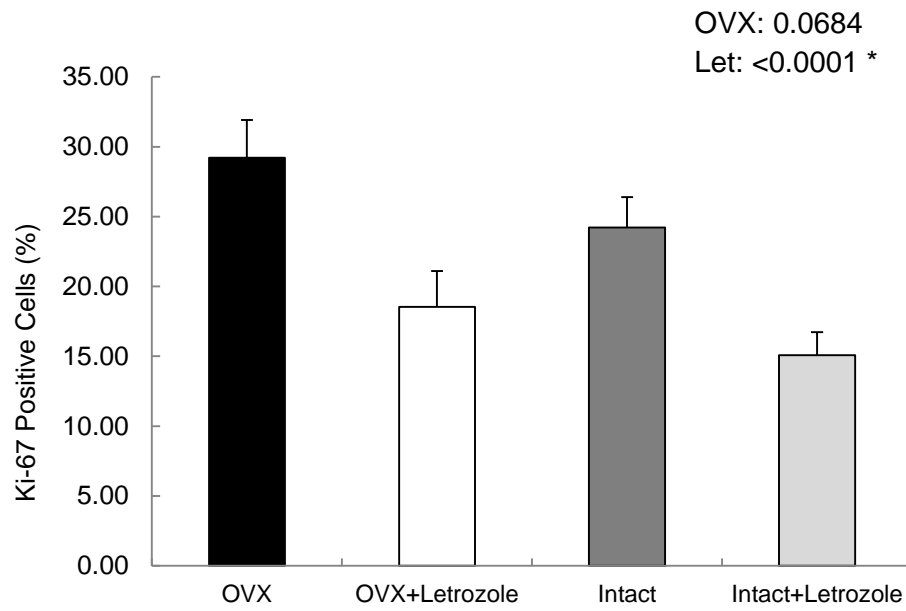


Figure 2.5 Letrozole reduced metastatic progression of 4T1 cells to lungs shown by H&E staining.

Tumor number and area from OVX and intact mice with or without letrozole injection are presented. (a) Tumor number of lungs with H&E staining. There are fewer tumors in OVX+Letrozole group than OVX group, and there are fewer tumors in Intact+Letrozole group than Intact group. Data are presented as mean \pm SEM. Bars with different letters are significantly different ($p < 0.05$). (b) Representative images of lungs selected from each group stained with H&E. Tumor cells are stained red in the cytosol and blue in the nucleus, while normal cells are black due to India ink staining. Top left: representative image from OVX group, showing a tumor with a large area; Top right: representative image from OVX+Letrozole group, showing a tumor with a small area; bottom left: representative image from Intact group, showing a tumor with a large area; bottom right: representative image from Intact+Letrozole group, showing a tumor with a small area.

Figure 2.6

(a)



(b)

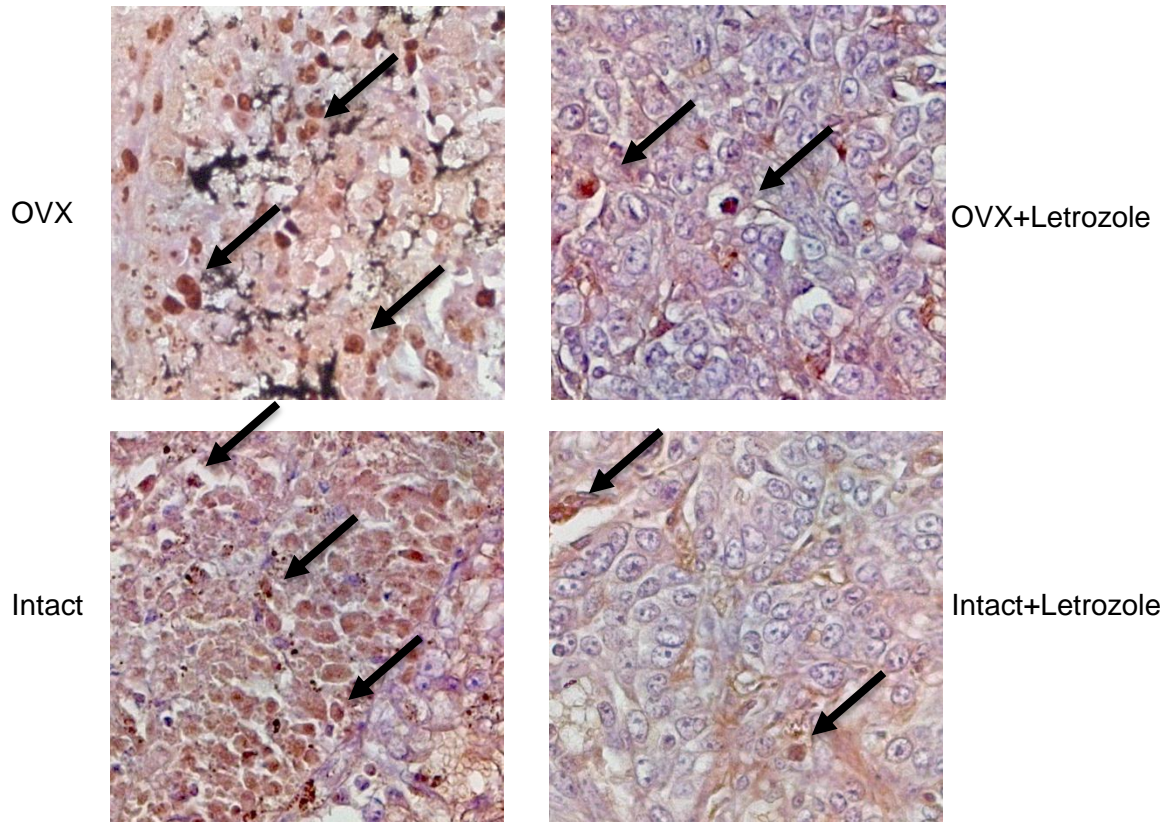


Figure 2.6 Letrozole reduced metastatic progression of 4T1 cells to lungs shown by Ki-67 staining.

Positive tumor cell percentages were calculated as the number of positive cells divided by the sum of positive and negative cells from metastatic lung tumors in mice. (a): Percentage of Ki-67 positive cells. Data are presented as mean \pm SEM. The significance levels of the major effect from OVX or Letrozole were shown above the figure. Groups treated with letrozole were compared with groups not treated with the drug. OVX groups were compared with intact groups. P values show that letrozole significantly reduced proliferative cell percentage. (b): Representative images of lungs selected from each group showing Ki-67 staining. Top left: representative image from OVX group, showing tumor area with a proportion of positive cells (indicated by arrows); Top right: representative image from OVX+Letrozole group, showing tumor area with few positive cells (indicated by arrows); bottom left: representative image from Intact group, showing tumor area with a proportion of positive cells (indicated by arrows); bottom right: representative image from Intact+Letrozole group, showing tumor area with few positive cells (indicated by arrows).

Chapter 3 Effects of a Low Calcium Diet on Breast Cancer Micro-metastatic Bone Tumor Growth and Lung Metastasis in Mice from a Time Course Study

Abstract

Breast cancer (BC) is the second most common cancer in women worldwide. Metastasis occurs in stage IV BC, when cancer starts to spread to major organs like bone and lungs. Low Calcium (LC) diet was reported to increase bone turnover and promote tumor growth in the bone of mice. Our goal was to study the effects of LC diet on BC metastases from bone to lungs, and effects on the bone microenvironment in mice inoculated with murine 4T1 cells. 76 female Balb/c mice were randomly assigned to 7 groups. Mice in the Control (C) diet and LC diet groups were sacrificed on day 5, day 10, and day 21. Mice in the sham group, which were not injected with cancer cells, were sacrificed on day 10. Bioluminescence imaging and India ink staining were used to evaluate tumor metastasis to the lungs. Our bioluminescence images showed that Mice in LC-D21 group had stronger integrated density on the bone tumor than C-D21 on Day 14 and Day 17. Among animals not inoculated with tumor, mice on LC diet had higher serum parathyroid hormone level than control. India ink stained lungs showed that mice in LC-D21 group had more tumor nodules on the surface of lung than C-D21 group. In summary, LC diet induced stronger tumor growth in the bone and increased BC metastatic tumor nodules on lung surface.

Introduction

According to American Cancer Society, in 2010, there were 200,000 women in the United States who are diagnosed with BC; among them, there were around 40,000 deaths.⁷⁶ BC frequently metastasizes to the bone. More than 70% of BC patients have bone metastasis¹⁶⁹, which usually leads to several skeletal complications, including pathological fractures, pain, debilitating neurologic symptoms, and hypercalcemia.¹⁷⁰ Though BC cells do not have the ability to resorb bone, they can cause destruction to the bone microenvironment by disrupting the equilibrium between osteoblasts and osteoclasts during bone remodeling by releasing growth factors for osteoclastic cells¹⁷⁰, which results in increased osteoclast activity that drives bone resorption¹⁶⁹ and formation of osteolytic lesions.¹⁷⁰

Most of late stage BC patients are post-menopausal women. Several studies reported that menopause and subsequently reduced estrogen levels result in a decrease in calcium absorption efficiency. Women entering menopause were reported to experience a sudden decline in calcium absorption corresponding to decreased serum estradiol levels, whereas women with ongoing menses experienced stable calcium absorption. Also reported is a decline in calcium absorption with age (around 0.2% per year). The one time decrease in calcium absorption at menopause is more than 10 times of the absorption decline per year (around 2.2%). Women would also have a decrease in calcium absorption following oophorectomy, which could be reversed with estrogen therapy.¹⁷¹

Inadequate calcium intake, vitamin D deficiency, and inadequate exercise increase the risk of osteoporosis and fractures, which are common among cancer patients. BC patients frequently have low dietary calcium intake and high bone turnover. Increased bone turnover, due to dietary calcium deficiency, promotes tumor growth in bone.¹⁷² For BC survivors, they are also at risk for bone loss because of the disease itself and other reasons like chemotherapy, irradiation, or anti-hormone therapy.¹⁷³

Though evidence is still inconclusive, some of epidemiological studies have linked a low calcium intake to breast cancer risk. Kawase *et al.* reported that calcium intake was inversely associated with BC risk. In analyses stratified to menopausal status, there is an inverse association between BC risk and calcium intake, modified by tumor receptor status, only among postmenopausal women.⁷² In another study, a 19% decrease in BC risk was found for those with highest quantile of calcium intake than the lowest quantile. These results suggested that calcium have a chemopreventive effect against BC.¹⁷⁴ It was also reported that women might have the lowest risk of BC with dietary calcium intake of about 600 mg/day.¹⁷⁵

Animal studies showed how LC diet increases BC risk by increasing bone turnover. Among BC metastases, osteosclerotic metastases account for 20% with the remainder osteolytic or mixed. Osteolytic metastases were shown to depend on bone resorption for growth in mice models.¹⁷⁶ Zheng *et al.* reported a low calcium diet increased tumor area compared with control in association with increased osteoclast numbers.¹⁷⁶ Another study evaluated effects of dietary calcium restriction, with chow containing 0.1% calcium (normal chow contained 0.79% calcium), on BC cell growth by implanting cancer cells intratibially in young growing nude mice. Over three days on this diet, nude mice developed secondary hyperparathyroidism with increased circulating levels of PTH, increased biochemical indices of bone resorption, and decreased bone density.⁶⁸

Materials and Methods

Materials

Heat-Inactivated Fetal Bovine Serum (HI-FBS) was purchased from Atlanta Biologicals (Lawrenceville, GA). Modified IMEM, Penicillin/Streptomycin, Fungizone, and Trypsin-EDTA were purchased from Invitrogen (Carlsbad, CA). L-Glutamine was purchased from Sigma Chemical Co. (St Louis, MO). Matrigel™ matrix was purchased from BD Biosciences (San Jose, CA). AIN-93G pellet diet was purchased from Research Diets (New Brunswick, NJ). D-luciferin potassium salt was purchased from Regis Technologies (Morton Grove, IL). Isoflurane was purchased from Baxter Healthcare Corporation (Deerfield, IL).

Cell Culture

Murine 4T1 mammary cancer cells tagged with firefly luciferase were provided by Dr. David Piwanica-Worms from Washington University (St. Louis, MO). 4T1 cells were cultured with IMEM, plus 10% HI-FBS, 100 unit/mL Penicillin, 100 µg/mL Streptomycin, 1% L-Glutamine, and 0.1% Fungizone in a humidified incubator containing 5% CO₂ at 37°C. 70% confluent cells were harvested, centrifuged, and resuspended in Matrigel^{TX} for injection.^{125,127}

BALB/c mice

Female Balb/c OVX mice were obtained from National Cancer Institute (Wilmington, MA). During the study, animals were singly caged and maintained under the standard light-dark cycle (12 h light and 12 h dark), with access to food and water. All studies were carried out under animal experiment protocols approved by the Institutional Animal Care and Uses Committee (IACUC) at the University of Illinois at Urbana-Champaign.

Methods

Seventy six female Balb/c mice (intact) were fed with AIN-93G diet for two days and then randomly assigned to four groups. The Control group (32 mice) was fed with normal diet (AIN-93G, contains 5g calcium per kilogram diet, or 0.5% w/w) and inoculated with 4T1 cells. The Control-Sham group (6 mice) was fed with normal diet with no cancer cell injected. The Low Calcium group (32 mice) was fed with low calcium diet (contains 80 mg calcium per kilogram diet, or 0.008% w/w) and inoculated with 4T1 cells. The Low Calcium-Sham group (6 mice) was fed with low calcium diet with no cancer cell injected. Animals were on their own diet for two weeks before cells were injected. They were 9 months old when cancer cells were injected into their tibia. Mice in the Control group and Low Calcium group were randomly assigned to three separate groups respectively: D5, D10, D21, with the numbers indicating the duration of days from tumor injection to sacrifice. Animals were weighed once a week and once more before sacrifice. Three weeks later, mice were sacrificed with CO₂ asphyxiation.

Intra-tibia Injection

Mice were anesthetized with isoflurane (mixed in oxygen) and placed in a supine position during operation. After an incision was made on the right knee of the animal, 1000 4T1 suspended in Matrigel were inoculated. A 26-gauge needle was first inserted into the bone marrow cavity to create space for inoculation, and a 27-gauge needle was then used for injection. The incision was sealed with tissue adhesive (3M Vetbond, No. 1469SB) and closed with a surgical staple. Banamine (2.3 µg/g body weight) was subcutaneously administered immediately and 12 hours later for pain relief after surgery.

Bioluminescence Imaging

Three minutes before BLI, mice were injected with 15 mg/mL luciferin dissolved in PBS at a dose of 10 µL luciferin per gram of body weight. Each mouse was anesthetized with continual administration of isoflurane gas from an inlet tube and imaged with BLI twice per week. The whole body scan takes three minutes per animal. BLI signals were detected by a camera set inside of the imaging unit. BLI images and movies were acquired and compiled by the Piper Control software (Stanford Photonics, Palo Alto, CA). Images obtained were later analyzed by the software Image J (NIH, Bethesda, MD) and Photoshop Elements (Adobe, San Jose, CA). The background image of the mouse body was combined with the image showing only the luminescence of the tumor. Tumor area and integrated density (the product of area and intensity of luminescence) on the bone were analyzed using ImageJ.

India ink staining

Lungs of mice were perfused with India ink to stain the lobes and visualize the tumor following the method described by Wexler.^{155,156} Briefly, ribs were cut to expose the lung and trachea, and India ink was slowly injected into the lung via trachea. The fully infused lung was harvested and fixed in fekete solution (90% of 70% ethanol, 9% of 37% formaldehyde, and 1% of 9% acetic acid). After placed in fresh fekete solution for 24 hours, tumor nodules on lung lobes were counted by three individuals. Tumors were distinguished as white extrudates not being stained while normal lung tissue was stained black. The mean value of the three individuals' counts is reported.

Uteri and serum collection

Blood was collected from each animal and centrifuged to separate serum from the blood cells. Serum was frozen and stored at -20°C freezer and sent to Dr. Iwaniec's lab in Oregon State University for parathyroid hormone (PTH) level measurement.

Statistical Analysis

BLI tumor area, integrated density, and serum PTH level were analyzed using Student t-test in Microsoft Excel to determine the significant difference between groups. Tumor nodule numbers on lung surface was analyzed using Wilcoxon rank sum test. All hypotheses were tested in a two sided way and significance was set at $p < 0.05$.

Results

Mice in LC-D21 group had stronger integrated density on the bone tumor than control

BLI is shown as effective to monitor tumor growth and progression and determine an appropriate ending point of a study.⁶ Tumor progression was monitored via BLI on day 4, 7, 11, 14, 17, and 20. Representative BLI images (Figure 3.1) show that mice on LC diet had larger bone tumor with stronger integrated density than mice on Control diet. It was confirmed later by tumor area and integrated density measurement on the bone (Figure 3.2). Mice in the LC-D21 group had stronger BLI integrated density of the micrometastatic bone tumor compared with mice in C-D21 group on both Day 14 ($p=0.05$) and Day 17 ($p<0.05$). A similar trend was shown in tumor area measurement on the bone, where LC-D21 seems to have a larger tumor area on the bone than C-D21, especially on Day 14 and D 17. The significance level between the two groups on Day 14 and D 17 is $p=0.07$, respectively.

Mice on LC diet had higher serum parathyroid hormone level than mice on Control diet

Serum PTH level in mice on a LC diet with no tumor inoculated is significantly higher than mice on a control diet with no tumor inoculated (Figure 3.3). However, there is no significant difference between LC group and Control group in those mice inoculated with cancer cells: D10 and D21 groups. Mice in the Control group that were inoculated with tumor in the bone also had higher serum PTH levels than those in the Control group without tumor inoculation.

Mice in LC-D21 group had more lung surface tumor nodules than mice in C-D21 group

Tumor colony numbers on lungs stained with India ink were counted to assess severity of lung metastases. Tumor nodule numbers of LC-D21 group were significantly higher ($p<0.05$) than that of C-D21 group; while there was no significant difference between LC and control in D5 and D10 groups (Figure 3.4).

Discussion

Previously we demonstrated that ovariectomy increased bone metastatic tumor area and integrated density as measured by bioluminescence imaging, which confirmed with previous findings that ovariectomy can enhance the growth of cancer cells in bone. However, whether this growth is facilitated by increased bone resorption induced by ovariectomy or other mechanisms remains unclear.⁶⁸ In this time course study, a similar model was utilized to investigate the effects of a low calcium diet on breast cancer bone metastatic tumor growth and lung metastasis. The tibias of animals in this study, together with carcasses were sent to our collaborators for bone mineral analysis and to study the damage that a low calcium diet induced with tumors in the bone microenvironment.

In this study, stronger integrated density of bone tumor were observed from BLI analysis in those mice fed with LC diet, compared with control, which confirms with previous findings from Ooi L.L. *et al.* They showed that mice deficient in calcium (0.1% calcium) with BC cells (MDA-MB-231) implanted intratibially had larger tumor histologically with increased lesion size as assessed radiologically than mice on control diet (0.79% calcium). Mice on calcium deficient diet also had increased circulating PTH, increased bone resorption and bone density.⁶⁸ In our study, increased PTH levels was also observed in low calcium fed sham animals (mice not injected with cancer cells) than control animals. However, for animals on control diet inoculated with tumors, their PTH levels seemed to be higher than mice with no tumor and no difference was found between LC and control in those tumor-bearing mice.

In this study, after analysis on the bone, our collaborators found increased bone mineral content and bone mineral density in those low calcium fed animals (data not shown). There was also some foreign tissue formed in the area close to the tumor inoculation site on the tibia of those tumor-bearing animals (data not shown). It needs to be elucidated whether this foreign tissue formation was due to the low calcium diet or tumor inoculation, or both. Such finding coincides with some previous reports that bone injection of breast cancer cells would cause osteogenesis. Liang H. *et al.* adopted the bone injection model in their study with MDA-MB-231 cells, and found osteogenesis in the bone tissue after tumor inoculation.⁷⁷ Compared with control, animals received tumor inoculation in the bone had decreased bone volume during the study while increased bone density throughout the first three weeks post-injection which was higher than the control, and suddenly dropped bone density in the last week.⁷⁷

In the current study, though mice were fed with a low calcium diet, the serum calcium levels of these animals were not assessed. The assumption is that the low calcium diet increased bone turnover, but due to the tight regulation of calcium level in blood, there is possibly not

much difference of serum calcium levels between LC and C groups. However, it was also reported that low calcium fed animals may also have a lower calcium level than control. Rader J.I. *et al.* fed male rats with calcium deficient diet and control diet in a study. They found that serum calcium levels for calcium-deficient rats continued to decline during the 5 week study, and control calcium level was higher than calcium-deficient rats. For serum PTH levels, calcium-depleted rats had rapidly increased PTH levels and much higher than control, which had a stable PTH level during the study¹⁷⁷, consistent with previous studies and our finding.

In clinical trials, there have been inconsistent study outcomes in regard to whether serum calcium level or dietary calcium would affect breast cancer risks in women. Since serum calcium was tightly regulated in the body, it may not be an accurate indicator of dietary calcium intake.⁷⁴ In our study, intact animals were used, to exclude any possible effects from ovariectomy on bone resorption, which if existing, may confound study results. In the lung metastasis results, increased tumor nodules on the surface in LC-D21 group were found.

In summary, it is found in this project stronger integrated density on BC metastatic tumor in the bone via BLI, and increased tumor nodule counts on the lung surface induced by a low calcium diet compared with control in mice inoculated with murine 4T1 cells intratibially. LC diet also increased serum PTH level. Further evidence is needed on LC and BC metastasis, possibly through a larger scale study with more animals per group and extensive investigations on metastatic sites.

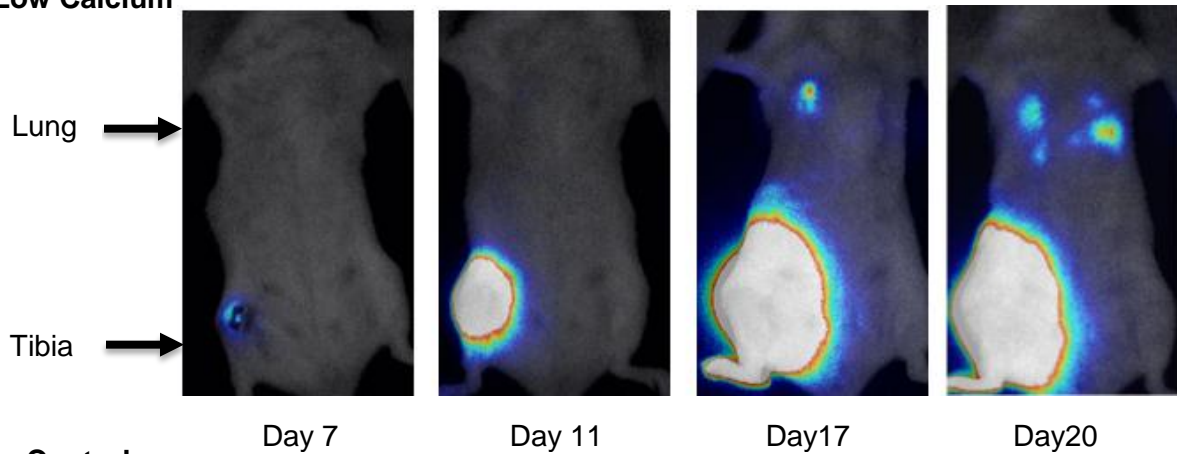
Acknowledgments

We thank the funding sources of this project as below: NCCAM BRC (P50 AT006268), DOD Breast Cancer Research Program from U.S. Army Medical Research and Materiel Command (W81XWH-09-1-0689; BC085882).

Figures

Figure 3.1

Low Calcium



Control

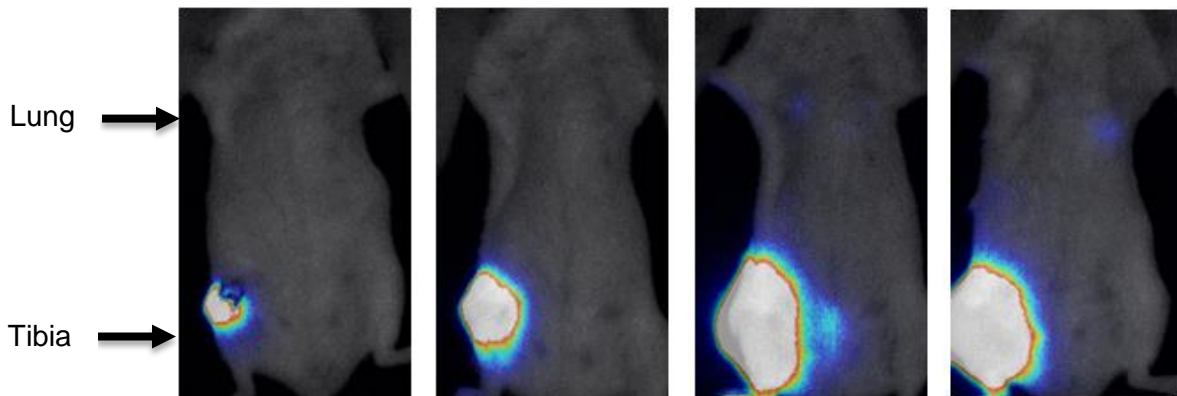
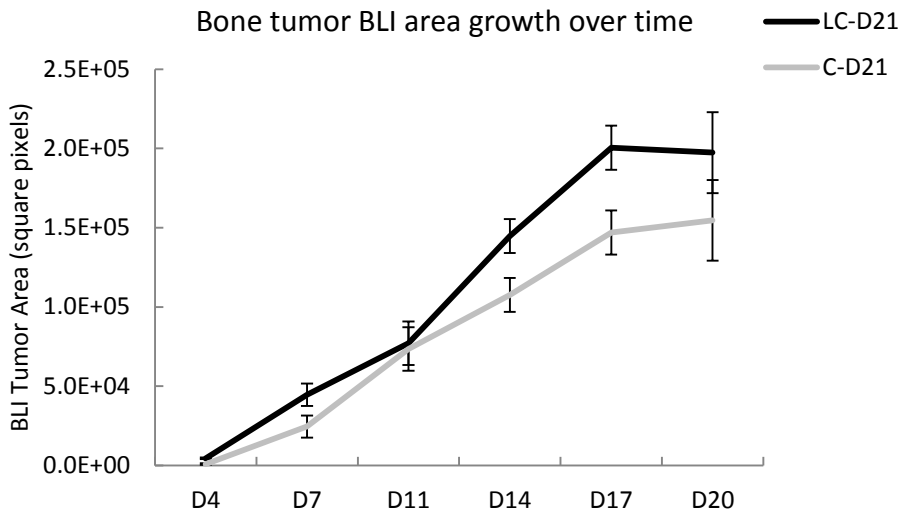


Figure 3.1 Metastatic progression of 4T1 cells monitored by bioluminescence imaging (BLI). The date for cell injection was set as day 1. BLI was conducted on six days of the study: day 4, 7, 11, 14, 17, and 20. Representative images of one animal in each group on day 7, 11, 17, and 20 are presented, showing progressive stages of tumor development. Images from a mouse in LC-D21 group are shown in the upper panel, showing tumor progressively metastasized to lungs with severe tumor growth developed in the bone; images from a mouse in C-D21 group are shown in the lower panel, showing tumor developed moderate metastases to lungs with sizable tumor growth in the bone.

Figure 3.2

(a)



(b)

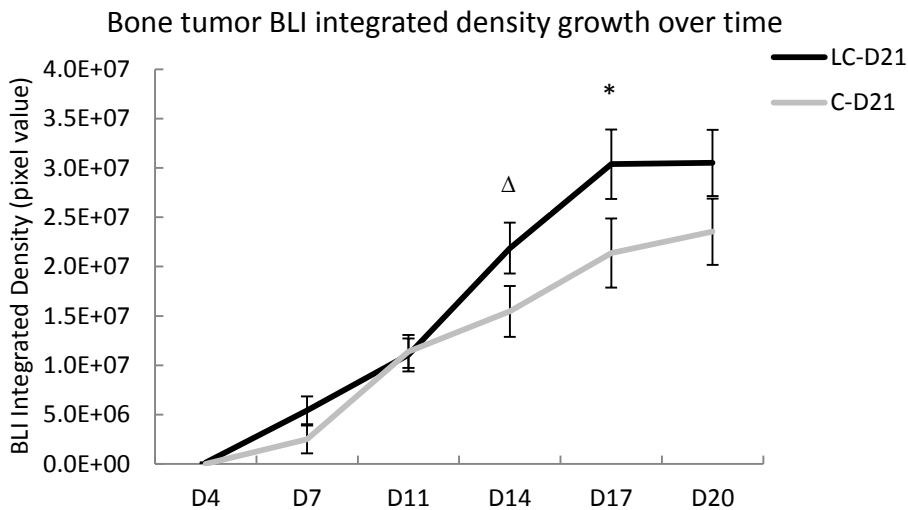


Figure 3.2 LC-D21 animals had greater integrated density on bone micrometastatic tumor on D14 and D17 shown by BLI.

(a) BLI tumor area: tumor area growth in bone over time from mice in LC-D21 and C-D21 groups is shown in Figure 2 a. (b) BLI integrated density: integrated density of tumor on the bone over time from mice in LC-D21 and C-D21 groups is shown in Figure 2 b. Data are presented as mean \pm SEM. Asterisk (*) indicates a significant difference between LC and control ($p < 0.05$); triangle (Δ) indicates a significant difference at the border-line level between LC and control ($p = 0.05$).

Figure 3.3

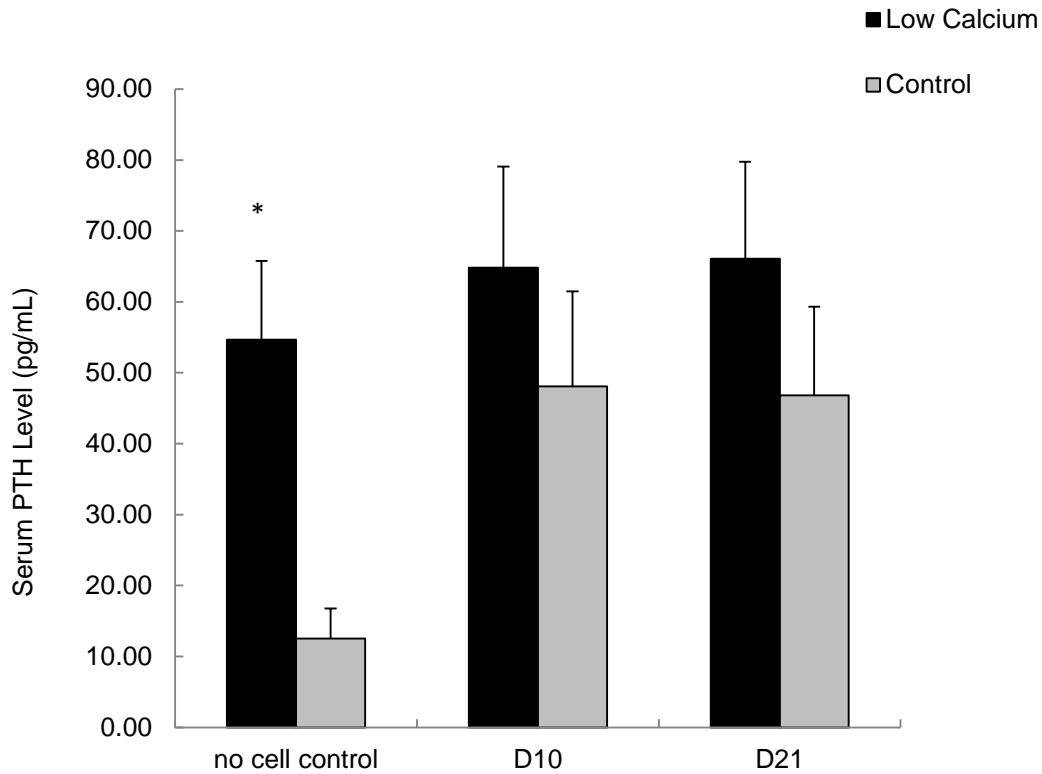


Figure 3.3 Mice on LC diet with no tumor inoculated had higher serum PTH level than control group with no tumor inoculated.

Serum was collected at necropsy and sent to be analyzed by research group in Oregon State University. Serum parathyroid hormone levels are shown in this figure and presented as mean \pm SEM. Among mice that were not inoculated tumor in the bone, LC diet increased serum PTH level than control.

Figure 3.4

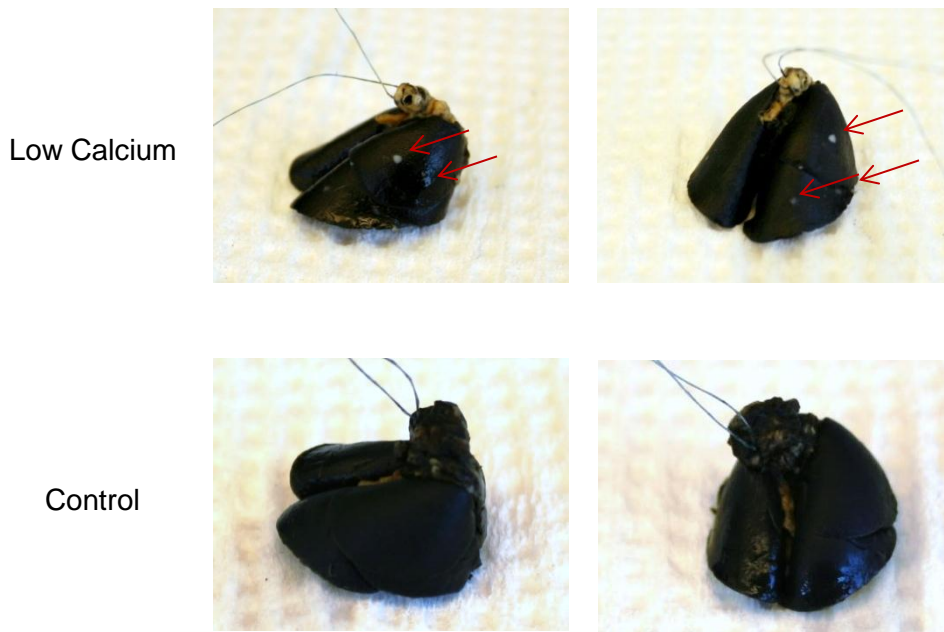
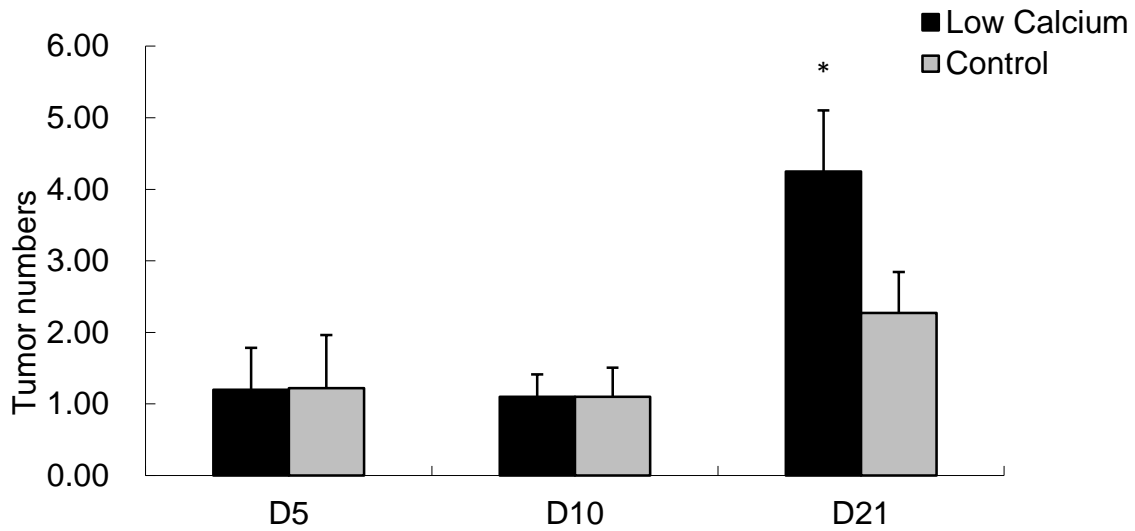


Figure 3.4 Mice in LC-D21 group had more metastatic tumors on lung surface than C-D21 group shown by India ink staining.

Tumor nodule numbers on lungs stained with India ink are presented. Mice in LC-D21 group had significantly more metastatic tumors on the surface of lung than C-D21 group. Data are presented as mean \pm SEM. Asterisk (*) indicates significant difference between LC group and control group ($p < 0.05$). Representative images of lungs stained with India ink from LC-D21 group and C-D21 group were also shown with arrows pointing to tumor nodules.

Chapter 4 Changes of Breast Cancer Metastasis in Mice Inoculated with Murine Breast Cancer Cells 4T1 and 4T1.2 Induced by a High Fat Diet

Abstract

Breast cancer (BC) is the leading cancer in women worldwide. Metastasis occurs in stage IV BC with bone and lung being common metastatic sites. Our goal is to study the effects of a High Fat Diet (HFD) on BC growth and metastases from bone to lungs in mice inoculated with murine 4T1 or 4T1.2 cells. 104 female ovariectomized BALB/c mice were randomly assigned to two groups. Mice on the Control Diet (CD) consumed 17.2% calories from fat; mice on the HFD consumed 46.9% calories from fat. After 30 days of feeding, 32 mice were injected with cancer cells into mammary gland, while the rest were injected intratibially. Animals were sacrificed three weeks after injection. Bioluminescence imaging (BLI) was used to monitor BC metastasis. Mice on HFD had higher body weight and lower energy intake than control. Mice on HFD with mammary injection had higher gonadal adipose weight than control, while mice with 4T1.2 cells had higher liver weight than 4T1 mice. BLI images showed that 4T1.2 cells metastasized from bone to lungs and other body parts, like abdominal cavity. Mice injected with 4T1.2 cells had significantly more lung surface tumors than those with 4T1 cells. H&E staining showed that HF-4T1.2 mice with bone injection had more lung tumors and more liver tumors than C-4T1.2 mice. In summary, mice with 4T1.2 cells developed more aggressive metastasis than mice with 4T1 cells; HFD increased BC metastasis to the lung and liver in mice with 4T1.2 cells injected in the bone shown by H&E staining.

Introduction

Breast cancer (BC) is the most commonly diagnosed cancer in women, the leading cause of cancer death in females worldwide,¹ and the second in American women (after lung cancer) according to CDC^{xxxix}. Stage IV of BC is the most advanced stage, in which cancer cells metastasize from the original site to distant organs like bone, lung and liver. The invasiveness and metastatic spread of BC are responsible for nearly all of the morbidity and mortality associated with BC.² Metastasis is considered as the primary cause of cancer treatment failure.¹² In developing countries, a large fraction of women with BC are diagnosed with advanced-stage disease and have no access to treatment or basic palliative care.¹¹ How we can transform existing knowledge about diet and BC into preventative or protective practices among BC patients and survivors becomes a critical issue.

The animal model utilized in this study mimics late stage BC in female patients by implanting a small number of metastatic murine mammary tumor cells into the marrow cavity of tibia to create a micrometastatic lesion. Subsequent metastasis to the lung is evaluated. Considered as a filter between the primary tumor and other secondary sites, lung is the organ mostly likely containing metastatic breast cancer at autopsy.¹³ Bone, as another frequent site for BC metastasis, has also stimulated extensive research. Once BC metastasizes to the bone, advanced disease of bone destruction and associated bone pain may occur, like fracture, hypercalcemia, and paralysis due to spinal cord compression. The most devastating consequence once BC has spread to bone is that the disease may be treatable but not curable.¹⁸

In this study, effects of a high fat diet (HFD) on BC growth and metastasis in mice were evaluated. HFD has been associated with BC growth and metastasis in previous studies; a few studies on HFD and BC metastasis were found. Rose D.P. *et al.* reported in 1991 that HFD increased the percentage of mice with palpable tumors, increased lung tumor surface area and lung metastasis incidence.⁹³ A high fat diet providing 60% Kcal from fat, as reported by Kim E.J. *et al.*, increased mammary tumor growth and metastasis, and increased mortality in obesity-resistant BALB/c mice.⁹

More studies focus on HFD and BC growth or development. Zhao Y. *et al.* reported that pubertal HFD affected mammary cancer development and reduced tumor latency. Three weeks of HFD induced a transient influx of eosinophils into the mammary gland, and elevated inflammatory and growth factor gene expression in the mammary gland.⁹¹ In transgenic mice spontaneously developing mammary cancers, HFD increased tumor weights in axillary and inguinal regions.¹⁷⁸ Another study using MCF-7 human BC cells in athymic nude mice reported

that HFD increased primary tumor weight and volume. HFD also modulated cell proliferation indicated by IHC^{xl} staining on mammary tumor.⁹² HFD were also used together with another dietary component as treatment. For example, it was reported that depending on whether the background diet is HFD or not, phytoestrogens may have differential effects on BC growth. Perinatal high-fat exposure accelerated onset of spontaneous mammary tumor growth compared with low-fat diet, when given alone or together with flax seed in Tg.NK(MMTV/c-neu) mice.¹⁷⁹

The murine 4T1 BC cell line used in this project has been extensively utilized in animal studies on BC, especially stage IV BC, due to high potential of metastasis to lung, liver, bone and other sites.¹²⁴ 4T1 cells have been regarded as an attractive model for studying late stage BC.^{124,125} They multiply rapidly and develop metastases aggressively once injected into the BALB/c mice, which closely imitate human BC.

According to Lelekakis M. *et al.*, clonogenic cells can be detected in the spines of 4T1 bearing mice.¹³¹ 4T1.2 cells are derived from its parental cell line 4T1 by single cell cloning, and metastasize to lung and bone following orthotopic inoculation into mammary fat pad. This cell line is highly metastatic to lymph nodes, bone, lungs and other organs; thus provides a rare and valuable model that closely resembles metastatic BC in humans, with spontaneous metastasis from the mammary gland to distal sites, including spine and femur.¹³² Tester AM *et al.* reported that Matrigel invasion in Boyden chamber was progressively higher in the more metastatic line 4T1.2 than other BC cell lines (66cl4 and 67NR cells), together with higher MMP-2 activation potential, MMP-9 secretion, and migration over type I or IV collagen.¹³⁰ To our knowledge, the current study is the first to compare 4T1.2 and its parental line 4T1 in animal models of diet and metastatic BC.

Materials and methods

Materials

Murine 4T1 cells tagged with firefly luciferase were provided by Dr. David Piwnica-Worms (Washington University, St. Louis, MO). Murine 4T1.2 cells tagged with firefly luciferase were provided by Dr. Robin L. Anderson (Peter MacCallum Cancer Centre, Melbourne, Australia). Heat-Inactivated Fetal Bovine Serum (HI-FBS) was purchased from Atlanta Biologicals (Lawrenceville, GA). Modified IMEM, Penicillin/Streptomycin, Fungizone, and Trypsin-EDTA were purchased from Invitrogen (Carlsbad, CA). L-Glutamine was purchased from Sigma Chemical Co. (St Louis, MO). Matrigel™ matrix was purchased from BD Biosciences (San Jose, CA). AIN-93G pellet diet was purchased from Research Diets (New Brunswick, NJ). D-luciferin potassium salt was purchased from Regis Technologies (Morton Grove, IL). Isoflurane was purchased from Baxter Healthcare Corporation (Deerfield, IL). Thermo Infinity Triglyceride Reagent was purchased from Thermo Fisher Scientific (Rockford, IL). Standard solution for liver triglyceride measurement was purchased from 9500 Verichem Lab Inc. (Providence, RI).

Cell culture

Both 4T1 and 4T1.2 murine mammary cancer cells were cultured with IMEM, supplemented with 10% HI-FBS, 100 unit/mL Penicillin, 100 μ g/mL Streptomycin, 1% L-Glutamine, and 0.1% Fungizone in a humidified incubator containing 5% CO₂ at 37°C.^{3,146} Cells were harvested at 70% confluence, centrifuged (0°C, 700 rpm, 5 minutes), and suspended in Matrigel™ for injection.

BALB/c mice

104 female BALB/c mice (OVX) were purchased from National Cancer Institute (Wilmington, MA). Mice were 5 weeks old when arrived. During the study, animals were singly caged and maintained under the standard light-dark cycle (12 h light and 12 h dark), with ad libitum access to food and water. All studies were carried out under animal experiment protocols approved by the Institutional Animal Care and Use Committee (IACUC) at the University of Illinois at Urbana-Champaign.

Mice were randomly assigned to 2 groups. Half of them were fed with a High Fat Diet (HFD) and the other half with Control Diet (CD) for 30 days. Then within each of the two diet groups, mice were randomly assigned to four groups (according to the cell line and whether cells were injected into the mammary gland or bone marrow cavity) as shown in Table 4.1. Mice on CD consumed 17.2% calories from fat; mice on HFD consumed 46.9% calories from fat. The 4T1 groups (18 mice each group) were inoculated with 4T1 cells via tibial injection. The 4T1-PT (Primary Tumor) groups (8 mice each group) were inoculated with 4T1 cells via mammary ductal injection. The 4T1.2 groups (18 mice each group) were inoculated with 4T1.2 cells via

tibial injection. The 4T1.2-PT (Primary Tumor) groups (8 mice each group) were inoculated with 4T1.2 cells into their mammary gland. Animals were weighed and food intake was measured once a week. Energy intake (Kcal/d) was calculated by multiplying their food intake with the amount of calories per gram of each diet. Macronutrient profile and diet composition were shown in Table 4.2 and Table 4.3, respectively. Three weeks after injection, mice were sacrificed with CO₂ asphyxiation. Major findings for mice in the bone injection model are presented in the Results section; major findings for mice in the mammary injection model are presented in Appendix B as supplemental materials.

Intra-tibial injection

Mice were anesthetized with isoflurane/oxygen and placed in a supine position during operation. After an incision was made on the right knee of the animal, 1,000 4T1 or 4T1.2 cells suspended in 2.5µL Matrigel™ were inoculated. A 26-gauge needle connected to a syringe was first inserted into the bone marrow cavity to create space for the subsequent injection, and then replaced by a 27-gauge for injection. The incision was sealed with tissue adhesive (3M Vetbond) and closed with a surgical staple. Banamine (2.3 µg/g body weight) was subcutaneously administered at surgery and 12 hours post-surgery for pain relief.

Mammary ductal injection

Mice were anesthetized with isoflurane/oxygen and placed in a supine position during operation. 1,000,000 4T1 or 4T1.2 cells suspended in 100 µL Matrigel™ were injected into the second rear right mammary gland of the animal via a syringe tipped with a 27-gauge needle.

Bioluminescence imaging

Three minutes before BLI, mice were injected with 15 mg/mL luciferin dissolved in PBS at a dose of 10µL luciferin per gram of body weight. Each mouse was anesthetized with continual administration of isoflurane gas from an inlet tube and imaged with BLI twice per week. The whole body scan of one mouse takes three minutes. BLI signals were detected by a camera set inside of the imaging unit. Images and movies were acquired and compiled by the Piper Control software (Stanford Photonics, Palo Alto, CA) on a computer. Images obtained were later analyzed by the software Image J (NIH, Bethesda, MD) and Photoshop Elements (Adobe, San Jose, CA). The image showing the luminescence of the tumor area was layered on top of the background image of the mouse body.

Primary tumor area measurement

The area of primary tumor was measured using a caliper during the study. At least four measurements were conducted before animals were sacrificed. The surface area of primary tumor was first swiped with a cotton ball soaked in 70% ethanol before measurement, so the

palpable tumor was easier to find. The length and width of the tumor were measured and recorded. Area was calculated as $\pi \times (\text{length}/2) \times (\text{width}/2)$. After sacrifice, tumor area was measured once again *ex vivo* after the tumor was removed from the body.

Primary tumor and organ collection

During necropsy, primary tumors in the mammary gland were collected. An incision was made next to the tumor; a number 15 scalpel was then used to gently loosen the mammary tumor from surrounding tissue. Primary tumor was cut into two halves. One half was kept in formalin first and changed to 70% ethanol 24 hours after sacrifice. The other half was frozen in liquid nitrogen and stored in -80°C freezer. Gonadal adipose tissue and liver were collected and weighed at necropsy. One lobe of liver was kept in formalin first and changed to 70% ethanol 24 hours after sacrifice.

Histopathological analysis

Lung sections from each animal in this study were embedded in paraffin, trimmed and sliced into 5 μm slices. Each slice was mounted on a glass slide, and tissue slides were deparaffinized, rehydrated, and stained with H&E. Stained tissues were observed and photographed using NanoZoomer Digital Pathology System (Hamamatsu, Hamamatsu City, Japan). Tumors on each slide were counted and tumor area was measured using the software NDP. View 2 (Hamamatsu, Hamamatsu City, Japan). Tumor area percentage on the lung from each animal was calculated by dividing the total tumor area (with individual tumor area added together) by the total area of lung lobes.

To evaluate proliferative cell percentage by Ki-67 staining, deparaffinized and rehydrated tissue slides were incubated with anti-Ki-67 antibody (PharMingen, San Diego, CA) and biotinylated secondary antibody (Vector Laboratories, Burlingame, CA). Slides were then stained by diaminobenzidine substrate and counter stained by hematoxylin. Proliferating cells expressing Ki-67 were stained brown and considered as positive cells. By contrast, cells stained blue by hematoxylin were considered as negative cells. Immunostained slides were photographed under NanoZoomer Digital Pathology System (Hamamatsu, Hamamatsu City, Japan). Tumor images were analyzed using Adobe Photoshop Elements. To assess the percentage of proliferating cells, proportion of Ki-67-positive nuclei was determined. According to H&E staining results, four animals with H&E tumor count most close to the group average were selected from each group. Ki-67 stained positive and negative cells were counted on slides of these four animals under high-power (40X objective) fields.

Liver Triacylglyceride (TAG) content measurement

A piece (around 50 mg) of the frozen liver sample was grinded in liquid nitrogen, homogenized in 0.3 mL saline (0.9% w/v NaCl) and weighed. Samples were diluted 2X with saline. 20 μ L of the diluted sample was mixed with 20 μ L 1% deoxycholate, and incubated at 37°C for 5 minutes. 10 μ L of sample or standard solution was added into each well of a 96 well plate. 200 μ L Thermo Infinity Triglyceride Reagent was added into each well. Plate was incubated at 37°C for 5 minutes, and read by a plate reader at $\lambda=562$ nm.

Statistical Analysis

Mice body weight and energy intake before cell injection were analyzed using student t-test. Mice body weight and energy intake after cell injection, gonadal adipose weight, liver weight, and proliferating cell percentage from Ki-67 staining were analyzed using ANOVA LSD test to determine the significant difference between groups. Tumor nodule counts on lung surface and tumor numbers inside lung tissue were analyzed using Wilcoxon rank sum test. Metastatic tumor incidence rate in liver was analyzed using Chi-Square test. All hypotheses were tested in a two-sided way and significance is set at $p<0.05$. All statistical tests were conducted in SAS (SAS Institute, Cary, NC).

Results

Mice in HFD groups had higher body weight and lower energy intake than control

As shown in Figure 4.1, before cell injection, HFD mice had higher body weight than control from week 2 to week 5; while they had lower energy intake than control at week 4 and week 5. After tumors were inoculated, HF-4T1.2 mice had higher body weight than C-4T1.2 during the first and third week after cell injection, and HF-4T1 had higher body weight than C-4T1 during the third week after cell injection. HF mice had lower energy intake than control during the first week after cell injection, then their energy intake became stable and were similar as control during the last two weeks.

Mice with 4T1.2 cells had more lung surface tumor nodules than mice with 4T1 cells in the bone injection model

Lung surface tumor nodule count shows that mice with 4T1.2 cells had significantly more metastatic lung tumors than 4T1 mice in the bone injection model (Figure 4.2). Bioluminescence images showed that mice injected with 4T1.2 cells in the bone had metastasis spread to different parts of the body, such as chest and abdominal cavity (Figure B.1). Representative pictures of lungs with surface tumors are shown (Figure 4.2). There is no difference on lung surface tumor nodule count between CD and HFD fed mice receiving bone injection. There is no difference on lung surface tumor nodule count among the four mammary injection groups (Figure B.2a). Measurement on primary tumor area of mice with mammary ductal injection shows that HF-4T1.2 mice had larger primary tumor area than C-4T1.2 on D9, D13 and D16 after cell injection (Figure B.3). There is no difference for the weight and area of primary tumors, recorded during and after necropsy, among the four mammary injection groups (data not shown).

HF-4T1.2 mice had more tumors in lung than C-4T1.2 in the bone injection model as shown by H&E staining

Among the four bone injection groups, HF-4T1.2 group had significantly more tumors inside lung than C-4T1.2 group from H&E staining results presented in Figure 4.3. There is no difference for tumor number inside lung between C-4T1 and HF-4T1 groups. HF-4T1.2 group had significantly more tumors inside lung than HF-4T1 group. There is no difference for tumor number inside lung among the four groups with mammary injection (Figure B.2b). There is no difference for tumor area percentage inside lung among the four groups with bone injection

(Figure B.4) or the four mammary injection groups (data not shown). There is no difference for Ki-67 positive cell percentage among all the 8 groups (Figure B.5).

HF-4T1.2 mice had more tumors in liver than C-4T1.2 among the four bone injection groups as shown by H&E staining

From H&E staining results presented in Figure 4, HF-4T1.2 group had significantly more metastatic tumor incidence rate inside liver than C-4T1.2 group among the four bone injection groups. No metastatic tumor was found in the liver of mice in C-4T1.2 group, while liver metastatic tumors were found in 7 out of 16 mice in the HF-4T1.2 group. Among these 7 mice of the HF-4T1.2 group which developed liver metastasis, the total metastatic tumor count in the liver is 16. No metastatic tumor was found in the liver of groups injected with 4T1 cells in the bone, or the four groups with mammary injection (data not shown).

4T1.2 mice had higher liver weight and higher liver triacylglyceride (TAG) content than 4T1 mice in the bone injection model

Liver weight at necropsy showed that mice with 4T1.2 cells injected in the bone had higher liver weight than mice with 4T1 cells injected in the bone (Figure 4.5). Mice with 4T1.2 cells injected in the bone also had higher liver triacylglyceride (TAG) content than mice with 4T1 cells injected in the bone (Figure 4.6). Among the four groups with mammary injection, there is no difference on liver TAG content (data not shown); while HFD groups had higher gonadal adipose weight than CD groups in the mammary injection model (Figure B.6). There is no difference for gonadal adipose weight between the four bone injection groups (data not shown).

Discussion

The reason why HFD is studied in this project not only lies in the fact that it reflects the considerably high dietary fat intake among westerners, but also stems from the inconsistent association of dietary fat and risk of BC. HFDs have been associated with BC progression and metastasis, indicated to increase BC risk by raising estradiol level.^{7,8}

In this study, it is found in this project that in mice inoculated with 4T1.2 cells, an HFD providing 46.9% Kcal from fat increased metastatic tumors inside lung and liver compared with CD which provided 17.2% Kcal from fat, as shown by H&E staining. Mice with 4T1.2 cells had more metastatic tumors on the surface of lung than mice with 4T1 cells; while there is no difference between HFD and CD on lung surface tumor nodule count. Several reasons may explain why there was no significant difference on lung surface tumor nodule counts between HFD and CD fed groups, as illustrated below.

First, dietary fat percentage may impact study results. Some previous studies on HFD and BC used a diet containing as high as 60% Kcal from fat.^{9,91,92,94} In this study, HFD provides 46.9% Kcal from fat, which is still higher than, yet much closer to dietary fat consumption in humans. Second, different sources of fat have different effects on BC patients. Diet high in animal fat relates to a higher BC risk in sedentary women, while consumption of plant fat products may reduce the risk.⁹⁵ Mammary adenocarcinomas from high olive oil fed animals showed a low histologic grade, few necrotic and invasive areas, and a high percentage of papillary areas; while adenocarcinomas from high corn oil diet fed animals had higher degree of morphological malignancy.¹⁸⁰ Dairy fat is a source of estrogenic hormones and relates to worse BC survival. Intake of high-fat dairy was related to a higher risk of mortality after BC diagnosis.¹⁸¹ Western diet (WD) high in fat, sucrose and cholesterol have been introduced in animal models, especially in studies on metabolic syndrome. With anhydrous milk fat as a fat source, WD induces whole-body oxidative stress and elevates adiposity in male C57B1/6N mice, compared with an equal caloric HFD with lard as a fat source.⁹⁶ Matthews S.B. *et al.* used anhydrous milk fat and corn oil as fat source for HFD and found that excess weight gain accelerated carcinogen induced mammary carcinogenesis in a rat model of premenopausal BC.⁹⁷

Besides, other factors, such as dietary lipid profile, feeding time frame and duration may also impact study results. Epidemiological studies found that different types of fat may have differential effects on BC risk in post-menopausal women. For example, polyunsaturated fatty acids may protect women from BC; while saturated fat may increase BC risk.¹⁸² Previous studies on HFD and BC in animals mostly have a longer feeding duration compared with our

study. Animals were usually fed from 12 weeks to 5 months before cell injection, and at least 1 month after injection as reported.^{9,92}

Another influential factor may relate to the mice strain used, since it was reported that response to HFD in mice may be strain-dependent. In this project, BALB/c mice were used, which were referred to as obesity-resistant by some previous studies on HFD and BC.⁹ Other studies on HFD and metabolism,^{101,106} and some on diet and cancer have used C57/BL mice,^{94,183} which are more prone to gain weight and become obese on HFD. Yet in the current project, our focus is not on obesity and BC; using BALB/c mice helps to justify our goal by excluding possible effects from obesity on BC in the study. Moreover it was still reported that in pubertal BALB/c mice, HFD increased mammary epithelial cell proliferation, while in pubertal C57BL/6 mice it caused stunted mammary duct elongation and reduced mammary epithelial cell proliferation.⁹⁴

In this study, slightly higher body weight from HFD fed animals than control was observed, as expected, and intriguingly lower energy intake in the HFD groups. Yet similar findings were reported before. Ishii Y *et al.* found comparable energy intake while higher body weight in HFD rats than control.¹¹⁵ Lane *et al.* reported lower energy intake in sedentary rats fed with HFD than those on standard diet.¹¹⁷ They pointed out that organisms can react to reductions in energy intake by reducing basal energy, activity and growth rate. HFD may induce thermogenesis, and affect tumor incidence.

Studies showed that a pro-inflammatory state induced by HFD may cause cancer. For example, chronic inflammation in mice fed HFD for one year, marked by increased macrophage infiltration and fibrotic changes in the adipose tissue, led to hepatocellular carcinoma.⁹⁹ HFD can also affect lipid metabolism in the liver and energy homeostasis in the adipose tissue by modulating gene expressions. Liver tumorigenesis induced by HFD in C57Bl/6 mice was accompanied with altered gene expression of inflammatory cytokines, such as MCP-1^{xi} and NADPH^{xiii} oxidase complex.¹⁰¹ In regard to fatty-acid and lipid metabolism in mice on HFD, Nishikawa S. *et al.* reported that vacuolation of hepatocytes was severe in nine-week HFD-fed BALB/c mice, with up-regulated genes in fatty acid uptake and biosynthesis, such as CD36^{xliii}, ACACA^{xliv}, ACLY^{xlv}, and FASn^{xlvi}.¹⁰² In contrast, Montgomery M.K. *et al.* reported that BALB/c mice were protected from detrimental effects by HFD, without accumulating excess lipid in the liver, potentially due to lower fatty acid uptake.¹⁰³ Waller-Evans H. *et al.* also showed BALB/c's resistance to HFD-induced nonalcoholic fatty liver disease, though HFD did change liver gene expression of PPAR^{xlvii} signaling, fatty acid metabolism, JAK-STAT^{xlviii} signaling and steroid biosynthesis in BALB/c.¹⁰⁴

In this study, conducted histological staining and Oil-Red-O staining were on liver trying to locate lipid vacuoles. However, we did not find significant amount of liver lipid accumulation in either control animals or HFD animals (data not shown), possibly due to the fact that BALB/c mice did not gain much weight on HFD in such a short time frame (one month pre-injection feeding and three weeks post-injection feeding). However, in liver TAG content analysis, it is found in this project that mice with 4T1.2 cells had significantly more liver lipid accumulation than mice with 4T1 cells, consistent with liver weight results that mice with 4T1.2 injected in the bone had higher liver weight than mice with 4T1 cells in the bone. This may be explained by the fact that mice with 4T1.2 cells developed more aggressive metastasis than mice with 4T1 cells, and thus tend to store more nutrients in liver such as TAG for survival in the extreme situation. Though 4T1.2 is considered more aggressive than its parental cell line 4T1, comparison of them in animal models responding to dietary modulations has not been directly addressed so far.

Besides affecting metabolism and cancer growth and progression, HFDs were reported to influence gene and protein expressions in rodents with BC. In F2 mice from a cross between a polygenic obese strain and a mammary cancer strain, HFD decreased BC latency and increased pulmonary metastases. HFD altered 211 hepatic gene expressions in tumor free F2 control mice, while only changed the expression of five genes in mammary tumors; four of which are downstream of the tumor suppressor PTEN, suggesting that diet affects cancer metastasis through tumor autonomous and non-autonomous mechanisms.¹⁸⁴ In another study on athymic mice, HFD decreased protein expression of PCNA^{xlix} and Cyclin D1 in mammary fat pads, which were involved in cell proliferation, while increased Ob-Rb^l, IGF-1R^{li}, Bcl-2^{lii}, and Bax^{liii} in mammary tumors.¹⁸³ Lamas B. *et al.* reported that HFD increased primary tumor weight and volume in athymic nude mice bearing MCF-7 human BC, and expression of genes such as VEGFR2^{liv} (angiogenesis), TRADD^{lv} (apoptosis), and PTEN^{lvi} (tumor suppressor) were increased; while key regulating genes on adiponectin metabolism and lipid metabolism were decreased.⁹² Besides, there may be epigenetic mechanisms involved in how HFD in pregnancy exerts trans-generational effects on BC development. Mammary tumorigenesis was found to be higher in daughters and granddaughters of HF rat dams.¹⁸⁵ It would be worthwhile to explore the mechanism of HFD's modulation on BC metastasis and differences between the two cell lines from this project utilizing gene expression analysis in the future.

In summary, it is found in this project that an HFD containing 46.9% Kcal from fat increased metastatic tumors inside lung and liver as shown by H&E staining in BALB/c mice inoculated with murine 4T1.2 cells in the tibia, compared with control diet containing 16.9% Kcal from fat. HFD increased gonadal adipose weight in animals injected with cancer cells in mammary gland.

Mice with 4T1.2 cells developed more aggressive metastasis as shown by lung tumor nodule counts. Liver weight and triacylglyceride content analysis showed that mice with 4T1.2 cells had higher liver weight and accumulated more TAG in the liver. Future studies with a longer feeding time frame and possibly a different diet composition and lipid profile are needed to further confirm whether HFD affects BC metastasis to secondary organs. Studies examining gene expression changes modulated by HFD in primary or secondary tumor site, such as lung and liver, are in need to investigate the mechanisms on how HFD affects metabolism and modulates BC metastasis.

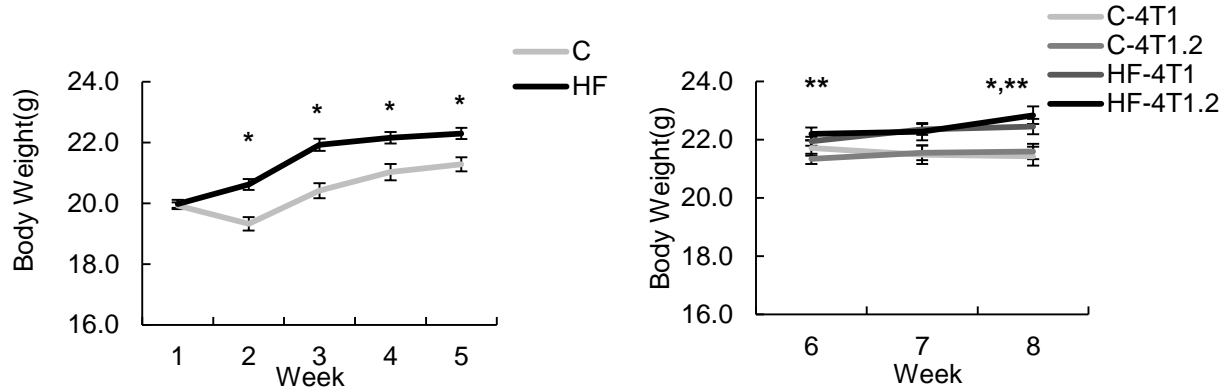
Acknowledgments

We thank the funding sources of this project as below: NCCAM BRC (P50 AT006268), DOD Breast Cancer Research Program from U.S. Army Medical Research and Materiel Command (W81XWH-09-1-0689; BC085882). This project was made possible by Grant Number P50AT006268 from the National Center for Complementary and Alternative Medicines (NCCAM), the Office of Dietary Supplements (ODS) and the National Cancer Institute (NCI). Its contents are solely the responsibility of the authors and do not necessarily represent the official views of the NCCAM, ODS, NCI, or the National Institutes of Health.

Figures and Tables

Figure 4.1

(a)



(b)

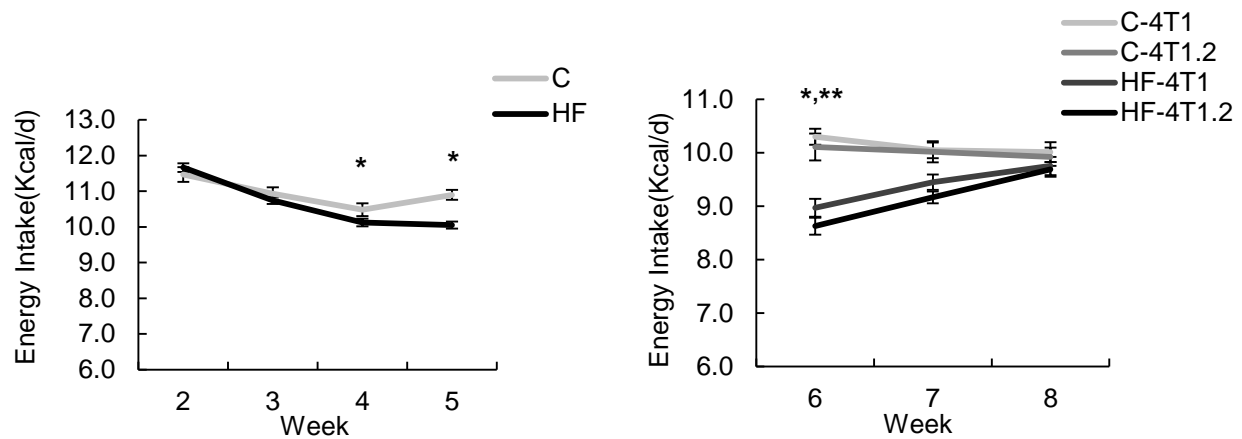


Figure 4.1 Mice on HFD had higher body weight and lower energy intake than control before and at certain time points after cell injection.

Star (*) before cell injection indicates a significant difference between HF group and C group by t-test ($p < 0.05$). After cell injection, single asterisk (*) indicates a significant difference between HF and C in mice injected with 4T1 cells; two asterisks (**) indicates a significant difference between HF and C in mice with 4T1.2 cells ($p < 0.05$). Before cell injection, all the mice were assigned to two groups, C or HF. After cell injection, mice were assigned to 8 groups. Here the body weight and energy intake of the four groups in the bone injection model is presented.

(a) Body weight of mice before and after cell injection.

(b) Energy intake of mice before and after cell injection

Figure 4.2

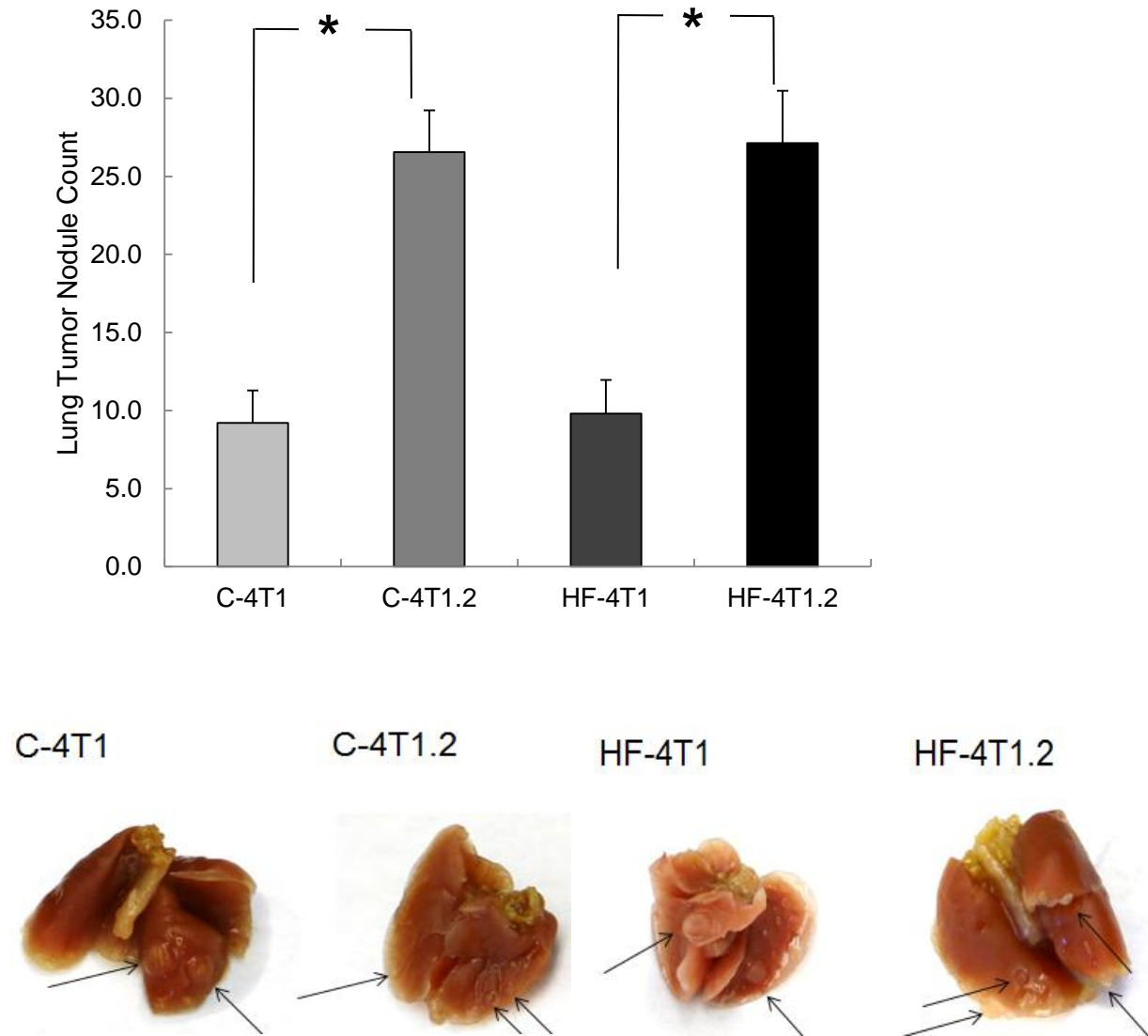


Figure 4.2 Lung tumor nodule counts in the bone injection model showed that mice with 4T1.2 cells had significantly more tumors on the surface of lung than mice with 4T1 cells.

Representative pictures of lungs with surface tumors are shown, with arrows pointing to lung surface tumor nodules. Asterisks between two columns indicate significant differences between two groups. Statistical analysis is done by Wilcoxon Rank Sum test, $p < 0.05$.

Figure 4.3

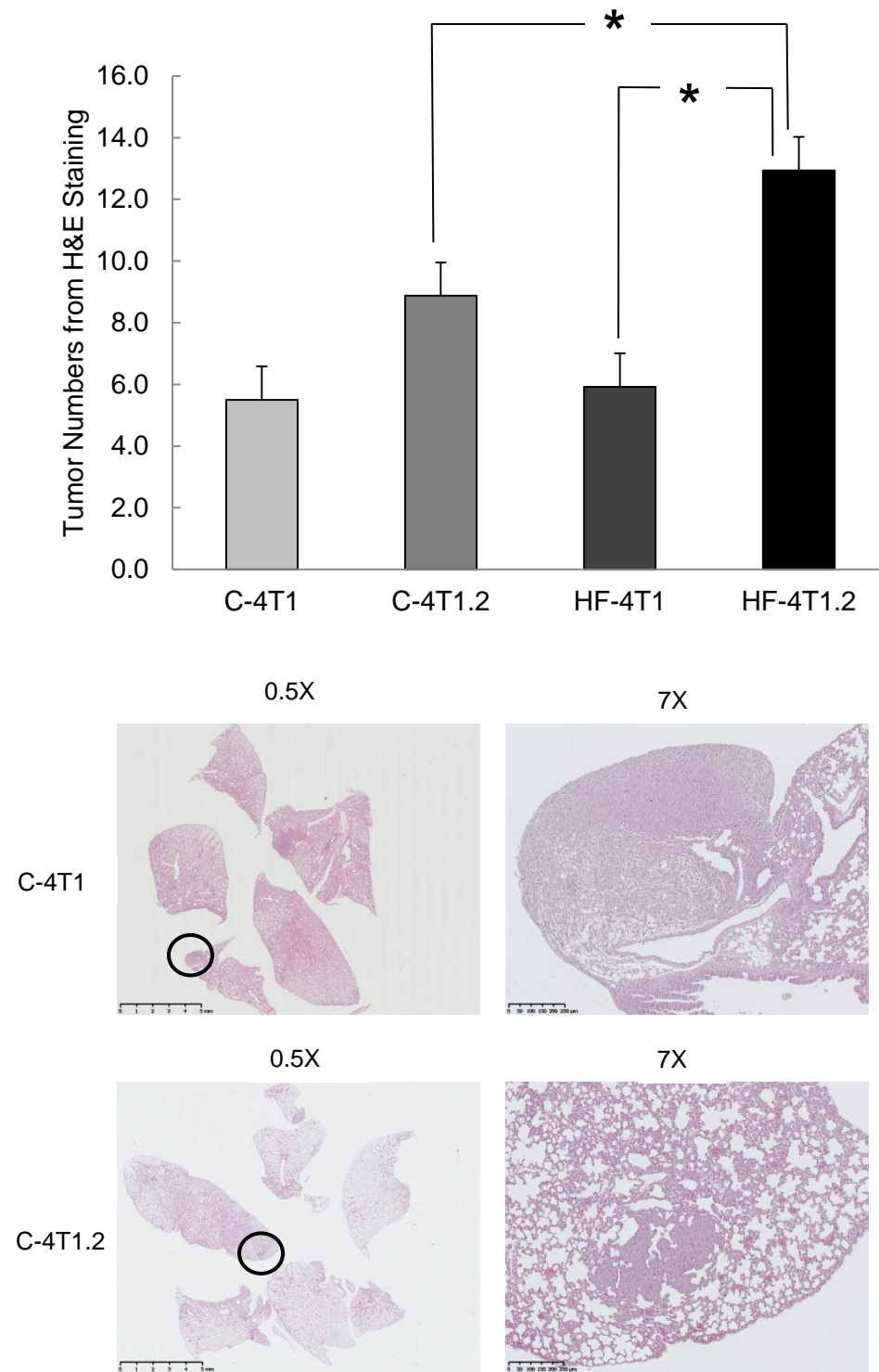


Figure 4.3 (cont.)

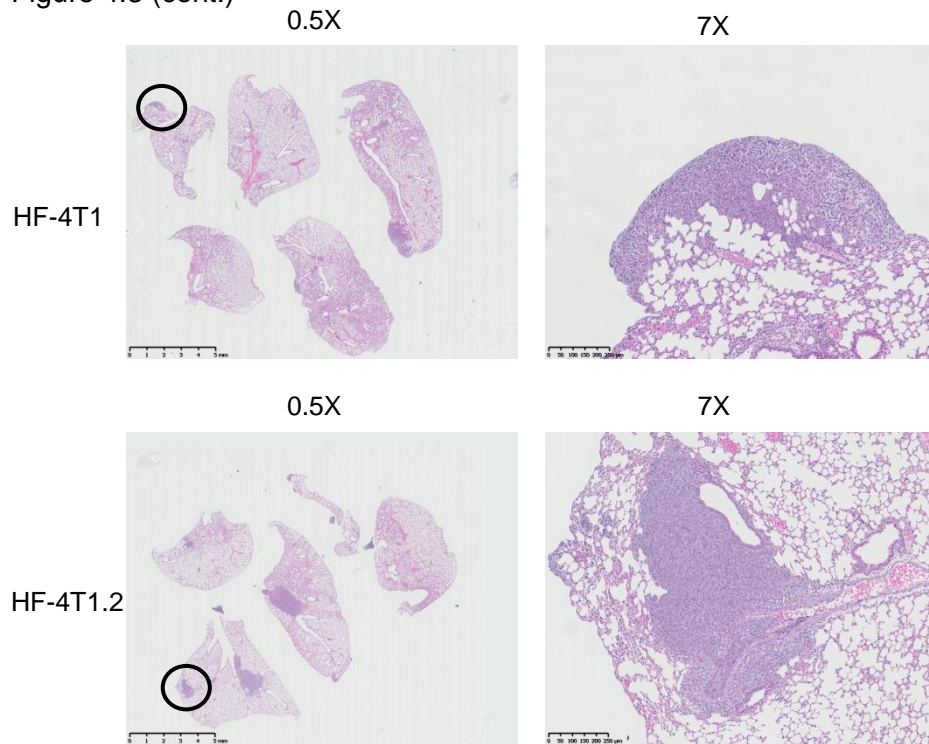


Figure 4.3 Tumor numbers inside lung in the bone injection model showed that HF-4T1.2 group had significantly more lung tumors than C-4T1.2 group as shown by H&E staining; HF-4T1.2 also had more tumors inside lung than HF-4T1.

Representative images of lung tumor by H&E staining under 0.5X and 7X objectives were shown. Circled areas indicate the specific locations of tumors displayed on the 7X images under the 0.5X lens. Asterisks between two columns indicate significant differences between two groups. Statistical analysis is done by Wilcoxon Rank Sum test, $p < 0.05$.

Figure 4.4

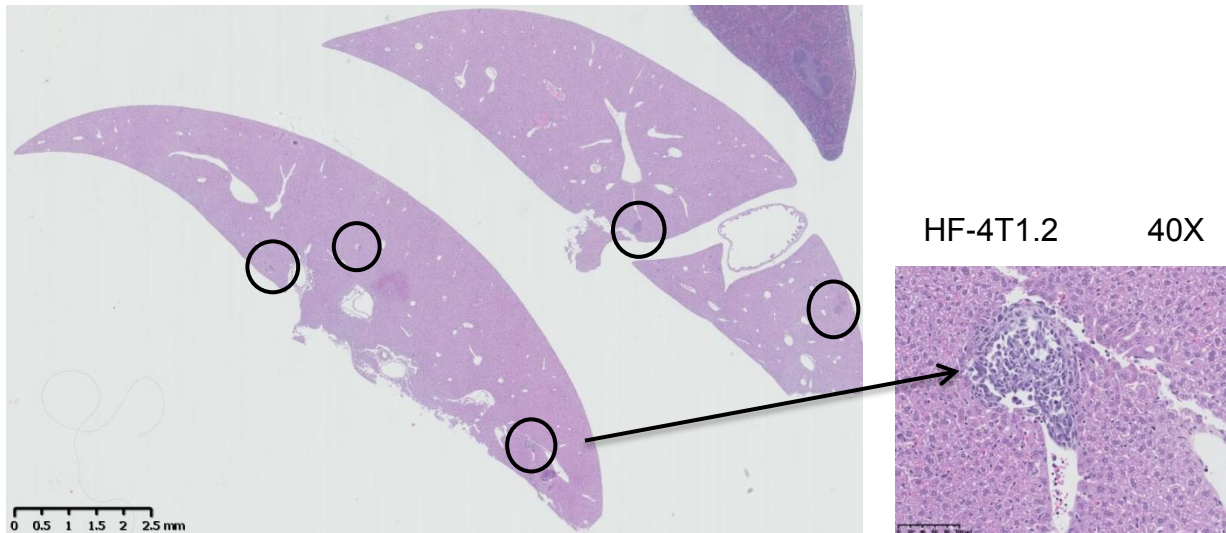
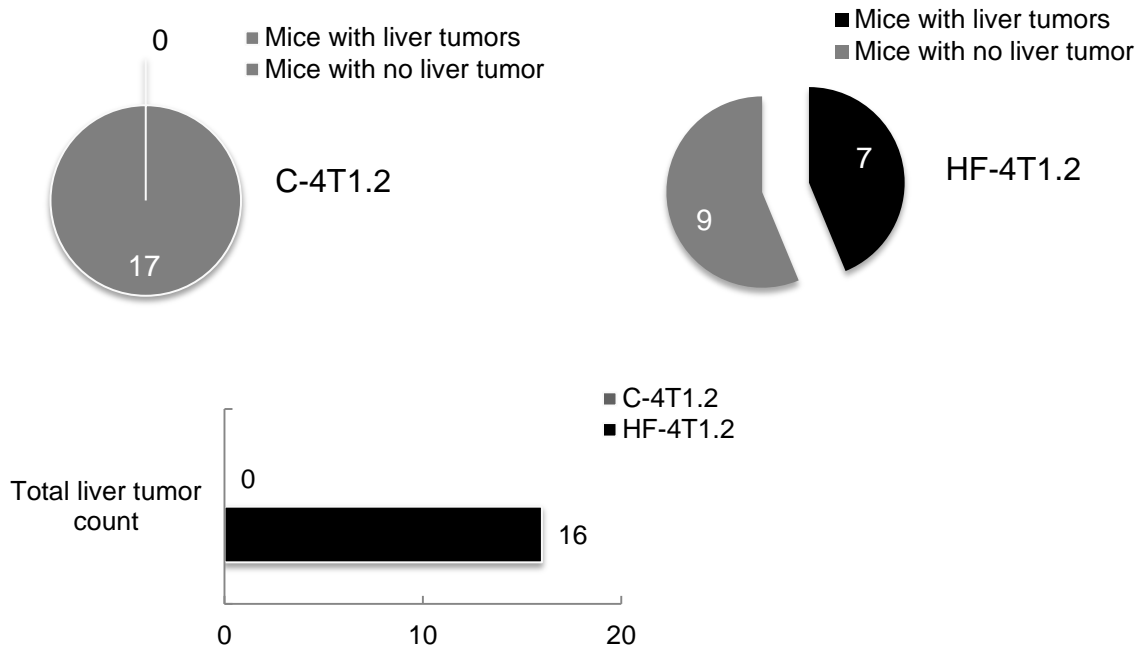


Figure 4.4 Liver metastatic tumor incidence rate in C-4T1.2 group and HF-4T1.2 groups in the bone injection model showed that HF-4T1.2 group had higher liver metastatic tumor incidence rate (7/16 with liver metastasis) than C-4T1.2 (0/17 with liver metastasis).

Representative metastatic liver tumor images by H&E staining were shown. Circles indicate the location of liver metastatic tumors from an animal in HF-4T1.2 group. The image for one of the metastatic tumors under 40X objective is also shown. Statistical analysis is done by Chi-Square test, $p < 0.05$.

Figure 4.5

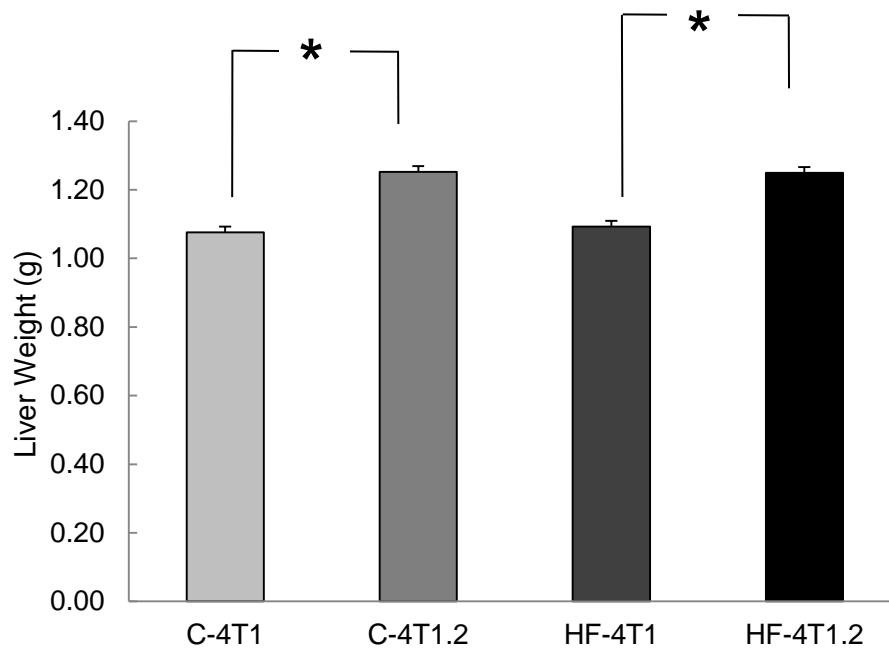


Figure 4.5 Liver weight at necropsy showed that mice with 4T1.2 cells in the bone injection model had higher liver weight than mice with 4T1 cells.

Asterisks between two columns indicate significant differences between two groups. Statistical analysis is done by ANOVA LSD, $p < 0.05$.

Figure 4.6

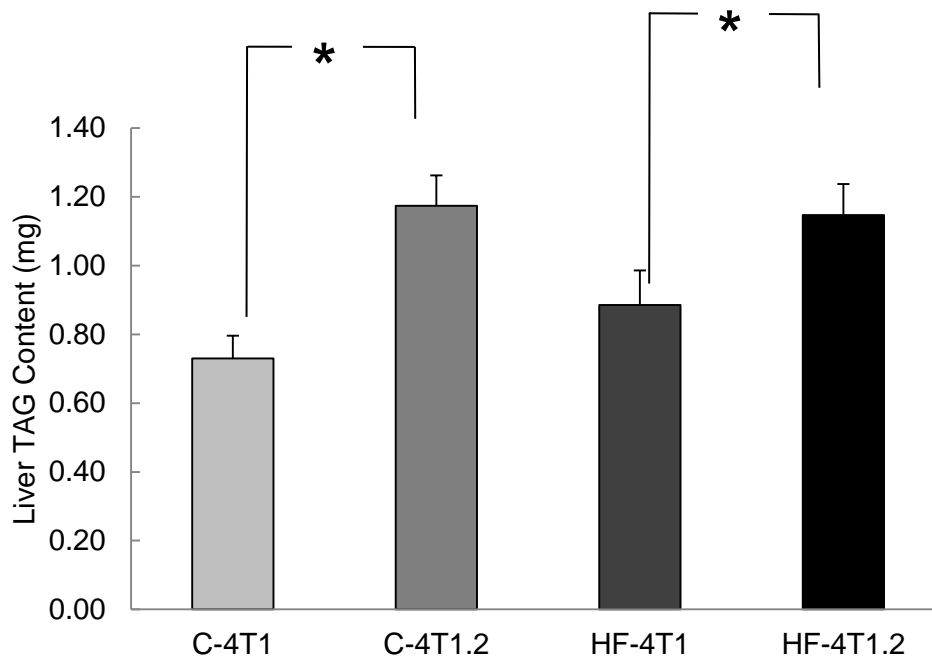


Figure 4.6 Liver Triacylglyceride (TAG) content after normalized to 50 mg liver weight showed that mice with 4T1.2 cells in the bone injection model had higher liver TAG content than mice with 4T1 cells.

Asterisks between two columns indicate significant differences between two groups. Statistical analysis is done by ANOVA LSD, $p < 0.05$.

Table 4.1 Experimental design and animal groups

Cell Injection Model	Cell Line	High Fat Diet	Control Diet
Tibial Injection Model	4T1	18 mice	18 Mice
	4T1.2	18 mice	18 Mice
Mammary Injection Model	4T1	8 Mice	8 Mice
	4T1.2	8 Mice	8 Mice

Table 4.2 Diet calories

Nutrients	High Fat Diet		Control Diet	
	Percentage by weight (g)	Percentage by energy (Kcal)	Percentage by weight (g)	Percentage by energy (Kcal)
Protein	21.2	18.4	17.7	18.8
Carbohydrate	40.2	34.8	60.1	63.9
Fat	24.0	46.8	7.2	17.2

Table 4.3 Diet composition

Macro-nutrient	Component	HFD (g/Kg)	Control Diet (g/Kg)
Carbohydrate	Corn starch	125	397
	Maltodextrin	158	132
	Sucrose	119	100
Fat	Soybean oil	83	70
	Lard	155	/

*In HFD, protein, vitamins, minerals and cellulose are increased in proportion to the increase in Kcal density.

Chapter 5 Conclusion and Future Research

In the first project, effects of the aromatase inhibitor letrozole on breast cancer metastasis from bone to the lung were evaluated. Mice that were ovariectomized had lower body estradiol level and lower uterine weight. They also had larger bone tumor area and greater integrated density on Day 14 and Day 17 as shown from BLI. Letrozole decreased serum estradiol level, reduced lung surface tumor nodules in intact mice, reduced tumor numbers inside lung as shown by H&E staining, and reduced proliferative cell percentage in lung shown by Ki-67 staining. In conclusion, ovariectomy induced more aggressive micrometastatic tumor growth in the bone and letrozole reduced BC lung metastasis by suppressing tumor proliferation. Future research of this project lies in several areas: first, molecular analysis *in vitro* would help to investigate possible mechanisms involved in letrozole's effects on reducing BC metastasis. For example, cell culture studies with 4T1 cells and letrozole given in different dosages would help to investigate whether letrozole has any effects on cell migration and invasion *in vitro*, which will provide further implication when compared with animal study. Second, expression of genes related to BC progression and metastasis can be tested in 4T1 cells cultured with letrozole, so that possible molecular pathways involved in this drug's effects on BC metastasis can be elaborated.

In the second project, effects of low calcium diet on BC metastasis in a similar murine model as the previous one was evaluated in this time-course study. Low calcium diet induced greater integrated density on the bone tumor on Day 14 and Day 17 according to BLI, and reduced lung surface tumor nodule counts in mice that were sacrificed on Day 21. Data from our collaborators showed that low calcium diet induced more damage to the bone microenvironment as well compared with the control diet. In the future, improvements can be made to further research this topic. First, a longer feeding time frame should be considered. In this project, mice were fed one month prior to cell injection. Future studies could feed several months longer. Second, tumor on the bone could be harvested from future study to conduct both histopathological staining and gene expression analysis, to show the changes from low calcium diet to the bone tumor growth as well as molecular pathways modulated by the diet. Third, analysis using 4T1 cells cultured *in vitro* with a low calcium diet can be conducted to examine whether the diet affects cell growth, invasion, or migration. Gene expression analysis can also be conducted to demonstrate molecular changes induced by a low calcium diet to the tumor cells.

In the third project, high fat diet increased tumor numbers inside both lung and liver in mice injected with 4T1.2 tumor cells as shown by H&E staining. Mice with the 4T1.2 cells had

significantly more aggressive lung metastasis shown by lung surface tumor counts. Future research for this project would be: molecular analysis on the liver tissue is needed to demonstrate the gene expression differences in liver induced by the high fat diet, especially genes related to inflammation and cancer metastasis. On the other hand, genes related to metabolism in liver, such as lipid or fatty acid synthesis and breakdown, or glycogen synthesis and breakdown, could be tested to see whether there is any difference between mice injected with the two different cells lines. The higher liver weight and more TAG accumulation in mice received 4T1.2 cell injection as seen from this current study could be attributed to the fact that more aggressive tumor growth in these animals would need more nutrient supply from their host organs. Further investigation in this arena would be both meaningful and intriguing.

References

1. Jemal A, Bray F, Center MM, Ferlay J, Ward E, Forman D. Global cancer statistics. *CA: A Cancer Journal for Clinicians*. 2011;61(2):69-90.
2. Eckhardt BL, Francis PA, Parker BS, Anderson RL. Strategies for the discovery and development of therapies for metastatic breast cancer. *Nat Rev Drug Discov*. 2012;11(6):479-497.
3. Kim EJ, Shin M, Park H, et al. Oral administration of 3,3'-diindolylmethane inhibits lung metastasis of 4T1 murine mammary carcinoma cells in BALB/c mice. *J Nutr*. 2009;139(12):2373-9.
4. Ju YH, Allred KF, Allred CD, Helferich WG. Genistein stimulates growth of human breast cancer cells in a novel, postmenopausal animal model, with low plasma estradiol concentrations. *Carcinogenesis*. June 2006;27(6):1292-1299.
5. Ju YH, Doerge DR, Woodling KA, Hartman JA, Kwak J, Helferich WG. Dietary genistein negates the inhibitory effect of letrozole on the growth of aromatase-expressing estrogen-dependent human breast cancer cells (MCF-7Ca) in vivo. *Carcinogenesis*. 2008;29(11):2162-2168.
6. Yang X, Belosay A, Du M, et al. Estradiol increases ER-negative breast cancer metastasis in an experimental model. *Clin Exp Metastasis*. 2013;30(6):711-721.
7. Shaharudin SH, Sulaiman S, Shahril MR, Emran NA, Akmal SN. Dietary changes among breast cancer patients in malaysia. *Cancer Nurs*. 2013;36(2):131-138.
8. Turner LB. A meta-analysis of fat intake, reproduction, and breast cancer risk: An evolutionary perspective. *Am J Hum Biol*. 2011;23(5):601-608.
9. Kim EJ, Choi MR, Park H, et al. Dietary fat increases solid tumor growth and metastasis of 4T1 murine mammary carcinoma cells and mortality in obesity-resistant BALB/c mice. *Breast Cancer Res*. 2011;13(4):R78.
10. Servick K. Breast cancer: A world of differences. *Science*. 2014;343(6178):1452-1453.
11. Anderson BO. Breast Cancer—Thinking globally. *Science*. 2014;343(6178):1403-1403.
12. Mitropoulou TN, Tzanakakis GN, Kletsas D, Kalofonos HP, Karamanos NK. Letrozole as a potent inhibitor of cell proliferation and expression of metalloproteinases (MMP-2 and MMP-9) by human epithelial breast cancer cells. *Int J Cancer*. 2003;104(2):155-60.
13. Lee YT. Breast carcinoma: Pattern of metastasis at autopsy. *J Surg Oncol*. 1983;23(3):175-180.
14. Planchard D, Soria JC, Michiels S, et al. Uncertain benefit from surgery in patients with lung metastases from breast carcinoma. *Cancer*. 2004;100(1):28-35.
15. Kolodziejcki L, Goralczyk J, Dyczek S, Duda K, Dymek H, Nabialek T. Analysis of indications and results of surgical treatment for patients with pulmonary metastasis. *Pneumonol Alergol Pol*. 1999;67(5-6):228-236.
16. Martin TJ, Moseley JM. Mechanisms in the skeletal complications of breast cancer. *Endocr Relat Cancer*. 2000;7(4):271-284.
17. Ding X, Fan Y, Ma F, et al. Prolonged administration of bisphosphonates is well-tolerated and effective for skeletal-related events in chinese breast cancer patients with bone metastasis. *Breast*. 2012;21(4):544-549.
18. Guise TA. Breast cancer bone metastases: It's all about the neighborhood. *Cell*. 2013;154(5):957-959.
19. Murphy BO, Joshi S, Kessinger A, Reed E, Sharp JG. A murine model of bone marrow micrometastasis in breast cancer. *Clin Exp Metastasis*. 2002;19(7):561-569.
20. Gupta GP, Nguyen DX, Chiang AC, et al. Mediators of vascular remodelling co-opted for sequential steps in lung metastasis. *Nature*. 2007;446(7137):765-770.
21. Gupta GP, Minn AJ, Kang Y, et al. Identifying site-specific metastasis genes and functions. *Cold Spring Harb Symp Quant Biol*. 2005;70:149-158.
22. Gupta GP, Massague J. Cancer metastasis: Building a framework. *Cell*. 2006;127(4):679-695.

23. Lucci A, Krishnamurthy S, Singh B, et al. Cyclooxygenase-2 expression in primary breast cancers predicts dissemination of cancer cells to the bone marrow. *Breast Cancer Res Treat.* 2009;117(1):61-68.
24. Wilson C, Holen I, Coleman RE. Seed, soil and secreted hormones: Potential interactions of breast cancer cells with their endocrine/paracrine microenvironment and implications for treatment with bisphosphonates. *Cancer Treat Rev.* 2012;38(7):877-889.
25. Pantel K, Otte M. Occult micrometastasis: Enrichment, identification and characterization of single disseminated tumour cells. *Semin Cancer Biol.* 2001;11(5):327-337.
26. Vincent-Salomon A, Bidard FC, Pierga JY. Bone marrow micrometastasis in breast cancer: Review of detection methods, prognostic impact and biological issues. *Journal of Clinical Pathology.* 2008;61(5):570-576.
27. Molino A, Giovannini M, Micciolo R, et al. Bone marrow micrometastases in breast cancer patients: A long-term follow-up study. *Clin Med Oncol.* 2008;2:487-490.
28. Braun S, Cevatli BS, Assemi C, et al. Comparative analysis of micrometastasis to the bone marrow and lymph nodes of node-negative breast cancer patients receiving no adjuvant therapy. *Journal of Clinical Oncology.* 2001;19(5):1468-1475.
29. Braun S, Vogl FD, Naume B, et al. A pooled analysis of bone marrow micrometastasis in breast cancer. *N Engl J Med.* 2005;353(8):793-802.
30. Jenkins DE, Hornig YS, Oei Y, Dusich J, Purchio T. Bioluminescent human breast cancer cell lines that permit rapid and sensitive in vivo detection of mammary tumors and multiple metastases in immune deficient mice. *Breast Cancer Res.* 2005;7(4):R444-54.
31. Hartkopf AD, Taran F, Wallwiener M, et al. Prognostic relevance of disseminated tumour cells from the bone marrow of early stage breast cancer patients – results from a large single-centre analysis. *Eur J Cancer.* 2014;50(15):2550-2559.
32. Riethdorf S, Wikman H, Pantel K. Review: Biological relevance of disseminated tumor cells in cancer patients. *International Journal of Cancer.* 2008;123(9):1991-2006.
33. Falck AK, Bendahl PO, Ingvar C, et al. Analysis of and prognostic information from disseminated tumour cells in bone marrow in primary breast cancer: A prospective observational study. *BMC Cancer.* 2012;12:403-2407-12-403.
34. Cristofanilli M, Budd GT, Ellis MJ, et al. Circulating tumor cells, disease progression, and survival in metastatic breast cancer. *N Engl J Med.* 2004;351(8):781-791.
35. Macedo LF, Sabnis G, Brodie A. Aromatase inhibitors and breast cancer. *Ann N Y Acad Sci.* 2009;1155:162-73.
36. Iwase H. Current topics and perspectives on the use of aromatase inhibitors in the treatment of breast cancer. *Breast Cancer.* 2008;15(4):278-290.
37. Kataoka M, Yamaguchi Y, Moriya Y, et al. Antitumor activity of chemoendocrine therapy in premenopausal and postmenopausal models with human breast cancer xenografts. *Oncol Rep.* 2012;27(2):303-310.
38. Park IH, Ro J, Lee KS, et al. Phase II parallel group study showing comparable efficacy between premenopausal metastatic breast cancer patients treated with letrozole plus goserelin and postmenopausal patients treated with letrozole alone as first-line hormone therapy. *J Clin Oncol.* 2010;28(16):2705-11.
39. Yao S, Xu B, Li Q, et al. Goserelin plus letrozole as first- or second-line hormonal treatment in premenopausal patients with advanced breast cancer. *Endocr J.* 2011;58(6):509-516.
40. Torrìsi R, Bagnardi V, Rotmensz N, et al. Letrozole plus GnRH analogue as preoperative and adjuvant therapy in premenopausal women with ER positive locally advanced breast cancer. *Breast Cancer Res Treat.* 2011;126(2):431-441.
41. Luthra R, Kirma N, Jones J, Tekmal RR. Use of letrozole as a chemopreventive agent in aromatase overexpressing transgenic mice. *J Steroid Biochem Mol Biol.* 2003;86(3-5):461-7.

42. Kubatka P, Sadlonova V, Kajo K, Nosalova G, Fetisovova Z. Preventive effects of letrozole in the model of premenopausal mammary carcinogenesis. *Neoplasma*. 2008;55(1):42-46.
43. Brodie A, Macedo L, Sabnis G. Aromatase resistance mechanisms in model systems in vivo. *J Steroid Biochem Mol Biol*. 2010;118(4-5):283-7.
44. Brodie A, Sabnis G, Macedo L. Xenograft models for aromatase inhibitor studies. *J Steroid Biochem Mol Biol*. 2007;106(1-5):119-24.
45. Masri S, Liu Z, Phung S, Wang E, Yuan YC, Chen S. The role of microRNA-128a in regulating TGFbeta signaling in letrozole-resistant breast cancer cells. *Breast Cancer Res Treat*. 2010;124(1):89-99.
46. Muraoka RS, Dumont N, Ritter CA, et al. Blockade of TGF-beta inhibits mammary tumor cell viability, migration, and metastases. *J Clin Invest*. 2002;109(12):1551-1559.
47. Nair BC, Vallabhaneni S, Tekmal RR, Vadlamudi RK. Roscovitine confers tumor suppressive effect on therapy-resistant breast tumor cells. *Breast Cancer Res*. 2011;13(3):R80.
48. Saha Roy S, Chakravarty D, Cortez V, et al. Significance of PELP1 in ER-negative breast cancer metastasis. *Mol Cancer Res*. 2011.
49. Macedo LF, Sabnis G, Brodie A. Preclinical modeling of endocrine response and resistance: Focus on aromatase inhibitors. *Cancer*. 2008;112(3 Suppl):679-88.
50. Sabnis G, Brodie A. Adaptive changes results in activation of alternate signaling pathways and resistance to aromatase inhibitor resistance. *Mol Cell Endocrinol*. 2010.
51. Yang X, Belosay A, Hartman JA, et al. Dietary soy isoflavones increase metastasis to lungs in an experimental model of breast cancer with bone micro-tumors. *Clin Exp Metastasis*. 2015;32(4):323-333.
52. Goss PE, Ingle JN, Martino S, et al. Randomized trial of letrozole following tamoxifen as extended adjuvant therapy in receptor-positive breast cancer: Updated findings from NCIC CTG MA.17. *Journal of the National Cancer Institute*. 2005;97(17):1262-1271.
53. Núñez NP, Jelovac D, Macedo L, et al. Effects of the antiestrogen tamoxifen and the aromatase inhibitor letrozole on serum hormones and bone characteristics in a preclinical tumor model for breast cancer. *Clinical Cancer Research*. 2004;10(16):5375-5380.
54. Goss PE, Qi S, Cheung AM, Hu H, Mendes M, Pritzker KPH. Effects of the steroidal aromatase inhibitor exemestane and the nonsteroidal aromatase inhibitor letrozole on bone and lipid metabolism in ovariectomized rats. *Clinical Cancer Research*. 2004;10(17):5717-5723.
55. Balakrishnan A, Ravichandran D. Early operable breast cancer in elderly women treated with an aromatase inhibitor letrozole as sole therapy. *Br J Cancer*. 2011;105(12):1825-1829.
56. Hadji P, Bundred N. Reducing the risk of cancer treatment-associated bone loss in patients with breast cancer. *Semin Oncol*. 2007;34, Supplement 4(0):S4-S10.
57. Servitja S, Nogués X, Prieto-Alhambra D, et al. Bone health in a prospective cohort of postmenopausal women receiving aromatase inhibitors for early breast cancer. *The Breast*. 2012;21(1):95-101.
58. Ingle JN. Postmenopausal women with hormone receptor-positive breast cancer: Balancing benefit and toxicity from aromatase inhibitors. *The Breast*. 2013;22, Supplement 2(0):S180-S183.
59. Mincey BA, Duh MS, Thomas SK, et al. Risk of cancer Treatment—Associated bone loss and fractures among women with breast cancer receiving aromatase inhibitors. *Clinical Breast Cancer*. 2006;7(2):127-132.
60. Ipekci SH, Baldane S, Ozturk E, et al. Letrozole induced hypercalcemia in a patient with breast cancer. *Case Rep Oncol Med*. 2014;2014:608585.
61. McCaig FM. A study of the effects of the aromatase inhibitors anastrozole and letrozole on bone metabolism in postmenopausal women with estrogen receptor-positive breast cancer. *Breast Cancer Res Treat*. 2010;119:643-651.

62. McCloskey EV, Hannon RA, Lakner G, et al. Effects of third generation aromatase inhibitors on bone health and other safety parameters: Results of an open, randomised, multi-centre study of letrozole, exemestane and anastrozole in healthy postmenopausal women. *Eur J Cancer*. 2007;43(17):2523-2531.
63. Goss P, Hadji P, Subar M, Abreu P, Thomsen T, Banke-Bochita J. Effects of steroidal and nonsteroidal aromatase inhibitors on markers of bone turnover in healthy postmenopausal women. *Breast Cancer Research*. 2007;9(4):R52.
64. Tang SC. Women and bone health: Maximizing the benefits of aromatase inhibitor therapy. *Oncology*. 2010;79(1-2):13-26.
65. Park IH, Ro J, Lee KS, et al. Phase II parallel group study showing comparable efficacy between premenopausal metastatic breast cancer patients treated with letrozole plus goserelin and postmenopausal patients treated with letrozole alone as first-line hormone therapy. *Journal of Clinical Oncology*. 2010;28(16):2705-2711.
66. Ruddy KJ, DeSantis SD, Barry W, et al. Extended therapy with letrozole and ovarian suppression in premenopausal patients with breast cancer after tamoxifen. *Clinical Breast Cancer*. 2014(0).
67. Guise T. Examining the metastatic niche: Targeting the microenvironment. *Semin Oncol*. 2010;37 Suppl 2:S2-14.
68. Ooi LL, Zheng Y, Stalgis-Bilinski K, Dunstan CR. The bone remodeling environment is a factor in breast cancer bone metastasis. *Bone*. 2011;48(1):66-70.
69. Weilbaecher KN, Guise TA, McCauley LK. Cancer to bone: A fatal attraction. *Nat Rev Cancer*. 2011;11(6):411-425.
70. Su X, Colditz GA, Collins LC, et al. Adolescent intakes of vitamin D and calcium and incidence of proliferative benign breast disease. *Breast Cancer Res Treat*. 2012;134(2):783-791.
71. Anderson LN, Cotterchio M, Vieth R, Knight JA. Vitamin D and calcium intakes and breast cancer risk in pre- and postmenopausal women. *Am J Clin Nutr*. 2010;91(6):1699-1707.
72. Kawase T, Matsuo K, Suzuki T, et al. Association between vitamin D and calcium intake and breast cancer risk according to menopausal status and receptor status in japan. *Cancer Sci*. 2010;101(5):1234-1240.
73. Abbas S, Linseisen J, Rohrmann S, et al. Dietary intake of vitamin D and calcium and breast cancer risk in the european prospective investigation into cancer and nutrition. *Nutr Cancer*. 2013;65(2):178-187.
74. Almquist M, Manjer J, Bondeson L, Bondeson AG. Serum calcium and breast cancer risk: Results from a prospective cohort study of 7,847 women. *Cancer Causes Control*. 2007;18(6):595-602.
75. Almquist M, Bondeson AG, Bondeson L, Malm J, Manjer J. Serum levels of vitamin D, PTH and calcium and breast cancer risk-a prospective nested case-control study. *Int J Cancer*. 2010;127(9):2159-2168.
76. Hu Z, Zhang Z, Guise T, Seth P. Systemic delivery of an oncolytic adenovirus expressing soluble transforming growth factor-beta receptor II-fc fusion protein can inhibit breast cancer bone metastasis in a mouse model. *Hum Gene Ther*. 2010;21(11):1623-1629.
77. Liang H, Ma SY, Mohammad K, Guise TA, Balian G, Shen FH. The reaction of bone to tumor growth from human breast cancer cells in a rat spine single metastasis model. *Spine (Phila Pa 1976)*. 2011;36(7):497-504.
78. D'Ambrosio J, Fatatis A. Osteoblasts modulate Ca²⁺ signaling in bone-metastatic prostate and breast cancer cells. *Clin Exp Metastasis*. 2009;26(8):955-964.
79. Peterlik M, Cross HS. Vitamin D and calcium insufficiency-related chronic diseases: Molecular and cellular pathophysiology. *Eur J Clin Nutr*. 2009;63(12):1377-1386.
80. Berube S, Diorio C, Masse B, et al. Vitamin D and calcium intakes from food or supplements and mammographic breast density. *Cancer Epidemiol Biomarkers Prev*. 2005;14(7):1653-1659.

81. Lin J, Manson JE, Lee IM, Cook NR, Buring JE, Zhang SM. Intakes of calcium and vitamin D and breast cancer risk in women. *Arch Intern Med*. 2007;167(10):1050-1059.
82. Peterlik M, Kallay E, Cross HS. Calcium nutrition and extracellular calcium sensing: Relevance for the pathogenesis of osteoporosis, cancer and cardiovascular diseases. *Nutrients*. 2013;5(1):302-327.
83. Lopez-Fernandez I, Schepelmann M, Brennan SC, Yarova PL, Riccardi D. The calcium-sensing receptor: Just one-of-a-kind. *Exp Physiol*. 2015.
84. Mihai R. The calcium sensing receptor: From understanding parathyroid calcium homeostasis to bone metastases. *Ann R Coll Surg Engl*. 2008;90(4):271-277.
85. Liu G, Hu X, Chakrabarty S. Calcium sensing receptor down-regulates malignant cell behavior and promotes chemosensitivity in human breast cancer cells. *Cell Calcium*. 2009;45(3):216-225.
86. Saidak Z, Boudot C, Abdoune R, et al. Extracellular calcium promotes the migration of breast cancer cells through the activation of the calcium sensing receptor. *Exp Cell Res*. 2009;315(12):2072-2080.
87. Leclercq G. Calcium-induced activation of estrogen receptor alpha--new insight. *Steroids*. 2012;77(10):924-927.
88. Divekar SD, Storch GB, Sperle K, et al. The role of calcium in the activation of estrogen receptor-alpha. *Cancer Res*. 2011;71(5):1658-1668.
89. Peters AA, Simpson PT, Bassett JJ, et al. Calcium channel TRPV6 as a potential therapeutic target in estrogen receptor-negative breast cancer. *Mol Cancer Ther*. 2012;11(10):2158-2168.
90. Britschgi A, Bill A, Brinkhaus H, et al. Calcium-activated chloride channel ANO1 promotes breast cancer progression by activating EGFR and CAMK signaling. *Proc Natl Acad Sci U S A*. 2013;110(11):E1026-34.
91. Zhao Y, Tan YS, Aupperlee MD, et al. Pubertal high fat diet: Effects on mammary cancer development. *Breast Cancer Res*. 2013;15(5):R100.
92. Lamas B, Nachat-Kappes R, Goncalves-Mendes N, et al. Dietary fat without body weight gain increases in vivo MCF-7 human breast cancer cell growth and decreases natural killer cell cytotoxicity. *Mol Carcinog*. 2013.
93. Rose DP, Connolly JM, Meschter CL. Effect of dietary fat on human breast cancer growth and lung metastasis in nude mice. *J Natl Cancer Inst*. 1991;83(20):1491-1495.
94. Olson LK, Tan Y, Zhao Y, Aupperlee MD, Haslam SZ. Pubertal exposure to high fat diet causes mouse strain-dependent alterations in mammary gland development and estrogen responsiveness. *Int J Obes (Lond)*. 2010;34(9):1415-1426.
95. Kruk J, Marchlewicz M. Dietary fat and physical activity in relation to breast cancer among polish women. *Asian Pac J Cancer Prev*. 2013;14(4):2495-2502.
96. Heinonen I, Rinne P, Ruuhonen ST, Ruuhonen S, Ahotupa M, Savontaus E. The effects of equal caloric high fat and western diet on metabolic syndrome, oxidative stress and vascular endothelial function in mice. *Acta Physiologica*. 2014:n/a-n/a.
97. Matthews SB, Zhu Z, Jiang W, McGinley JN, Neil ES, Thompson HJ. Excess weight gain accelerates 1-methyl-1-nitrosourea-induced mammary carcinogenesis in a rat model of premenopausal breast cancer. *Cancer Prev Res (Phila)*. 2014;7(3):310-318.
98. Sun X, Zhang J, Gupta R, Macgibbon AK, Kuhn-Sherlock B, Krissansen GW. Dairy milk fat augments paclitaxel therapy to suppress tumour metastasis in mice, and protects against the side-effects of chemotherapy. *Clin Exp Metastasis*. 2011;28(7):675-688.
99. Itoh M, Suganami T, Nakagawa N, et al. Melanocortin 4 receptor-deficient mice as a novel mouse model of nonalcoholic steatohepatitis. *Am J Pathol*. 2011;179(5):2454-2463.
100. Kampschulte M, Stockl C, Langheinrich AC, et al. Western diet in ApoE-LDLR double-deficient mouse model of atherosclerosis leads to hepatic steatosis, fibrosis, and tumorigenesis. *Lab Invest*. 2014.
101. Tajima K, Nakamura A, Shirakawa J, et al. Metformin prevents liver tumorigenesis induced by high-fat diet in C57Bl/6 mice. *Am J Physiol Endocrinol Metab*. 2013;305(8):E987-98.

102. Nishikawa S, Sugimoto J, Okada M, Sakairi T, Takagi S. Gene expression in livers of BALB/C and C57BL/6J mice fed a high-fat diet. *Toxicol Pathol*. 2012;40(1):71-82.
103. Montgomery MK, Hallahan NL, Brown SH, et al. Mouse strain-dependent variation in obesity and glucose homeostasis in response to high-fat feeding. *Diabetologia*. 2013;56(5):1129-1139.
104. Waller-Evans H, Hue C, Fearnside J, et al. Nutrigenomics of high fat diet induced obesity in mice suggests relationships between susceptibility to fatty liver disease and the proteasome. *PLoS One*. 2013;8(12):e82825.
105. Rizki G, Arnaboldi L, Gabrielli B, et al. Mice fed a lipogenic methionine-choline-deficient diet develop hypermetabolism coincident with hepatic suppression of SCD-1. *J Lipid Res*. 2006;47(10):2280-2290.
106. Figarola JL, Singhal P, Rahbar S, Gugiu BG, Awasthi S, Singhal SS. COH-SR4 reduces body weight, improves glycemic control and prevents hepatic steatosis in high fat diet-induced obese mice. *PLoS One*. 2013;8(12):e83801.
107. Huang X, Yang C, Luo Y, Jin C, Wang F, McKeenan WL. FGFR4 prevents hyperlipidemia and insulin resistance but underlies high-fat diet induced fatty liver. *Diabetes*. 2007;56(10):2501-2510.
108. Ye R, Jung DY, Jun JY, et al. Grp78 heterozygosity promotes adaptive unfolded protein response and attenuates diet-induced obesity and insulin resistance. *Diabetes*. 2010;59(1):6-16.
109. Satyanarayana A, Klarmann KD, Gavrilova O, Keller JR. Ablation of the transcriptional regulator Id1 enhances energy expenditure, increases insulin sensitivity, and protects against age and diet induced insulin resistance, and hepatosteatosis. *FASEB J*. 2012;26(1):309-323.
110. Marcelin G, Liu SM, Li X, Schwartz GJ, Chua S. Genetic control of ATGL-mediated lipolysis modulates adipose triglyceride stores in leptin-deficient mice. *J Lipid Res*. 2012;53(5):964-972.
111. Bjorndal B, Berge C, Ramsvik MS, et al. A fish protein hydrolysate alters fatty acid composition in liver and adipose tissue and increases plasma carnitine levels in a mouse model of chronic inflammation. *Lipids Health Dis*. 2013;12:143-511X-12-143.
112. West DB, Blohm FY, Truett AA, DeLany JP. Conjugated linoleic acid persistently increases total energy expenditure in AKR/J mice without increasing uncoupling protein gene expression. *The Journal of Nutrition*. 2000;130(10):2471-2477.
113. Johnston SL, Souter DM, Tolcamp BJ, et al. Intake compensates for resting metabolic rate variation in female C57BL/6J mice fed high-fat diets. *Obesity (Silver Spring)*. 2007;15(3):600-606.
114. Hambly C, Adams A, Fustin JM, Rance KA, Bunger L, Speakman JR. Mice with low metabolic rates are not susceptible to weight gain when fed a high-fat diet. *Obes Res*. 2005;13(3):556-566.
115. Ishii Y, Ohta T, Sasase T, et al. A high-fat diet inhibits the progression of diabetes mellitus in type 2 diabetic rats. *Nutr Res*. 2010;30(7):483-491.
116. Lane HW, Teer P, Keith RE, White MT, Strahan S. Reduced energy intake and moderate exercise reduce mammary tumor incidence in virgin female BALB/c mice treated with 7,12-dimethylbenz(a)anthracene. *The Journal of Nutrition*. 1991;121(11):1883-1888.
117. Lane HW, Keith RE, Strahan S, White MT. The effect of diet, exercise and 7,12-dimethylbenz(a)anthracene on food intake, body composition and carcass energy levels in virgin female BALB/c mice. *J Nutr*. 1991;121(11):1876-1882.
118. Haramizu S, Nagasawa A, Ota N, Hase T, Tokimitsu I, Murase T. Different contribution of muscle and liver lipid metabolism to endurance capacity and obesity susceptibility of mice. *J Appl Physiol (1985)*. 2009;106(3):871-879.
119. Vaanholt LM, Jonas I, Doornbos M, et al. Metabolic and behavioral responses to high-fat feeding in mice selectively bred for high wheel-running activity. *Int J Obes (Lond)*. 2008;32(10):1566-1575.
120. Hino S, Sakamoto A, Nagaoka K, et al. FAD-dependent lysine-specific demethylase-1 regulates cellular energy expenditure. *Nat Commun*. 2012;3:758.

121. Pessentheiner AR, Pelzmann HJ, Walenta E, et al. NAT8L (N-acetyltransferase 8-like) accelerates lipid turnover and increases energy expenditure in brown adipocytes. *J Biol Chem*. 2013;288(50):36040-36051.
122. Altintas MM, Rossetti MA, Nayer B, et al. Apoptosis, mastocytosis, and diminished adipocytokine gene expression accompany reduced epididymal fat mass in long-standing diet-induced obese mice. *Lipids Health Dis*. 2011;10:198-511X-10-198.
123. Morita M, Oike Y, Nagashima T, et al. Obesity resistance and increased hepatic expression of catabolism-related mRNAs in Cnot3^{+/-} mice. *EMBO J*. 2011;30(22):4678-4691.
124. Tao K, Fang M, Alroy J, Sahagian GG. Imagable 4T1 model for the study of late stage breast cancer. *BMC Cancer*. 2008;8:228.
125. Xanthopoulos JM, Romano AE, Majumdar SK. Response of mouse breast cancer cells to anastrozole, tamoxifen, and the combination. *J Biomed Biotechnol*. 2005;2005(1):10-19.
126. Wang T, Wyrick KL, Meadows GG, Wills TB, Vorderstrasse BA. Activation of the aryl hydrocarbon receptor by TCDD inhibits mammary tumor metastasis in a syngeneic mouse model of breast cancer. *Toxicological Sciences*. 2011;124(2):291-298.
127. Banka CL, Lund CV, Nguyen MTN, Pakchoian AJ, Mueller BM, Eliceiri BP. Estrogen induces lung metastasis through a host Compartment-Specific response. *Cancer Research*. 2006;66(7):3667-3672.
128. Gupta PB, Kuperwasser C. Contributions of estrogen to ER-negative breast tumor growth. *J Steroid Biochem Mol Biol*. 2006;102(1-5):71-78.
129. Iyer V, Klebba I, McCready J, et al. Estrogen promotes ER-negative tumor growth and angiogenesis through mobilization of bone marrow-derived monocytes. *Cancer Res*. 2012;72(11):2705-2713.
130. Tester AM, Ruangpanit N, Anderson RL, Thompson EW. MMP-9 secretion and MMP-2 activation distinguish invasive and metastatic sublines of a mouse mammary carcinoma system showing epithelial-mesenchymal transition traits. *Clin Exp Metastasis*. 2000;18(7):553-560.
131. Lelekakis M, Moseley JM, Martin TJ, et al. A novel orthotopic model of breast cancer metastasis to bone. *Clin Exp Metastasis*. 1999;17(2):163-170.
132. Sloan EK, Stanley KL, Anderson RL. Caveolin-1 inhibits breast cancer growth and metastasis. *Oncogene*. 2004;23(47):7893-7897.
133. Guise T. Breast cancer bone metastases: It's all about the neighborhood. *Cell*. 2013;154(5):957-959.
134. Martin M, Bell R, Bourgeois H, et al. Bone-related complications and quality of life in advanced breast cancer: Results from a randomized phase III trial of denosumab versus zoledronic acid. *Clinical Cancer Research*. 2012;18(17):4841-4849.
135. Santen RJ, Yue W, Heitjan DF. Occult breast tumor reservoir: Biological properties and clinical significance. *Horm Cancer*. 2013;4(4):195-207.
136. Chen YC, Prabhu KS, Das A, Mastro AM. Dietary selenium supplementation modifies breast tumor growth and metastasis. *Int J Cancer*. 2013;133(9):2054-2064.
137. Yoneda T, Sasaki A, Mundy G. Osteolytic bone metastasis in breast cancer. *Breast Cancer Res Treat*. 1994;32(1):73-84.
138. Fidler IJ, Kim S, Langley RR. The role of the organ microenvironment in the biology and therapy of cancer metastasis. *J Cell Biochem*. 2007;101(4):927-936.
139. Nassa G, Tarallo R, Guzzi PH, et al. Comparative analysis of nuclear estrogen receptor alpha and beta interactomes in breast cancer cells. *Mol Biosyst*. 2011;7(3):667-676.
140. Campos SM. Aromatase inhibitors for breast cancer in postmenopausal women. *The Oncologist*. 2004;9(2):126-136.
141. Herold CI, Blackwell KL. The impact of adjuvant endocrine therapy on reducing the risk of distant metastases in hormone-responsive breast cancer. *Breast*. 2008;17 Suppl 1:S15-24.
142. Puglisi F, Minisini AM. Adjuvant endocrine therapy in postmenopausal breast cancer patients: Does hormone receptor status influence decision-making? *Crit Rev Oncol Hematol*. 2010.

143. Del Mastro L, Clavarezza M, Venturini M. Reducing the risk of distant metastases in breast cancer patients: Role of aromatase inhibitors. *Cancer Treat Rev.* 2007;33(8):681-7.
144. Bauer KR, Brown M, Cress RD, Parise CA, Caggiano V. Descriptive analysis of estrogen receptor (ER)-negative, progesterone receptor (PR)-negative, and HER2-negative invasive breast cancer, the so-called triple-negative phenotype. *Cancer.* 2007;109(9):1721-1728.
145. Gupta PB, Proia D, Cingoz O, et al. Systemic stromal effects of estrogen promote the growth of estrogen Receptor–Negative cancers. *Cancer Research.* 2007;67(5):2062-2071.
146. You S, Zuo L, Li W. Optimizing the time of doxil injection to increase the drug retention in transplanted murine mammary tumors. *Int J Nanomedicine.* 2010;5:221-229.
147. Dabydeen SA, Kang K, Diaz-Cruz ES, et al. Comparison of tamoxifen and letrozole response in mammary preneoplasia of ER and aromatase overexpressing mice defines an immune-associated gene signature linked to tamoxifen resistance. *Carcinogenesis.* 2015;36(1):122-132.
148. Martin LA, Pancholi S, Farmer I, et al. Effectiveness and molecular interactions of the clinically active mTORC1 inhibitor everolimus in combination with tamoxifen or letrozole in vitro and in vivo. *Breast Cancer Res.* 2012;14(5):R132.
149. Fowler AM, Chan SR, Sharp TL, et al. Small-animal PET of steroid hormone receptors predicts tumor response to endocrine therapy using a preclinical model of breast cancer. *J Nucl Med.* 2012;53(7):1119-1126.
150. Brodie A, Sabnis G, Macedo L. Xenograft models for aromatase inhibitor studies. *J Steroid Biochem Mol Biol.* 2007;106(1-5):119-124.
151. Jelovac D, Macedo L, Handratta V, et al. Effects of exemestane and tamoxifen in a postmenopausal breast cancer model. *Clin Cancer Res.* 2004;10(21):7375-7381.
152. Jelovac D, Macedo L, Goloubeva OG, Handratta V, Brodie AM. Additive antitumor effect of aromatase inhibitor letrozole and antiestrogen fulvestrant in a postmenopausal breast cancer model. *Cancer Res.* 2005;65(12):5439-5444.
153. Allred CD, Allred KF, Ju YH, et al. Dietary genistein results in larger MNU-induced, estrogen-dependent mammary tumors following ovariectomy of Sprague–Dawley rats. *Carcinogenesis.* 2004;25(2):211-218.
154. Churchwell MI, Camacho L, Vanlandingham MM, et al. Comparison of life-stage-dependent internal dosimetry for bisphenol A, ethinyl estradiol, a reference estrogen, and endogenous estradiol to test an estrogenic mode of action in sprague dawley rats. *Toxicological Sciences.* 2014.
155. Filardi MJ, Lininger L, McKneally MF. Adaptation of an automatic bacterial colony counter for measuring lung tumor growth in mice. *Cancer Res.* 1977;37(8 Pt 1):2726-2728.
156. Wexler H, Chretien PB, Ketcham AS, Sindelar WF. Induction of pulmonary metastases in both immune and nonimmune mice. effect of the removal of a transplanted primary tumor. *Cancer.* 1975;36(6):2042-2047.
157. Fidler IJ. The pathogenesis of cancer metastasis: The 'seed and soil' hypothesis revisited. *Nat Rev Cancer.* 2003;3(6):453-458.
158. Kakonen SM, Mundy GR. Mechanisms of osteolytic bone metastases in breast carcinoma. *Cancer.* 2003;97(3 Suppl):834-839.
159. de Almeida PE, van Rappard JRM, Wu JC. In vivo bioluminescence for tracking cell fate and function. *American Journal of Physiology - Heart and Circulatory Physiology.* 2011;301(3):H663-H671.
160. Sun A, Hou L, Prugpichailers T, et al. Firefly luciferase-based dynamic bioluminescence imaging: A noninvasive technique to assess tumor angiogenesis. *Neurosurgery.* 2010;66(4):751-7; discussion 757.
161. Ju YH, Fultz J, Allred KF, Doerge DR, Helferich WG. Effects of dietary daidzein and its metabolite, equol, at physiological concentrations on the growth of estrogen-dependent human breast cancer (MCF-7) tumors implanted in ovariectomized athymic mice. *Carcinogenesis.* April 2006;27(4):856-863.

162. Pulaski BA, Ostrand-Rosenberg S. Mouse 4T1 breast tumor model. In: *Current protocols in immunology*. John Wiley & Sons, Inc.; 2001. 10.1002/0471142735.im2002s39.
163. Heshmati HM, Khosla S, Robins SP, O'Fallon WM, Melton LJ, Riggs BL. Role of low levels of endogenous estrogen in regulation of bone resorption in late postmenopausal women. *Journal of Bone and Mineral Research*. 2002;17(1):172-178.
164. Michigami T, Hiraga T, Williams PJ, et al. The effect of the bisphosphonate ibandronate on breast cancer metastasis to visceral organs. *Breast Cancer Res Treat*. 2002;75(3):249-258.
165. Zhang S, Kim K, Jin UH, et al. Aryl hydrocarbon receptor agonists induce MicroRNA-335 expression and inhibit lung metastasis of estrogen receptor negative breast cancer cells. *Molecular Cancer Therapeutics*. 2012;11(1):108-118.
166. Hoefnagel L, van dV, van Slooten H, et al. Receptor conversion in distant breast cancer metastases. *Breast Cancer Research*. 2010;12(5):R75.
167. MacRitchie AN, Jun SS, Chen Z, et al. Estrogen upregulates endothelial nitric oxide synthase gene expression in fetal pulmonary artery endothelium. *Circ Res*. 1997;81(3):355-362.
168. Koehler KF, Helguero LA, Haldosén L, Warner M, Gustafsson J. Reflections on the discovery and significance of estrogen receptor β . *Endocrine Reviews*. 2005;26(3):465-478.
169. Canon J, Bryant R, Roudier M, Branstetter DG, Dougall WC. RANKL inhibition combined with tamoxifen treatment increases anti-tumor efficacy and prevents tumor-induced bone destruction in an estrogen receptor-positive breast cancer bone metastasis model. *Breast Cancer Res Treat*. 2012;135(3):771-780.
170. Costa-Rodrigues J, Moniz KA, Teixeira MR, Fernandes MH. Variability of the paracrine-induced osteoclastogenesis by human breast cancer cell lines. *J Cell Biochem*. 2012;113(3):1069-1079.
171. Tevaarwerk A, Burkard ME, Wisinski KB, et al. Aromatase inhibitors and calcium absorption in early stage breast cancer. *Breast Cancer Res Treat*. 2012;134(1):245-251.
172. Zheng Y, Zhou H, Modzelewski JR, et al. Accelerated bone resorption, due to dietary calcium deficiency, promotes breast cancer tumor growth in bone. *Cancer Res*. 2007;67(19):9542-9548.
173. Kim SH, Cho YU, Kim SJ, Lee JE, Kim JH. Low bone density in breast cancer survivors in Korea: Prevalence, risk factors and associations with health-related quality of life. *Eur J Oncol Nurs*. 2012.
174. Chen P, Hu P, Xie D, Qin Y, Wang F, Wang H. Meta-analysis of vitamin D, calcium and the prevention of breast cancer. *Breast Cancer Res Treat*. 2010;121(2):469-477.
175. Hong Z, Tian C, Zhang X. Dietary calcium intake, vitamin D levels, and breast cancer risk: A dose-response analysis of observational studies. *Breast Cancer Res Treat*. 2012;136(1):309-312.
176. Zheng Y, Zhou H, Fong-Yee C, Modzelewski JR, Seibel MJ, Dunstan CR. Bone resorption increases tumour growth in a mouse model of osteosclerotic breast cancer metastasis. *Clin Exp Metastasis*. 2008;25(5):559-567.
177. Rader JI, Baylink DJ, Hughes MR, Safilian EF, Haussler MR. Calcium and phosphorus deficiency in rats: Effects on PTH and 1,25-dihydroxyvitamin D3. *Am J Physiol*. 1979;236(2):E118-22.
178. Gordon RR, Hunter KW, La Merrill M, Sorensen P, Threadgill DW, Pomp D. Genotype X diet interactions in mice predisposed to mammary cancer: II. tumors and metastasis. *Mamm Genome*. 2008;19(3):179-189.
179. Luijten M, Thomsen AR, van den Berg JA, et al. Effects of soy-derived isoflavones and a high-fat diet on spontaneous mammary tumor development in tg.NK (MMTV/c-neu) mice. *Nutr Cancer*. 2004;50(1):46-54.
180. Costa I, Moral R, Solanas M, Escrich E. High-fat corn oil diet promotes the development of high histologic grade rat DMBA-induced mammary adenocarcinomas, while high olive oil diet does not. *Breast Cancer Res Treat*. 2004;86(3):225-235.
181. Kroenke CH, Kwan ML, Sweeney C, Castillo A, Caan BJ. High- and low-fat dairy intake, recurrence, and mortality after breast cancer diagnosis. *J Natl Cancer Inst*. 2013;105(9):616-623.

182. Lof M, Sandin S, Laggiou P, et al. Dietary fat and breast cancer risk in the swedish women's lifestyle and health cohort. *Br J Cancer*. 2007;97(11):1570-1576.
183. Ray A, Nkhata KJ, Grande JP, Cleary MP. Diet-induced obesity and mammary tumor development in relation to estrogen receptor status. *Cancer Lett*. 2007;253(2):291-300.
184. La Merrill M, Gordon RR, Hunter KW, Threadgill DW, Pomp D. Dietary fat alters pulmonary metastasis of mammary cancers through cancer autonomous and non-autonomous changes in gene expression. *Clin Exp Metastasis*. 2010;27(2):107-116.
185. de Assis S, Warri A, Cruz MI, et al. High-fat or ethinyl-oestradiol intake during pregnancy increases mammary cancer risk in several generations of offspring. *Nat Commun*. 2012;3:1053.

Appendix A Supplemental Figures for Chapter 2

Figure A.1

(a)

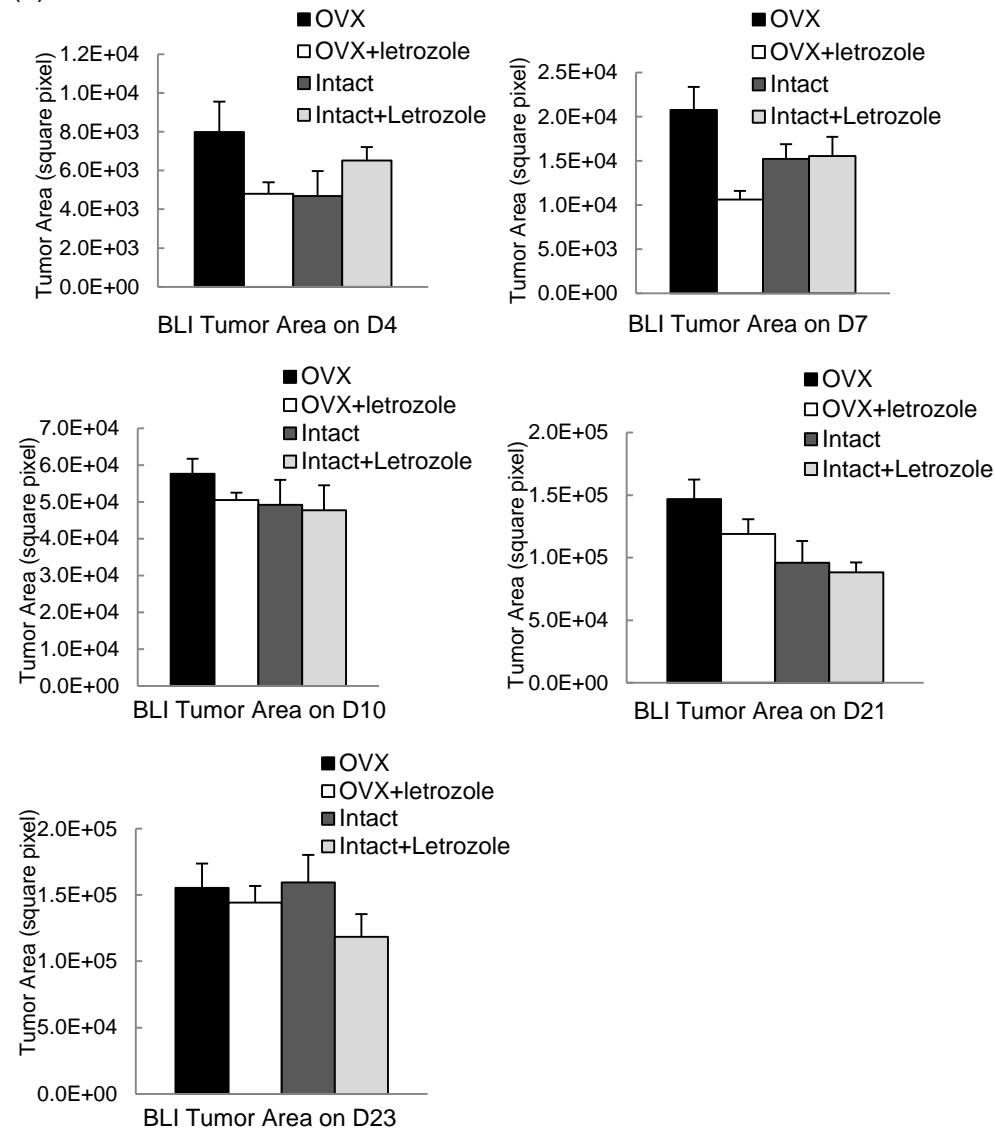


Figure A.1 (cont.)

(b)

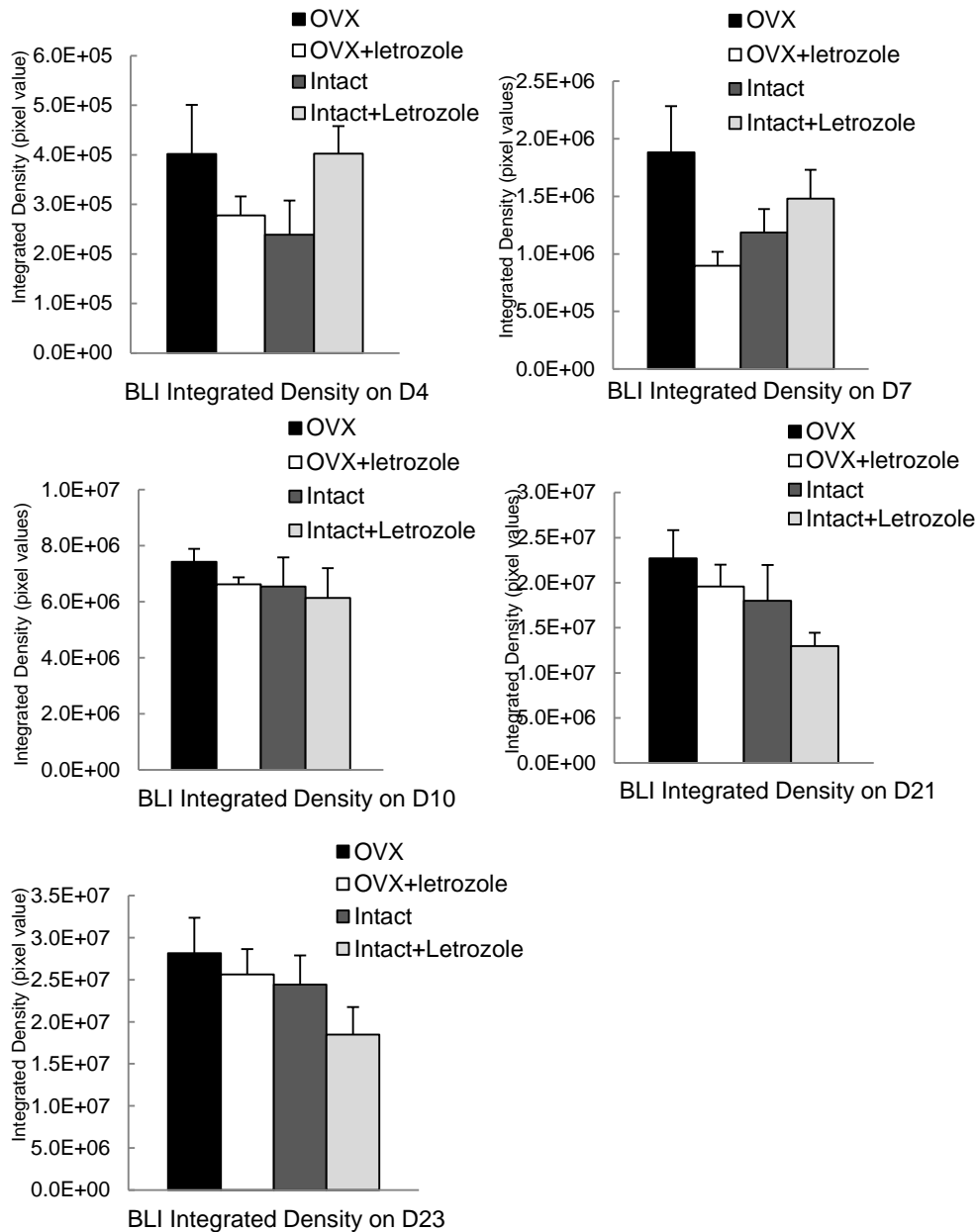


Figure A.1 BLI tumor area and integrated density measurement on D4, D7, D10, D21, and D23

(a) BLI tumor area

(b) BLI integrated density

There is no significant difference between groups in tumor area and integrated density of the micrometastatic tumor on bone measured on Day 4, Day 7, Day 10, Day 21 and Day 23.

Figure A.2

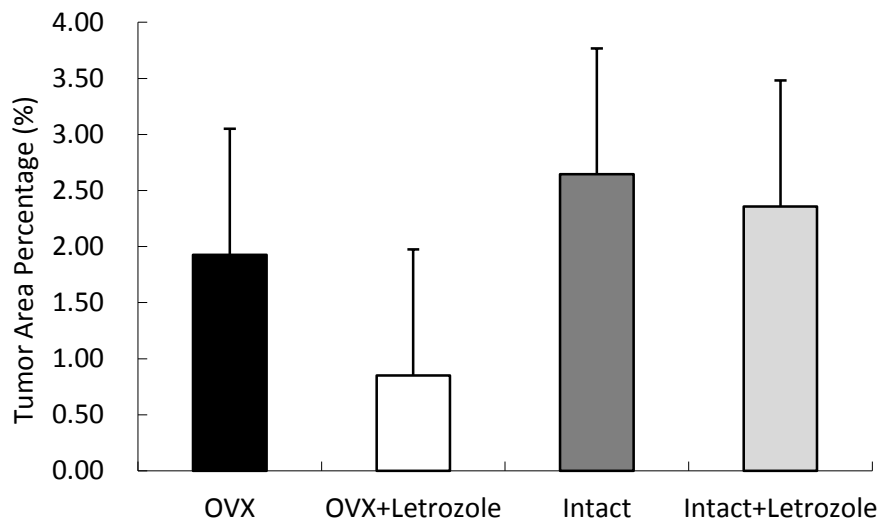


Figure A.2 Tumor area percentage on the lung from H&E staining showed no major effect of either ovariectomy or letrozole between groups

Tumor area percentage was calculated from H&E stained lung slides, as described in Methods and Materials. There is no significant effect from either ovariectomy or letrozole.

Appendix B Supplemental Figures for Chapter 4

Figure B.1

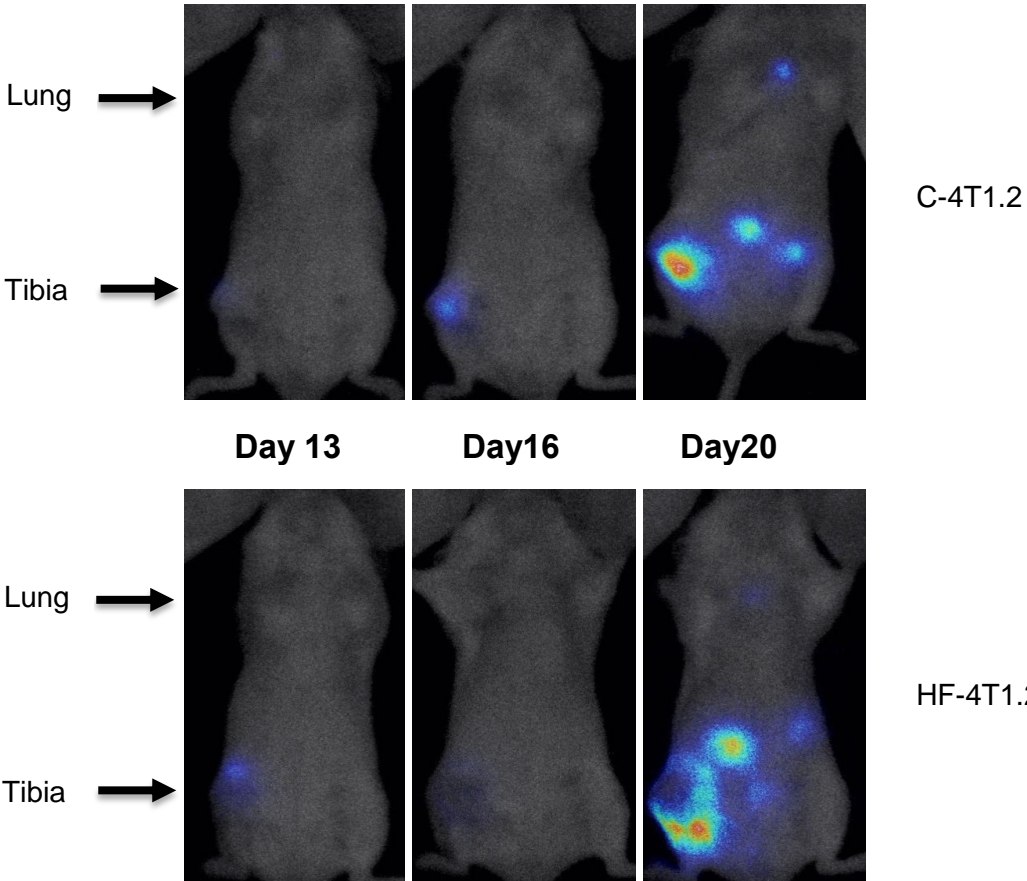
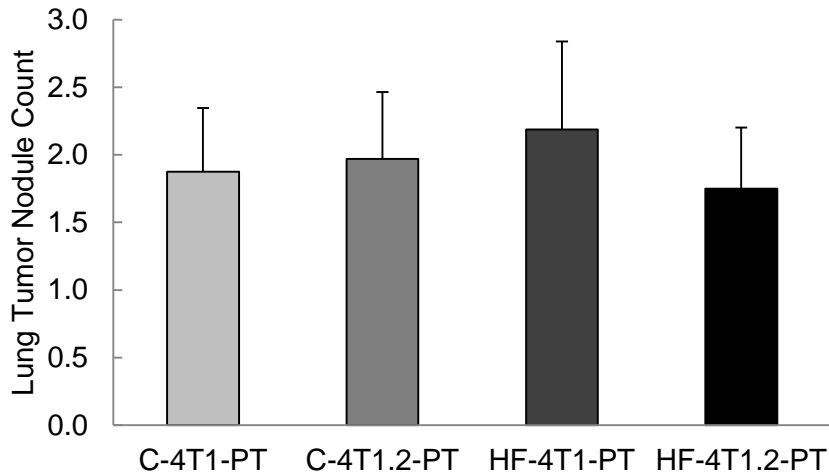


Figure B.1 Images from Bioluminescence Imaging showed that mice with 4T1.2 cells in the bone injection model developed metastasis to secondary sites in the body, such as chest and abdominal cavity.

Figure B.2

(a)



(b)

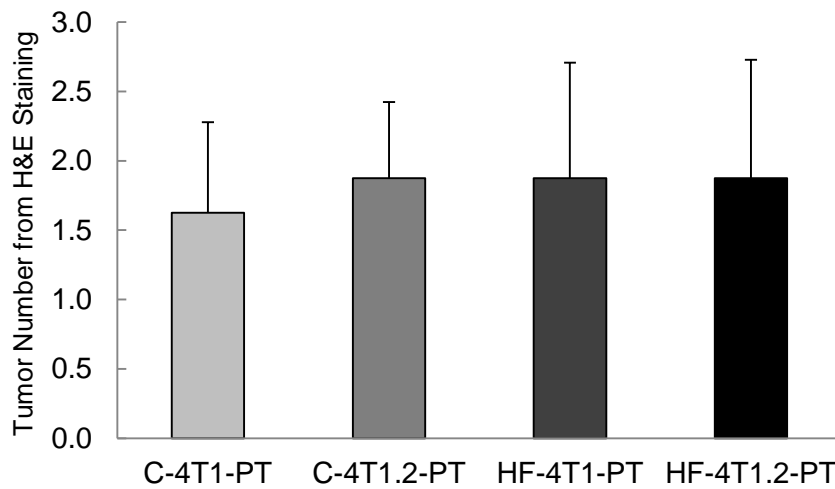


Figure B.2 There is no difference on lung surface tumor nodule count among the four groups in the mammary injection model; there is no difference on tumor numbers inside lung from H&E staining among the four groups in the mammary injection model.

(a) Lung tumor nodule count among mammary injection groups

(b) Tumor numbers inside lung from H&E staining among mammary injection groups

Figure B.3

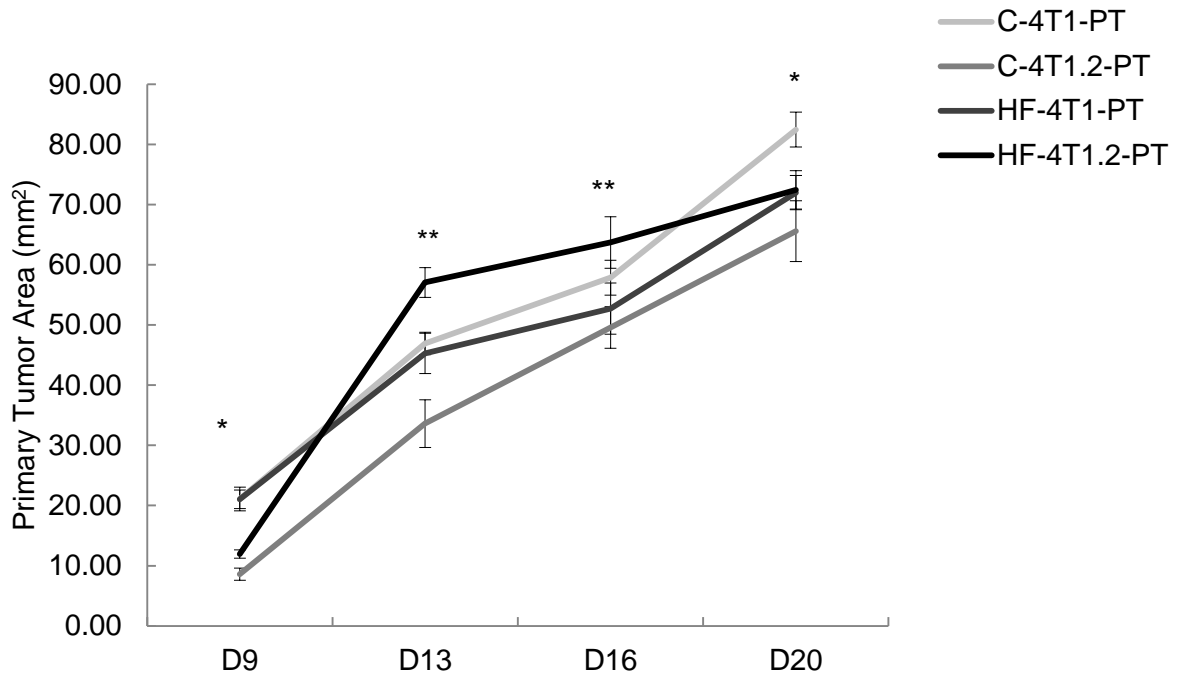


Figure B.3 Primary tumor area of mice with mammary ductal injection showed that HF-4T1.2-PT mice had larger primary tumor area than C-4T1.2-PT on Day 9, Day 13 and Day 16. Single asterisk (*) indicates a significant difference between HF and C in mice injected with 4T1 cells; two asterisks (**) indicate a significant difference between HF and C in mice with 4T1.2 cells. ($p < 0.05$)

Figure B.4

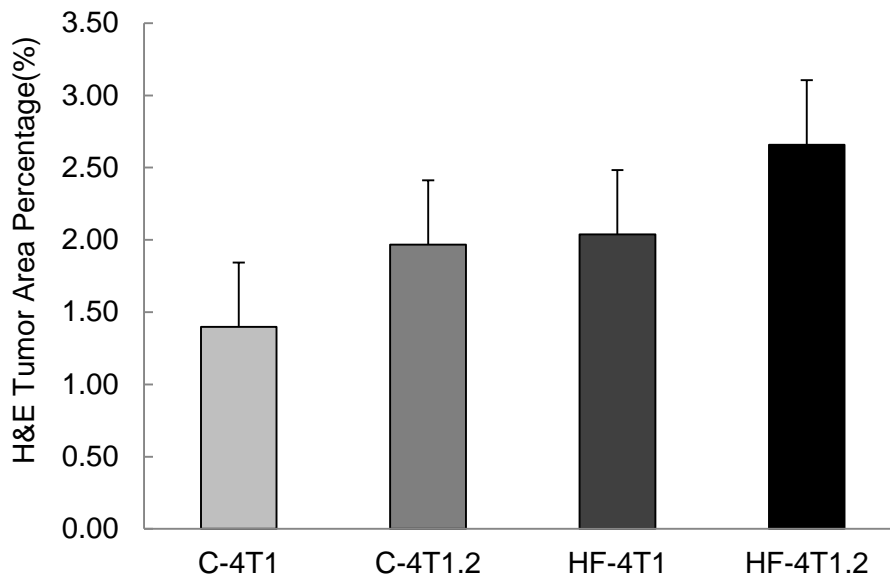


Figure B.4 There is no significant effect from either the diet or the cell line on metastatic tumor area percentage from H&E staining inside lung among the four groups in the bone injection model. Tumor area percentage was calculated from H&E stained lung slides, as described in Methods and Materials.

Figure B.5

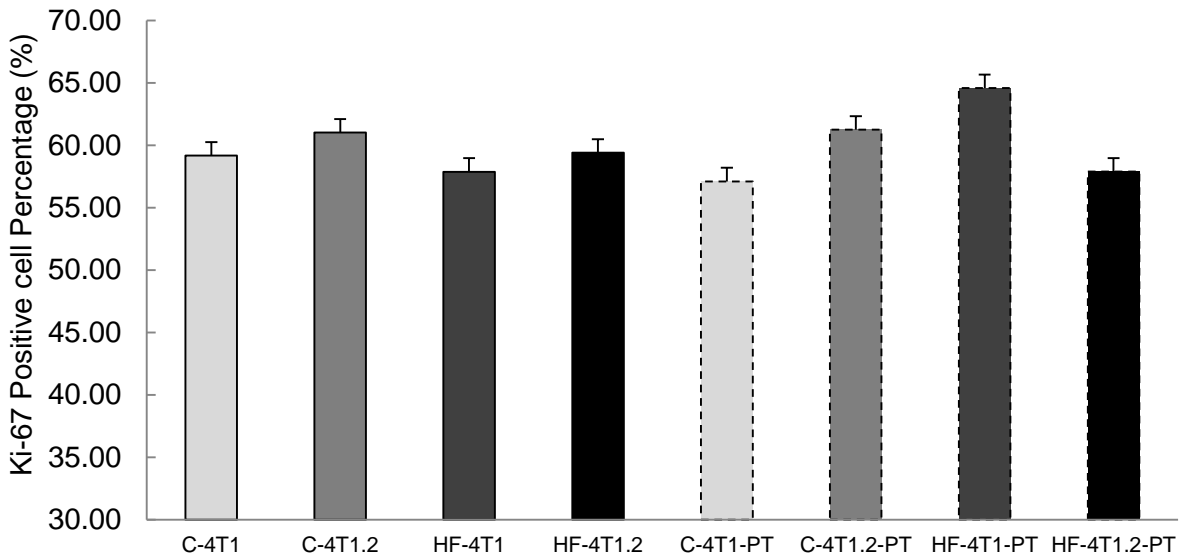


Figure B.5 There is no difference from either the diet or the cell line on Ki-67 positive cell percentage on the lung metastatic tumors in all the 8 groups. Ki-67 positive cell percentage indicates proliferative cell percentage. It was calculated as the number of positive cells divided by the sum of positive and negative cells on metastatic lung tumors in mice. Columns with dashed outlines represent the four mammary injection groups.

Figure B.6

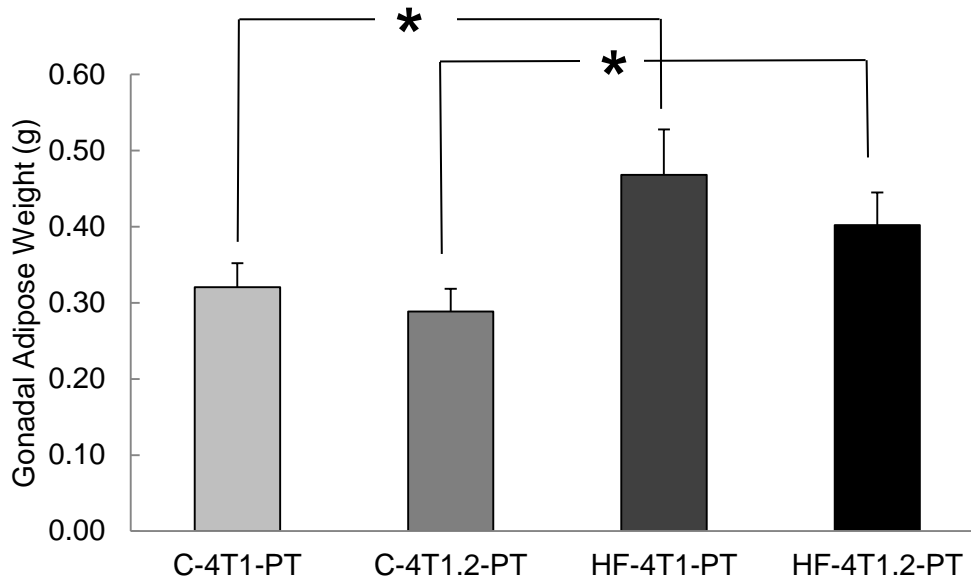


Figure B.6 Mice on a high fat diet had higher gonadal adipose weight than control in the mammary injection model. Asterisks between two columns indicate significant differences between two groups. Statistical analysis is done by ANOVA LSD, $p < 0.05$.

ⁱ CDC: Center for Disease Control and Prevention

ⁱⁱ EREG: Epiregulin

ⁱⁱⁱ COX 2: cyclooxygenase 2

^{iv} MMP: matrix-remodeling metalloproteinase

^v SPARC: secreted protein acidic and rich in cysteine, also known as osteonectin or BM-40

^{vi} CXCL1: Chemokine (C-X-C motif) ligand 1

vii VCAM1: vascular cell adhesion molecule 1
viii IL13RA2: Interleukin-13 receptor subunit alpha-2
ix ROBO1: Roundabout homolog 1
x ID-1: DNA-binding protein inhibitor
xi TGF- β : Transforming growth factor beta
xii NF- κ B: nuclear factor kappa-light-chain-enhancer of activated B cells
xiii ApoE: Apolipoprotein E
xiv LDLR: low density lipoprotein receptor
xv MCP-1: monocyte chemotactic protein-1
xvi NADP: Nicotinamide adenine dinucleotide phosphate
xvii SREBP1-c: sterol regulatory element-binding protein 1
xviii SCD-1: Stearoyl-CoA desaturase-1
xix CPT-1a: Carnitine palmitoyltransferase I
xx Hmgcr: 3-hydroxy-3-methyl-glutaryl-CoA reductase
xxi GPAT: Glycerol-3-phosphate acyltransferase
xxii PCK1: Phosphoenolpyruvate carboxykinase 1
xxiii G6P: Glucose-6-phosphatase
xxiv ACO: acyl-coenzyme A oxidase
xxv AMPK: AMP-activated protein kinase
xxvi PGC-1 α/β : Peroxisome proliferator-activated receptor gamma coactivator 1
xxvii VLAD: very long chain acyl dehydrogenase
xxviii BAT: brown adipose tissue
xxix Cidea: Cell death-inducing DFFA-like effector a
xxx IKK ϵ : Inhibitor- κ B kinase ϵ
xxxi TIF2: transcriptional mediators/intermediary factor 2
xxxii UCP: uncoupling protein
xxxiii WAT: white adipose tissue
xxxiv C/EBPs: Ccaat-enhancer-binding proteins
xxxv ADD1: Alpha-adducin
xxxvi RXR: Retinoid X receptor
xxxvii GATA: Erythroid transcription factor also known as GATA-binding factor
xxxviii KLF-4: Kruppel-like factor 4
xxxix CDC: Center for Disease Control and Prevention
xl IHC: Immunohistochemistry
xli MCP-1: monocyte chemotactic protein-1
xlii NADP: Nicotinamide adenine dinucleotide phosphate
xliiii CD-36: Cluster of Differentiation 36
xliv ACACA: Acetyl-CoA carboxylase 1
xlv ACLY: ATP citrate lyase
xlvi FASN: Fatty acid synthase
xlvii PPAR: Peroxisome proliferator-activated receptor
xlviii JAK-STAT: Janus kinase- Signal Transducer and Activator of Transcription
xlix PCNA: Proliferating cell nuclear antigen
l Ob-Rb: Leptin receptor
li IGF-1R: insulin-like growth factor 1 (IGF-1) receptor
lii Bcl-2: B-cell lymphoma 2
liii Bax: Bcl-2-associated X protein
liiv VEGFR2: receptors for vascular endothelial growth factor.
lv TRADD: Tumor necrosis factor receptor type 1-associated DEATH domain protein
lvi PTEN: Phosphatase and tensin homolog